UNIVERSITY OF CALIFORNIA

Los Angeles

Optimal Vehicle Grid Integration

A dissertation submitted in partial satisfaction of the

requirements for the degree Doctor of Philosophy

in Mechanical Engineering

by

Yingqi Xiong

2019

ABSTRACT OF THE DISSERTATION

Optimal Vehicle Grid Integration

by

Yingqi Xiong

Doctor of Philosophy in Mechanical Engineering

University of California, Los Angeles, 2019

Professor Rajit Gadh, Chair

With the increase in electric vehicle (EV) adoption in recent years, the impact of EV charging activity to the power grid has become increasingly significant. Although an EV is considered beneficial to the environment by reducing greenhouse gases, large amounts of un-coordinated EV charging could be detrimental to the power grid and thereby degrade power quality. Recent developments in Vehicle to Grid (V2G) technology has converted an EV to a distributed energy resource (DER). A modern smart grid with intelligent IoT devices, solar generation and battery storage provides additional opportunities but also additional challenges to the grid operator. To alleviate the negative effects of massive EV charging load and turn them into grid assets, the current dissertation performs research in designing and developing optimal EV charging strategies to integrate EVs into the smart power grid.

Using the UCLA Smart Grid Energy Research Center (SMERC) smart EV charging network infrastructure as the testbed, data has been collected regarding EV driver charging behavior for

five years. Based on historical charging records, both deterministic and generative EV user behavior models are proposed to combine statistical analysis and machine learning to predict day-ahead EV driver itinerary and energy demand. Optimal Vehicle Grid Integration strategy is designed to realize different objectives including EV charging cost minimization, power grid stabilization, computational burden decentralization, increasing convergence speed, mitigating solar over-generation, etc. A distributed optimal bi-directional charging scheduling algorithm with asynchronous converging feature has been designed for load curve flattening; A two-stage optimization and a distributed water-filling algorithm have been developed for aggregating EVs to participate in energy market and demand response program. Both large-scale simulation and real-world implementation are conducted to validate and evaluate the performance of these algorithms. Results show that the proposed distributed optimal bi-directional charging scheduling algorithm is able to flatten power peak load by 35% when implemented in a test-bed located within the parking structure 9 in UCLA. A daily energy cost saving of 18% is achieved when the two-stage optimization algorithm is performed to control the EVs in a parking structure in the Civic Center Garage of the City of Santa Monica to participate in wholesale energy markets. Smart meter data collected in the Santa Monica parking lot shows the proposed charging control algorithm is able to mitigate the solar over-generation in the building by 50% on a daily basis. It can be concluded that our Vehicle Grid Integration strategy is effective in stabilizing power grid load, reducing charging cost and solving solar power over-generation problem. In addition to the development of EV user behavior models and Vehicle Grid Integration strategy, this dissertation also solves practical engineering problems for a scalable, reliable and safe EV bi-directional smart charging infrastructure.

The dissertation of Yingqi Xiong is approved.

Adrienne Lavine

Tsu-Chin Tsao

Xiaochun Li

Rajit Gadh, Committee Chair

University of California, Los Angeles

2019

To my wife, Mengying Chen

and my daughter, Claire Xiong

Table of Contents

LIST OF FIGURES

LIST OF TABLES

ACKNOWLEDGEMENTS

This work has been sponsored in part by grants from the LADWP/DOE (fund 20699, Smart Grid Regional Demonstration Project), the California Energy Commission (fund EPC-14-056, Demonstration of PEV Smart Charging and Storage Supporting Grid Operational Needs) and UC-National Lab Collaborative Research and Training Awards (UC-Lab Center for Electricity Distribution Cybersecurity).

To my PhD advisor, Dr. Rajit Gadh, many thanks to his inspirations, valuable advice, continuous support and guidance through the course of my research. This dissertation could not have been finished without the experiences and suggestions from him. At UCLA Smart Grid Energy Research Center (SMERC), I have not only learned how to conduct independent research, but also implemented my research to the real-world applications.

To my committee, Dr. Adrienne Lavine, Dr. Tsu-Chin Tsao, and Dr. Xiaochun Li, for offering me great comments and suggestions on my research and dissertation.

I would like to express my gratitude to the staffs at UCLA SMERC: Dr. Chi-Cheng Chu, who gave me great support and guidance on implementation of my theoretical research works; Dr. Ching-Yen Chung, who was my mentor during the first year in SMERC. I would like to thank the students at UCLA SMERC: Dr. Bin Wang, Dr. Yubo Wang, Dr. Hamidreza Nazaripouya, Dr. Tianyang Zhang, Zhiyuan Cao, Yu-Wei Chung, Shashank Gowda and Behnam Khaki for their collaborations, supports and advice.

Finally, I am grateful for my family. Their love and support are always with me.

VITA

Educations

Master of Science, Northwestern University, Evanston, IL, September 2012 – June 2014

Bachelor of Engineering, Northeastern University, China, September 2008 – June 2012

Professional Experience

Data Scientist Intern, Microsoft Corporation, Bellevue, WA, June 2018 – September 2018

Publications

Yingqi Xiong, Bin Wang, Chi-cheng Chu, Rajit Gadh, “Vehicle grid integration for demand response with mixture user model and decentralized optimization”, Applied Energy, Volume 231, 2018, Pages 481-493.

Y. Xiong, B. Wang, C. Chu and R. Gadh, "Electric Vehicle Driver Clustering using Statistical Model and Machine Learning," 2018 IEEE Power & Energy Society General Meeting (PESGM), Portland, OR, USA, 2018, pp. 1-5.

Y. Xiong, B. Khakit, C. Chu and R. Gadh, "Real-Time Bi-Directional Electric Vehicle Charging Control with Distribution Grid Implementation," 2018 IEEE/PES Transmission and Distribution Conference and Exposition (T&D), Denver, CO, 2018, pp. 1-5.

Y. Xiong, C. Chu, R. Gadh and B. Wang, "Distributed optimal vehicle grid integration strategy with user behavior prediction," 2017 IEEE Power & Energy Society General Meeting, Chicago, IL, 2017, pp. 1-5.

Y. Xiong, B. Wang, Z. Cao, C. Chu, H. Pota and R. Gadh, "Extension of IEC61850 with smart EV charging," 2016 IEEE Innovative Smart Grid Technologies - Asia (ISGT-Asia), Melbourne, VIC, 2016, pp. 294-299.

1 Chapter I. Introduction

1.1 Backgrounds

1.1.1 Electric Vehicle Smart Charging

The popularity of electric vehicles is growing rapidly among consumers due to their environmental and technological advantages, such as zero emission and energy efficiency, etc., as well as the incentives from the government. For instance, California has renewed its target of electric vehicle (EV) penetration in the transportation system to 1.5 million by 2025, and at least 5 million by 2030 [1]. Five million EVs in the US will consume 50 GW of potentially available power if each EV is grid-integrated with an average of 10 kW of charging power. Currently, there is a lack of policies to regulate EV charging. All charging activities are spontaneous without coordination and consideration of any grid circumstances. However, uncoordinated EV charging activities will have a significant negative impact on the economics and resiliency of the energy system [2]. Specifically, the uncontrolled charging load from heterogeneous EV drivers will potentially create new system load peaks, which may degrade the power quality of the distribution systems, e.g., voltage drop [3]. For commercial sites or microgrids, the additional load peak may also contribute to an extra demand charge, e.g., the tariff structure E-19 in PG&E territory in northern California, which is calculated as the product of monthly load peak and demand charge rates [4]. Thus, there is a growing demand for smart energy management strategies for the large-scale integration of electric vehicles. Smart charging can solve these issues by optimizing the EV charging schedule and energy allocation [5][6][7]. Significant studies have been conducted to incorporate bi-directional power flow and grid service support from EVs, upgrading EVs from traditional dumb

consumptions to controllable distributed energy resources (DERs) [8]. If one can design a strategy to combine EV charging and V2G together, EVs will become valuable assets to the power grid. However, distributed EV batteries must be aggregated on a large scale, so that they can participate in the wholesale energy market to provide grid services. Such aggregation would require huge computational resources if it's performed in the traditional centralized control scheme. Smart bi-directional charging scheduling also depends on good understanding of EV driver behaviors.

1.1.2 Renewable Energy Generation

With the development of photovoltaic harvesting technology, solar panels become more and more affordable, and the energy conversion rate is also increasing over time. The installed capacity of solar photovoltaics (PV) continues to grow rapidly in the US. High penetrations of solar power can create operation and reliability challenges due to the characteristics of solar generation, which is highly intermittent and periodical in nature [9]. There is a demand for new methods to better integrate and manage the growing amount of these renewable distributed energy resources in the power grid. Big solar generation in the daytime decreases the load demand of fossil fuel based thermal generations. The power grid will face the so-called "duck curve" problem, *i.e.*, the power grid net load curve looks like the shape of the back of a duck, due to over-generation from solar power [10]. In this situation, conventional generations may be no longer able to support the ramp rate and range needed to fully utilize a big amount of solar generation [11].

1.1.3 Vehicle to Grid (V2G) Technology

Vehicle to Grid (V2G) technology refers to the technology which make it possible for bi-directional energy flow in plug-in electric vehicles to the power grid, which can be used to provide various grid services. It implies mobile storages that could – during long phases of immobility – provide services for the electricity sector. V2G requires electric vehicle users to temporarily abstain from the usage of their batteries for V2G [12]. By using V2G technology, electric vehicles are no longer only dumb loads on the power grid but also can act as distributed energy resources to support the power grid when needed. The charging station with V2G capability can be operated with more flexibility in response to various pricing and control signals, making it more effective in improving the grid economics and resiliency [13]. V2G covers the obvious benefits of economic savings, emissions, and renewable energy integration, several other novel benefits were also identified. The second and third most common discussed EV benefits were noise reduction and better performance [14]. V2G is actively tested in German which proved to be able to support transmission grid balancing, and local flexibility markets can provide reasonable remuneration for electric vehicle owners [15].

1.1.4 Demand Response Program

Demand Response (DR) provides an opportunity for consumers to participate in the power grid operation by bidding in the day-ahead energy wholesale market, reducing or shifting their electricity demands during peak load hours in response to the Time of Use (TOU) rate and some other ancillary service [16]. As one type of distributed energy resources (DER), EVs can be aggregated together as one large controllable resource to participate in multiple energy and demand

response markets [17]. EV load can also be seen as deferrable load, which can be shifted to different time windows to achieve various grid service objectives [18]. Authors in [19] proposed a method based on the idea of 'virtual battery' to the aggregated individual EV's charging flexibility, considering the heterogeneous charging session parameters, such as start charging time, plug-in duration and the total energy consumption per session. To maximize the benefits of EV-grid integrations, [20] discussed an approach to integrate the aggregated EV resources into multiple California energy and demand response markets, such as TOU and peak-day pricing (PDP) plans offered by the utility company and proxy demand response (PDR) and ancillary service markets from California Independent System Operator (CAISO). However, constraints on the real-world EV charging behaviors are barely modeled in most of the previous research.

1.1.5 Cybersecurity

The power grid is becoming more and more complex with increasing amount of smart grid equipment connected to the grid. Numerous data and controls are transferring in the power grid at every second. With the advancement in V2G and autonomous vehicle technology, we are expecting more data exchanges and interactions the power grid would have with public Internet [21]. Improved sensing, communication, and control capabilities have the potential to enormously enhance the performance of the electric grid, but at the cost of increased vulnerabilities to deliberate attacks and accidental failures, threatening the grid's functionality and reliability [22]. It is necessary to take cybersecurity into consideration when developing vehicle grid integration strategies.

1.1.6 Standards and Protocols

Currently there are three EV charging standards for EV charging in the North America market. The most popular among them is SAE J1772 [23], which specifies the hardware and communication requirement for level 1 and level 2 AC charging. The power output limit of SAE J1772 for AC charging is 15kW. As an example, a Nissan Leaf needs 6 hours to be fully charged using SAE J1772 charging station for a maximum traveling range of 100 miles. The Japanese EV charging standard CHAdeMO is used by all Japanese manufactured EVs such as Nissan Leaf and Mitsubishi MiEV for DC charging. There are many fast DC charging stations complied with CHAdeMO which can provide 30kW max output power. A Nissan Leaf as our benchmark can be fully charging in 30 minutes using a CHAdeMO DC fast charging station. Another charging standard currently available in the U.S. is SAE Combo Charging Standard (CCS). It provides DC fast charging support as an extension of SAE J1772. But CCS standard is not widely used in public yet. CCS is in the process of being combined with ISO 15118 [24], which is a charging standard currently widely used in Europe countries. There is a high possibility that CCS and ISO 15118 will be merged and become the most important and widely used charging standard in the U.S. and Europe.

1.2 Challenges and Objectives

Previous works on EV charging only partially covered the field of electric vehicle and power grid integration. With the fast increasing EV adoption rate, fast evolving charging and V2G technology and a smarter power grid, new challenges keep emerging in the field of EV smart charging scheduling. The objectives of this research are summarized in the following paragraphs.

First, most of the previous research and projects on EV charging scheduling are based on assumption and simulation. There is no real-world implementation of their proposed algorithms and no real-world data available to validate the results. Strong assumptions are made by many EV charging scheduling research that the traveling patterns and state of charge (SoC) information are known before the charging scheduling algorithm is executed. In reality, an SAE J1772 AC charging station is not able to obtain SoC information and never know when there would be future charging activities. However, user behavior, specifically speaking, the arrival time and departure time of an EV to the charging station, and the energy demand are critical constraints to make an optimal EV charging scheduling meaningful. These user behaviors are generally not available for the charging service provider. Considering privacy issue and fully automatic requirement, it is challenging but necessary to design methods to estimate user charging demand and predict user behavior for day-ahead optimal charging scheduling. The user behavior predictive model should only be learned from real-world EV driver charging record, but not from any assumptions or making up data. Second, most of the previous research and projects are working on an individual topic such as solar generation for demand response, EV charging control for load balancing, etc. None of them is systematically dealing with a real and integrated system with solar generation, EV charging stations, battery storage and energy management control center. A control strategy jointly consider every component in the energy system is most meaningful for real-world implementation. Third, the influence of V2G to the power grid in real-world is less studied in the literature.

In this research, all predictive models and control strategies are designed based on the real-world implementation of smart electric vehicle charging network infrastructure. We investigate methods to estimate EV user behavior, distributed optimization algorithm for EV charging scheduling, strategy of vehicle grid integration for demand response and other ancillary services. This research

also involves designing and developing hardware and system for the smart EV charging infrastructure.

1.3 Dissertation Structures

Chapter 2 gives an introduction of the smart EV charging network infrastructure. Chapter 3 covers methods for EV user behavior estimation and prediction. Chapter 4 discusses the decentralized optimal EV charging scheduling algorithm and distributed grid implementation. Chapter 5 investigates the Vehicle Grid Integration strategy for demand response program, energy market and solar generation duck curve mitigation. Chapter 6 provides hardware and system design for some key components in smart charging infrastructure. And Chapter 7 concludes this dissertation.

2 Chapter II. System Introduction

2.1 Smart Charging Network Infrastructure

Pioneer researchers in UCLA Smart Grid Energy Research Center (SMERC) have developed advanced smart charging infrastructure with an aggregated control center and network to coordinate EV charging activity with the variable current charging and power-sharing feature [25][26]. Considering the energy sharing strategies, uncertainties of user behaviors and energy prices, smart charging algorithms developed by SMERC in [27][28][29] have been successfully implemented on UCLA campus with real-world EV drivers.

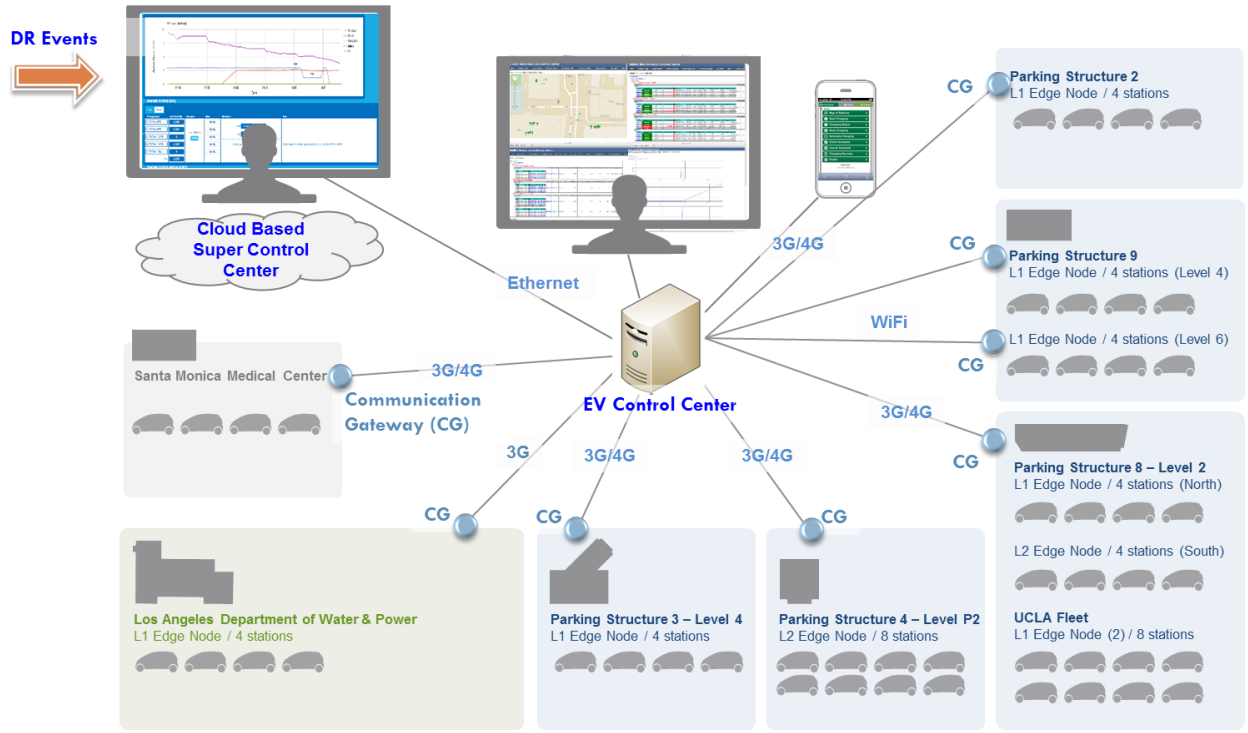

Figure 1. Smart EV charging network infrastructure architecture

The smart charging infrastructure, shown in Figure 1, consists of three major components: the control center, smart electric vehicle service equipment (EVSEs) and mobile app, they communicate with each other via the internet. Smart EVSEs are the foundations of this infrastructure. They are installed in different parking lots and different cities. Each smart EVSE is equipped with a local charging controller whose electronic circuit and firmware designed under SAE J1772 standard. The key features of this EVSE are capabilities of variable current charging and multiplexing charging. The input power source can be split up to 4 plug-in EVs with different power outlets by the firmware, using its smart charging algorithm. A gateway is integrated with each EVSE, which connects the EVSE to the internet through multiple protocols. Real-time energy consumption data with EV info and EVSE ID are retrieved by the infrastructure's control center through the gateway and stored in the database system. Optimal Charging strategy is generated for each charging session by the smart charging algorithm in the control center, based on real-time monitoring data, historical charging record, and grid-side signals, as well as coordination with other charging sessions. The charging strategy determines the current and power allocation plan for the EVSE, meanwhile related control commands are transmitted to certain EVSE through internet and gateway. Each user has a mobile app to perform user charging control and monitoring. SMERC mobile app provides a user interface to manually set their charging preference such as schedule, power demand and energy price. The user can start and stop charging any time using the mobile app. Mobile app sends user charging control and preference to control center. Control center receives these user request and takes them as parameters in the smart charging algorithm, providing charging strategy accordingly.

2.2 EV Control Center

The SMERC Monitoring and Control Center is a high-performance server that allows administrators/operators to monitor and control all EV charging stations, registered to the network. The system defines control algorithms, provides real-time and historical data for analysis, and allows the editing of information about charging boxes and EVs. UCLA SMERC has developed Application Programming Interface (API) to provide more efficient and reliable services for the charging infrastructure's communication and control. The current version, API v2.0 has a well-structured OOP (Object-Oriented Programming) architecture with separate function interfaces for server-based smart algorithms, web-based Apps and Web Services. API v2.0 provides the foundation for server-based charging applications and the other system components. In addition, OpenADR 2.0 [30] is integrated into the current API to provide interfaces for both utilities and other third parties to issue demand response signals, which support load curtailment and throttling. Both Level I and Level II charging boxes within WINSmartEVTM system is capable of dynamically adjusting current (duty-cycles) or on/off control according to the diverse DR signals and real-time EV charging load. Currently, the Control Center server platform is hosted on a high-performance server and the system has been updated.

In Figure 2, the monitoring page for the EV charging behaviors at the UCLA campus can be utilized for showing the real-time charging events. The EV info and the corresponding EVSE where this user's vehicle is in charging are shown. The user names are blocked in this figure for privacy concern. The available charging stations will be indicated as "Standby." Meanwhile, the real-time charging power, voltage, current and the accumulated energy consumed for the particular meter are recorded.

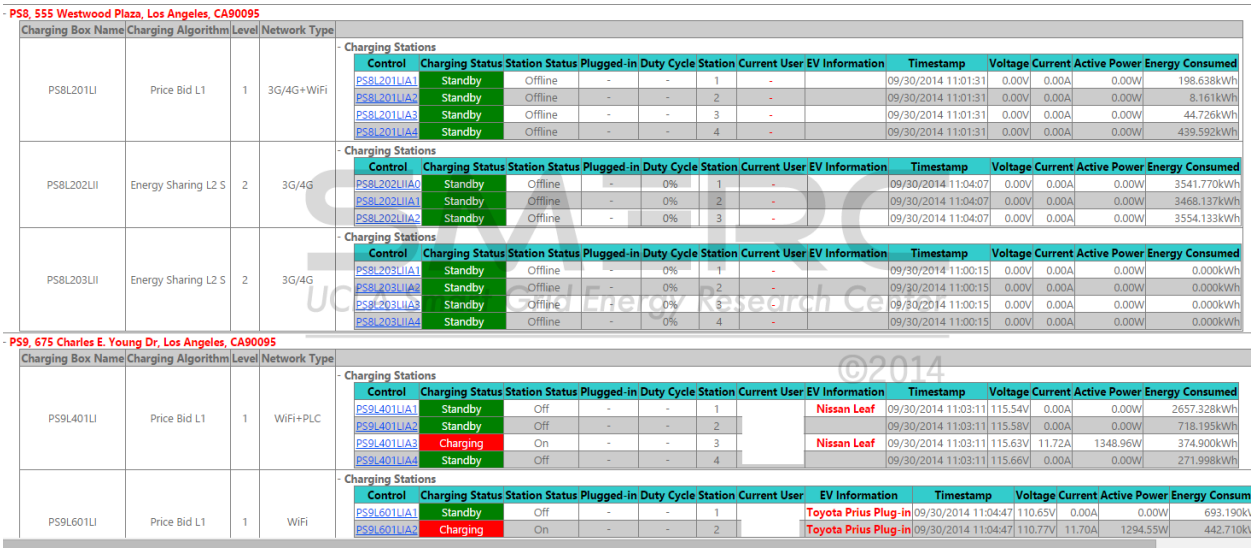

Figure 2. Monitoring of EV User Behaviors

2.3 Vehicle to Grid Control System

The architecture of the V2G system is shown in Figure 3. The V2G system is integrated into SMERC smart charging infrastructure to share data and receive aggregated control command. The V2G charging station is an advanced equipment with remote control communication interface and equipped with V2G capability. It has one CHAdeMO charging port. This charging port can perform regular DC fast charging to any vehicle using CHAdeMO standard. V2G can also be performed by the same charging port but currently only limited to Nissan Leaf with V2G technology enabled. There is a communication device built inside the charging station so that the charging station can be reached via the internet. The energy price and demand response signal are obtained from the power grid service providers to the SMERC control center on a real-time basis. Charging and discharging control command are passed to corresponding V2G charging station controller register using Modbus TCP interface.

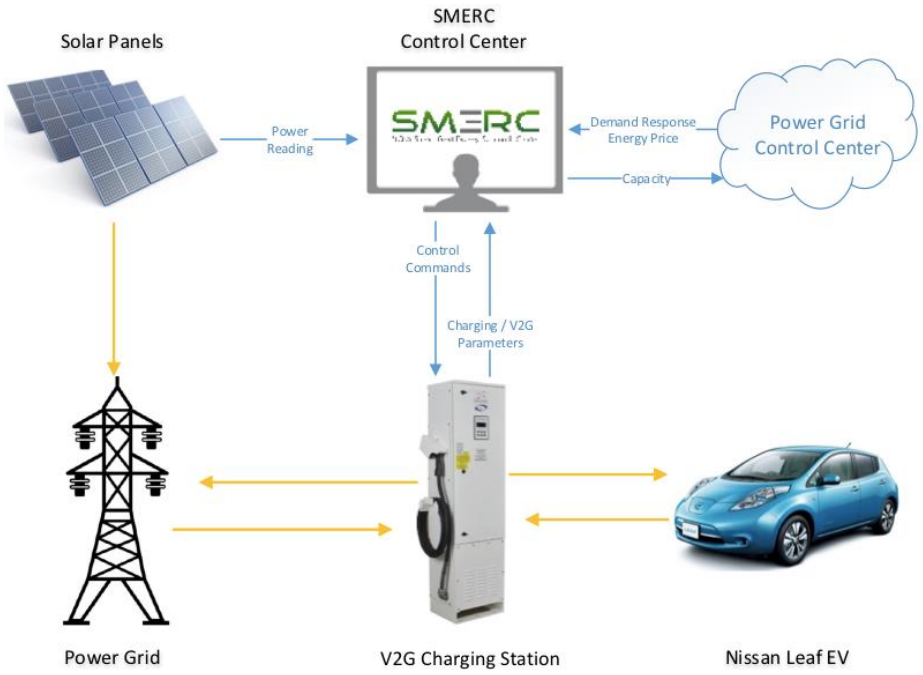

Figure 3. SMERC V2G system architecture

3 Chapter III. EV User Behavior Prediction

3.1 Introduction

To effectively manage the aggregated EV load, many approaches have been proposed by previous researches. For instance, Demand Response (DR) programs are offered to EV load aggregators to regulate the EV charging load according to the time-varying energy prices [29]. Also, EV charging load can be deferred intelligently to different time windows for different grid objectives, such as cost minimization [28][31][32] system load flattening and the valley-filling [33]. However, most of these approaches are based on assumptions that the charging session parameters, i.e., charging start-time, stop-time and energy consumption are pre-known without uncertainties, which is not realistic in most real-world cases. Thus, accurate session parameter prediction of the driver behavior is needed by both smart charging and demand response program. There are many well-

investigated forecasting methods for microgrid load, building load, solar generation [31][34][35], etc. However, there is a lack of research works regarding EV driver clustering and EV load prediction. There are challenges to make day-ahead forecasting for EV load due to the following factors: 1) EV users are individuals with uncertain behaviors; 2) Due to the size of the population, it is hard and not practical to model or label each EV user; 3) Load demand and capacity varies among different EV models.

Previous studies have partially covered some of those challenges discussed previously. A predictive EV charging control algorithm is proposed in [31] and [36] where the randomness of user behavior is described by Kernel Density Estimation (KDE), which eliminates the restriction from specific distribution model, but no load forecasting has been performed. The uncertainty of EV user behaviors is also addressed in [37], where Markov Decision Process (MDP) and Queue Theory (QT) are utilized. [38] compares the performance of different EV load prediction methods including k-Nearest Neighbors (kNN) and Lazy-learning Algorithm. However, to the best of authors' knowledge, none of them provides a comprehensive solution to address the whole implementation cycle of such forecasting that can resolve all the aforementioned challenges.

3.2 Electric Vehicle User Behavior Dataset

The volume of historical charging session data is large. These data require effective data mining methods to extract useful information. In [39][40][41] various data mining techniques were utilized to address challenges in the energy sector, such as load forecasting and profiling. In [42][43][44] data mining modeling frameworks were applied to electricity consumption data to support the characterization of end-user demand profiles. EV user charging record data has been collected for more than five years since the system was online in 2013. Timestamps of plugging-

in, charging start, charging stop, charger disconnection have all been stored in the database, as well as charging current and power consumption. Three typical types of user records are shown in Figure 4 to illustrate the statistical features of their behaviors.

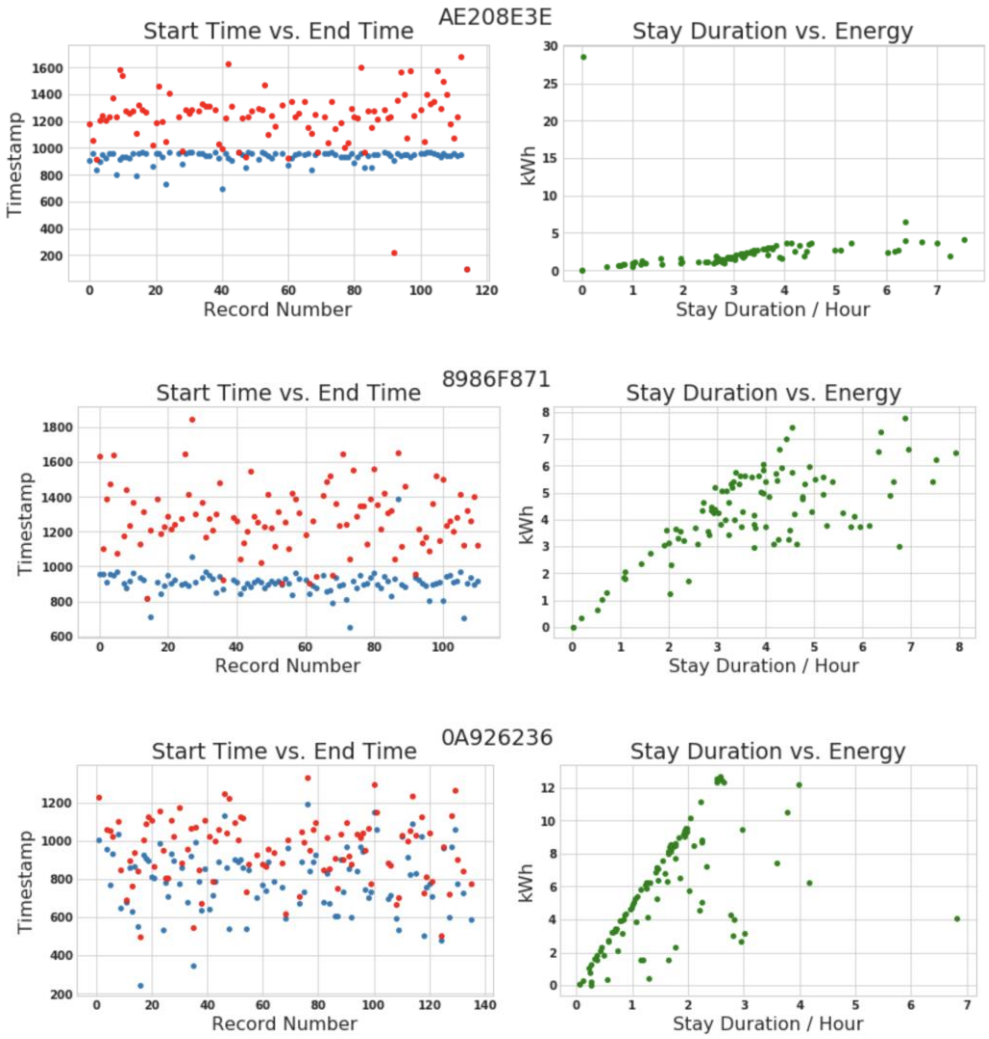

Figure 4. Typical EV user behavior

In Figure 4, the left column shows EV arrival time (blue dots) and departure time (red dots) for 100 days; the right column shows the relationship between energy consumption (kWh) and plug-in duration (h). It can be seen that there is no general distribution which can describe and model all user behaviors easily. By visualization of different user records, we can tell that there are

roughly several groups of users who share the same characteristics. Using the charging records shown in Figure 4 as an example, we can find that user #AE208E3E has a traveling schedule which is relatively easy to be predicted, and the energy consumption is linearly related to the charging duration. User #8986F871 usually arrives at the parking lot in the morning around 9 am, with variance less than 1 hour, but departure time is relatively random. The energy consumption is not entirely related to the stay duration which means the EV battery state of charge (SoC) may reach 100% before physically disconnected from the charger. Another type of user has a comparatively random itinerary, such as user #0A926236. These types of users could be fleet drivers, who frequently parks and drives their vehicle through the day.

3.3 Statistical Estimation Method

Historical charging data of randomly selected 4 EV users are plotted in Figure 5 to show the relationship between charging start time and end time.

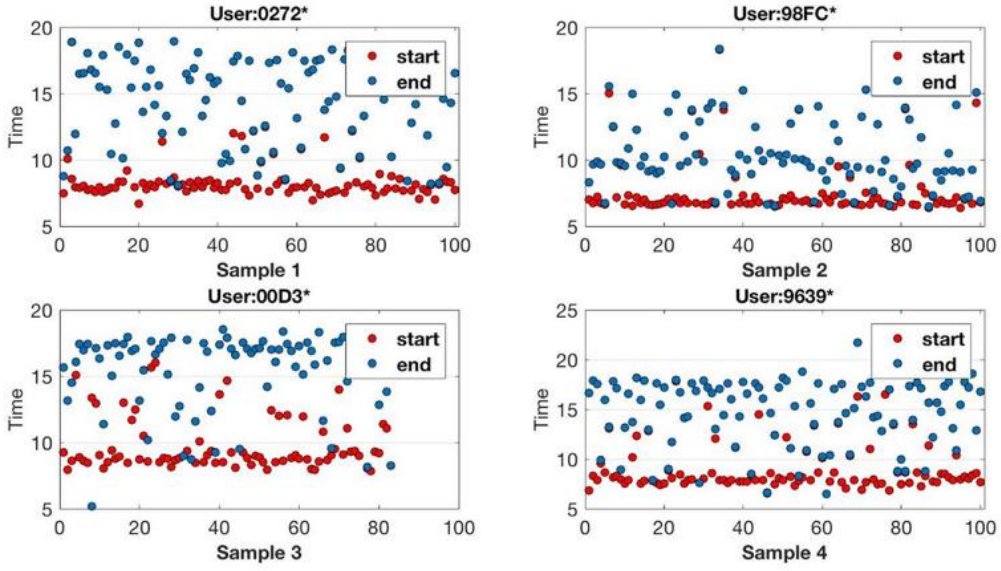

Figure 5. EV user charging time preference

From Figure 5 it can be seen that the charging start-time and end-time of these 4 EV drivers follow some patterns. Most of the charging activities start and stop at a particular time in the day, which may represent the EV user weekdays routine. Mean estimation is used to predict the charging behavior of these EV users,. The charging start time and end time can be obtained using following equations: The charging start time and end time can be obtained using following equations:

$$t_{start}^{pred} = \frac{1}{M}\sum_{i=1}^{M} t_{start}^{i} \tag{3.1}$$

$$t_{end}^{pred} = \frac{1}{M}\sum_{i=1}^{M} t_{end}^{i} \tag{3.2}$$

Where t_{start}^{pred} is the predicted charging start time using the mean method, and t_{end}^{pred} is the end time. M is the number of samples used in prediction analysis.

EV charging duration t_{stay} can be obtained by taking the difference between start time and end time. Figure 6 shows the relationship between charging duration and energy consumption for one of the users.

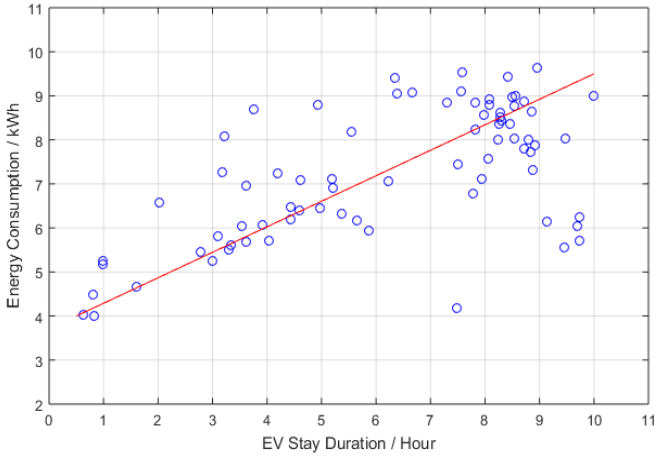

Figure 6. EV charging power consumption versus duration

It can be seen from Figure 6 the relationship between charging duration and energy consumption is almost linear. Additional features, such as last trip energy consumption, driver' home distance from campus, etc. will be utilized in the regression model in the future. By using linear regression, the prediction model for EV charging consumption can be obtained. Let $X = [t_{stay}^{1}, t_{stay}^{2}, \ldots t_{\text{stay}}^{\text{M}}]$ denote the pool of sample charging duration and $y = [E^{1}, E^{2}, \ldots E^{M}]$ contains corresponding energy consumption, linear regression parameter θ can be calculated by:

$$\theta = \left[X^{\text{T}} X\right]^{-1} X^{\text{T}} y \tag{3.3}$$

The predicted energy consumption can then be calculated by:

$$E^{pred} = \theta\left(t_{end}^{pred} - t_{start}^{pred}\right) \tag{3.4}$$

Most of the charging behaviors from different EV drivers in our database share similar patterns with EV drivers in Figure 6. They have a routine charging start time and end time with predictable energy consumption values. By using the mean estimation and linear regression method, we can predict EV user charging behaviors for the proposed bi-directional charging control algorithm [33].

3.4 Clustering and Neural Network

In this section, we utilize both supervised learning and unsupervised learning approaches to find patterns in EV user charging records and make predictions. K-means clustering is applied to categorize EV user behavior and the neural network is used for further classification. The combination of both techniques is built for an online real-time EV user model to describe the uncertainty and eliminate the needs for hand labeling user behavior or revisiting historical dataset.

The user model can be used by different kinds of scheduling algorithms for generating optimal predictive control scheme [45].

3.4.1 EV User Clustering

K-Means clustering [46] is an unsupervised learning algorithm which can be used to partition data into k clusters based on some certain properties within each individual data point. We use this algorithm to process our historical charging records and generate assumptions of EV user behavior for EV charging scheduling.

From the visualization of historical EV charging record, it can be observed that user behavior can be categorized into four groups. We choose the mean and standard deviation of arrival and departure time and the Pearson correlation coefficient between stay duration and energy consumption as clustering criteria. There are k centroids $\mu_j \in R^5, j \in [1,k]$.

$$\mu := \left(\bar{t}_{arrival}, \bar{t}_{departure}, \sigma_{arrival}, \sigma_{departure}, cor\right) \tag{3.5}$$

Where cor is the Pearson correlation coefficient. The charging record data of each user are also processed into the same tuple structure as the clustering centroids. Assuming there are m user records which give us the user clustering matrix $X \in R^{m\times k}$. The clustering algorithm updates the user group tag of each user in every iteration step by:

$$c^i := \arg\min_j \left\| x^i - \mu_j \right\|^2 \tag{3.6}$$

where c^i represents the user group tag of each user x^i, while $x^i \in X, i \in [1,m]$. Equation (3.6) changes the tag of each user to its closest user group. After updating all user group tags, the group centroid positions are then updated based on the users belonging by (3.7)

$$\mu_j := \frac{\sum_{i=1}^{m} I\{c^i = j\} x^i}{\sum_{i=1}^{m} I\{c^i = j\}} \tag{3.7}$$

The complete steps for EV user clustering are summarized in algorithm 3.1 as follows:

Algorithm 3.1: EV User Behavior Clustering

Process EV charging record for each user into tuple described in (3.5) to form the user clustering matrix X

Randomly initialize user group centroids $\mu_j, j = 1,2, \dots, k$ from user clustering matrix X

While $\sum_{i=1}^{m} \|x^i - \mu_{j^i}\|^2 > \varepsilon$:

For i = 1, 2, 3, … m:

Calculate (3.6)

End

For j = 1, 2, …, k:

Calculate (3.7)

End

End

The cost function selected for the K-means algorithm is Euclidian distance. By minimizing the cost function in (3.8) we can get the optimal group number:

$$\underset{j}{\operatorname{argmin}} \sum_{i=1}^{m} \|x^i - \mu_{j^i}\|^2 \tag{3.8}$$

3.4.2 EV User Classification

Multilayer perceptron [47], also known as artificial neuron network, is a powerful tool to make classification over the labelled dataset. It can capture features which are relatively hard to be observed by data visualization. We use multilayer perceptron to process EV user charging record data and make a classification based on both clustering labels from the K-means algorithm and

hand-labeling by data visualization. The neuron network is trained using backpropagation and can be utilized for future classification on any new users without processing the whole dataset again. The structure of the neuron network used in the proposed work is shown in Figure 7.

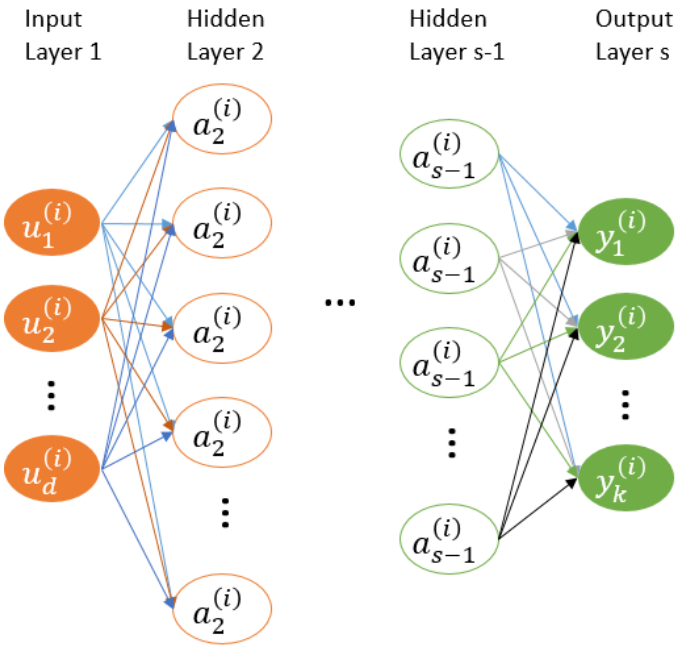

Figure 7. Multilayer perceptron network structure

For each user in the database charging records of d days are randomly picked to form the user charging record matrix $U \in R^{d \times m}$, the EV user number is denoted by m for consistency, and d is set up so that the feature length of each user is the same. User charging record matrix is transferred into the neuron network as input. The output of the neuron network is a vector representing EV user groups. In the neuron network, each mapping from layer s-1 to layer s follows the forward propagation rule:

$$a_s = g(\theta^{s-1} a_{s-1}) \tag{3.9}$$

Where g(x) is the activation function which chosen to be sigmoid. θ^{s-1} is the weight matrix for mapping from layer s-1 to s. By forward propagation, features in the input user charging record matrix are extracted by each hidden layers and user behaviors are classified in the output vector.

Backpropagation is used to train the neuron network. The output of user classification results is compared with labels from the clustering algorithm and labels from visualization. Errors are computed for the output layer. Errors associated with output layer are then used to back-calculate the error with its preceding layer. The calculation is back propagated in the way until the input layer. Errors associated with each layer are used to calculate the partial derivatives to perform gradient descent to minimize the cost function:

$$J(\theta) = -\frac{1}{u}\left[\sum_{i=1}^{u}\sum_{k}^{K} y_k^i \log\left(g\left(\theta a^i\right)\right) + \left(1 - y_k^i\right)\log\left(1 - g\left(\theta a^i\right)\right)\right]$$

$$+ \frac{\gamma}{2u}\sum_{s=1}^{s-1}\sum_{i=1}^{t_s}\sum_{j=1}^{t_{s+1}}\left(\theta_{ji}^s\right)^2 \qquad (3.10)$$

Where *s* denotes the layer index and t is the number of neurons in that particular layer. The iteration goes on until convergence criteria is satisfied. The hyper-parameters, i.e., the number of hidden layers and the number of neurons in each layer is selected by random search and cross-validation, which is performed by first defining search ranges for each hyper-parameter, then randomly select parameters from search pools to train the neural network. The best hyper-parameter combination is recorded.

3.4.3 EV User Model

From the user groups obtained by previous algorithms, we can generate the day-ahead predictive energy demand boundary. This demand boundary is used to construct the EV user model. We define there would be N EVs using charging stations within the network in the following day. Each EV has a charging/discharging rate $r_n(t)$ with $n \in N = [1, 2, \dots, N]$ at time slot $t \in T = [1, 2, \dots, T]$. T is the time span where the control can be performed.

The maximum charging rate and V2G rate of EVs made by different manufacturers are varied. We use $\overline{r_n}$ and $\underline{r_n}$ to denote maxithe mum charging rate and maximum V2G rate of EV n, respectively. V2G rate limit $\underline{r_n}$ is a negative value since the power flow is reversed. Thus, we have the bi-directional charging rate limits for each EV:

$$\underline{r_n} \leq r_n(t) \leq \overline{r_n}, \text{ for } n \in N \text{ and } t \in T \tag{3.11}$$

Within the control algorithm implementation interval, not all EVs are online in every time slot. When an EV is charging, the charging rate limits in (3.11) is effective. When an EV is not online, we set both the upper and lower bound of this EV charging rate to zero.

Energy consumption of each EV is denoted by E_n. It represents the energy demand of the particular EV during its stay in the parking facility. It is obvious that the summation of the products of EV charging rate and time interval equals to the total energy demand:

$$\sum_{T} r_n(t) \cdot \Delta t = E_n \tag{3.12}$$

where Δt is a constant since the control time span is evenly divided into T sections.

According to the Central Limit Theorem (CLT), when the sample number reach some large value, the distribution of sample will converge to the normal distribution. The availability time interval $[t_{arrival}, t_{departure}]$ of each EV can therefore be generated from clustering user groups using the mean and standard deviation. The energy consumption of EVs are then derived using the stay duration and the correlation in the user groups. We use a parameter $\beta_i, i \in [1, 2, \dots, l]$ to define the portions of each user group to all EV users and generate l charging rate boundaries from the l different user groups. The combined day-ahead EV user model is then:

$$R^{bound} = \sum_{l=1}^{l} \sum_{i=1}^{n} r_i^{bound} \beta_l \tag{3.13}$$

$$E^{total} = \sum_{l=1}^{l} \sum_{i=1}^{n} E_i \, \beta_l \tag{3.14}$$

3.4.4 Prediction Performance Analysis

EV user charging records collected by the smart charging infrastructure for the past four years are used as the dataset for testing the proposed prediction algorithm. K-fold cross-validation method is used to help train the neuron network and selected hyper-parameters. We divide the dataset into ten partitions, i.e., K=10. The descriptions dataset and partition setup are shown in Table I and Figure 8 respectively.

Table I. EV User Charging Records

	Training Set	Test Set
Number of Partitions	9	1
Number of Users	110	20
Number of Records	11000	2000
Number of Clusters	4	4

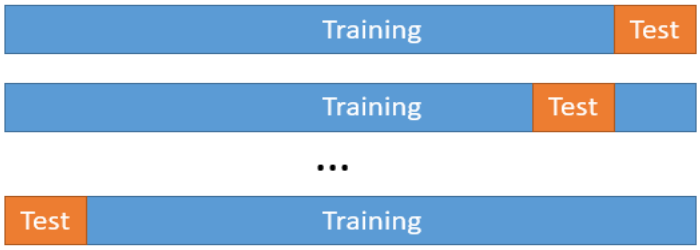

Figure 8. 10-fold cross-validation

The clustering algorithm processes the historical EV user data in our database and divides EV user behaviors into four groups, as shown in Figure 9. EV user behavior clusters. Three of the five features in the tuple are used for visualization with standard deviation normalized by the mean. User group labeled by green has highly predictable behavior. Their arrival and departure schedule are fixed at certain timestamps with little variance. Their energy consumption is linearly related to

stay duration with Pearson score close to 1. On the contrary user group label in black has an almost random traveling schedule, using them as resources to participate in charging scheduling is highly unreliable.

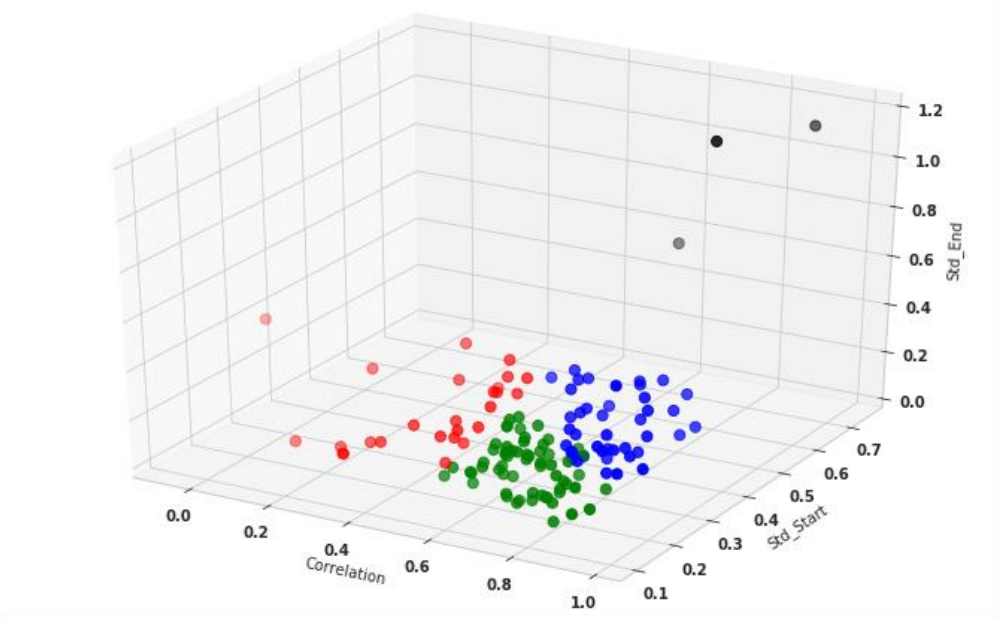

Figure 9. EV user behavior clusters

Multilayer perceptron neuron network is trained using collected EV user charging records and labels from both the clustering algorithm and data visualization-based hand-labeling. Cross-validation is used to determine the hidden layer number and neurons per layer. According to the grid search results, the optimal hidden layer number is 3 and neurons in each layer is 273, 212 and 169 respectively. By using the EV user model described in Section III part C, day-ahead EV user demand can be generated. The EV demand forecasting from clustering EV user model and from the multilayer perceptron EV user model are plotted in Figure 10. Day-ahead EV load demand from user models. It can be seen that the deviation between the two curves is negligible.

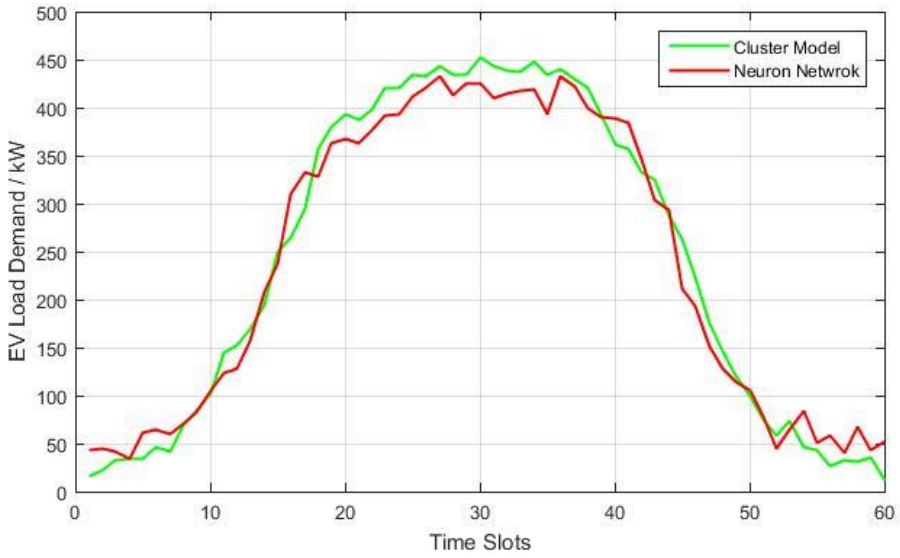

Figure 10. Day-ahead EV load demand from user models

More performance results are listed in Table II, which shows the neuron network classification accuracy with respect to the training set and test set. The neuron network model can achieve an average of 85% accuracy in the training set and around 78% in the test set. The EV load demand prediction is evaluated by Mean absolute percentage error (MAPE) [48]. It can be seen that the EV user model derived from multilayer perceptron is qualified for charging control scheduling with a tolerable error.

Table II. Multi-layer Perceptron User Model Performance Evaluation

Cross-Validation Case #	Classification Accuracy w.r.t Training Set	Classification Accuracy w.r.t Test Set	EV Load Demand MAPE
1	82%	78%	0.254
2	76%	72%	0.351
3	79%	74%	0.312
4	91%	82%	0.145
5	88%	84%	0.176
6	87%	73%	0.221
7	83%	72%	0.213
8	85%	75%	0.267

3.4.5 Conclusion

In this section, a data-driven method is introduced to model the EV user behavior based on EV user charging records collected in public charging facilities over four years. A novel approach which combines K-Means clustering and multilayer perceptron is developed and tested. The cross-validation experimental results and performance evaluation show that the proposed technique is capable of being used for various kinds of charging control scheduling. This method makes labeling dataset become an automatic process and eliminates the need to perform clustering whenever a new user joins in the charging network and once trained, can be used parallel with real-time control.

3.5 Latent Semantic Analysis and Mixture User Model

Latent Semantic Analysis (LSA) [49] is a topic modeling technique which has been successfully implemented in many text mining tasks. In this section, we adopt LSA to perform EV user behavior analysis and use it to process our historical charging records and generate a mixture model of EV users for EV charging scheduling. We name the modified algorithm Clustering-LSA (CLSA) [50].

3.5.1 Electric Vehicle User Classification

From the visualization of historical EV charging record, it can be observed that user behavior can be categorized into four groups. We choose arrival and departure time, energy consumption and their standard deviation as behavior features. From the historical charging records, we found that many EV users would connect their EV to the charging station at the time of parking and disconnect their EV from the charging station when they leave. Many charging sessions ended before the vehicle was physically disconnected from the charging station, due to the EV already fully charged. This also motivates us to design multiplexing charger which can connect to 4 EVs

at the same time. Some users also prefer to preset the amount of energy they need using our mobile App when they plug in their EVs. Since we have uncertainties of energy consumption, we treat energy consumed per session as one of the user behaviors to be investigated. Each behavior feature is divided into *l* intervals as shown in Figure 11.

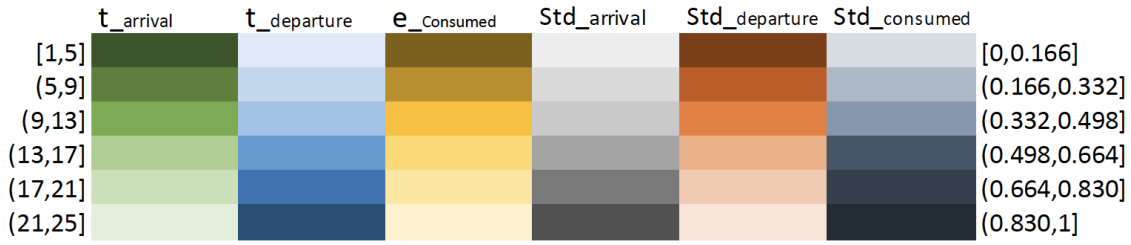

Figure 11. EV user behavior model features

Assuming there are *k* user behavior categories, each category is defined by a user behavior model $\theta_i, i \in [1, k]$. Each term in the user behavior model is a vector with *l* elements representing the conditional probability of different intervals within that feature.

$$\theta_i := \left(P(\bar{t}_{arr}|\theta_i), P(\bar{t}_{dept}|\theta_i), P(\bar{e}_{consumed}|\theta_i), P(\sigma_{arr}|\theta_i), P(\sigma_{dept}|\theta_i), P(\sigma_{consumed}|\theta_i)\right) \quad (3.15)$$

The conventional implementation of LSA assumes that each sample can belong to multiple topics. In CLSA, we enforce that each user can belong to only one user behavior model. This restriction makes the likelihood function slightly different. In our control center database, we extract a collection of m user records $X = \{u_1, \ldots, u_m\}$. The mixture of k user behavior model will be

$$\Theta = \{\{\theta_i\}; \{P(\theta_i)\}\}, i \in [1, k] \quad (3.16)$$

Where θ_i represents the features of user behavior model i and $P(\theta_i)$ indicates the popularity of user behavior model *i*. For each user u_m in the dataset *X*, CLSA scans through all charging records and count the number of times one record falls in certain feature intervals as c(*f*, *u*), where u denotes current user and $f \in F$ is the feature interval. The likelihood function for one user can be derived. We maximize the likelihood over all users to estimate our user behavior models:

$$\Theta^* = \underset{\Theta}{argmax} \prod_{m=1}^{N} P(u_m|\Theta) = \underset{\Theta}{argmax} \prod_{m=1}^{N} \sum_{i=1}^{k} \left[P(\theta_i) \prod_{F} P(f|\theta_i)^{c(f,u_m)} \right] \quad (3.17)$$

Expectation Maximization (EM) algorithm [51] is then used to perform the maximum likelihood estimation. First, we initialized all parameter in the user behavior model randomly. Then expectation and maximization steps are performed in iteration until convergence:

	Algorithm 3.2: EM for CLSA
1	Initialize all model parameters randomly
2	Introduce latent variable $L_u \in [1, k]$ represent the
3	model can be used to generate user u
4	**While** $\|\mathrm{P}^{n+1}(X\|\Theta) - \mathrm{P}^{n}(X\|\Theta)\| \geq \varepsilon$:
5	**E-Step:** infer behavior model to users
6	$\mathrm{P}^{n}(L_u = i\|u) \propto \mathrm{P}^{n}(\theta_i) \prod_F \mathrm{P}(f\|\theta_i)^{\mathrm{c}(f,u_m)}$
7	s.t. $\sum_{i=1}^{k} \mathrm{P}^{n}(L_u = i\|u) = 1$
8	**M-Step:** recalculate all parameters
9	$\mathrm{P}^{n+1}(\theta_i) \propto \sum_{m=1}^{N} \mathrm{P}^{n}\left(L_{u_m} = i\|u_m\right)$
10	$\mathrm{P}^{n+1}(f\|\theta_i) \propto \sum_{m=1}^{N} \mathrm{c}(f, u_m) \mathrm{P}^{n}\left(L_{u_m} =$
11	$i\|u_m\right)$
12	s.t. $\sum_{i=1}^{k} \mathrm{P}^{n+1}(\theta_i) = 1$
	$\sum_{f \in F} \mathrm{P}^{n+1}(f\|\theta_i) = 1$
	End

After EM algorithm converged, EV users are clustered into four behavior models. Figure 12 shows the feature distribution of behavior model No. 1 as an example. It has highly predictable behavior. Their arrival and departure schedule are fixed at specific timestamps with little variance. Their energy consumptions are relatively high on average due to longer stay duration. Other behavior model feature distributions also convey characteristics of different categories of users. Behavior

model No. 4 has an almost random traveling schedule, using them as resources to participate DR program is unreliable. Model No. 2 and 3 are intermediate users with behavior between predictive and random.

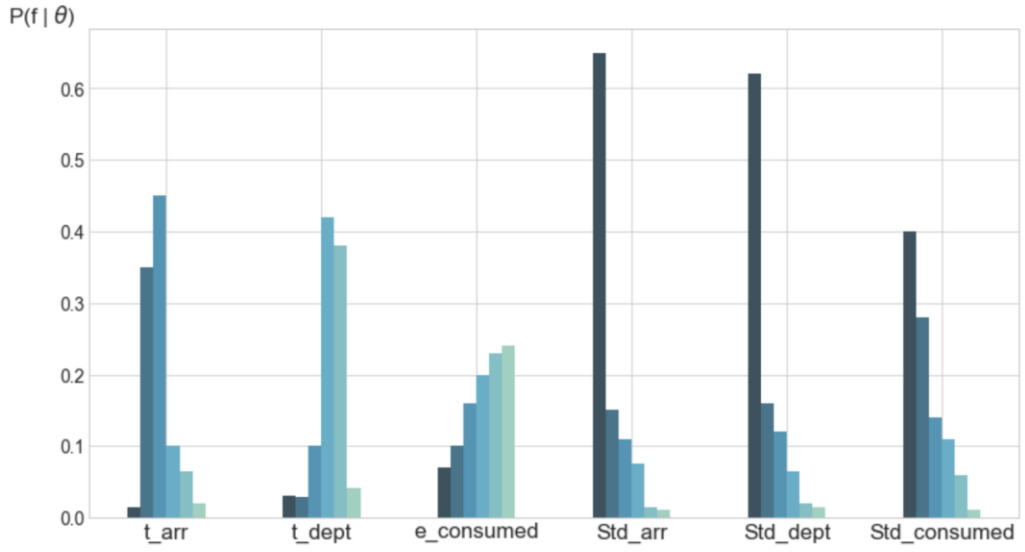

Figure 12. Estimated feature distribution of one behavior model after CLSA

3.5.2 Electric Vehicle User Mixture Model

From the user behavior model obtained by CLSA, we can generate the day-ahead predictive energy demand boundary. This demand boundary is used to construct mixture user model. We define there would be *N* EVs using charging stations within the network in the following day. Each EV has a charging/discharging rate $r_n(t)$ with $n \in N = [1, 2, \dots, N]$ at time slot $t \in T = [1, 2, \dots, T]$. T is the time span where the DR control will be performed. The entire EV bi-directional charging profile $R^{N \times T}$ can be written as:

$$R = \begin{bmatrix} r_1(1) & \cdots & r_1(T) \\ \vdots & \ddots & \vdots \\ r_N(1) & \cdots & r_N(T) \end{bmatrix} \tag{3.18}$$

The maximum charging rate and discharging rate of EVs made by different manufacturers are varied. We use $\overline{r_n}$ and $\underline{r_n}$ to denote the maximum charging rate and maximum discharging rate of

EV n, respectively. discharging rate limit $\underline{r_n}$ is a negative value since the power flow is reversed. Thus, we have the bi-directional charging rate limits for each EV:

$$\underline{r_n} \leq r_n(t) \leq \overline{r_n}, \text{for } n \in N \text{ and } t \in T \tag{3.19}$$

Within the control algorithm implementation interval, not all EVs are online in every time slot. When an EV is charging, the charging rate limits in (3.19) is effective. When an EV is not online, we set both the upper and lower bound of this EV charging rate to zero:

$$\overline{r_n} = \begin{cases} r_n^{max}, t \in [t_{arrival}, t_{departure}] \\ 0, \qquad\qquad otherwise \end{cases} \tag{3.20}$$

$$\underline{r_n} = \begin{cases} 0, \qquad\qquad otherwise \\ r_n^{min}, t \in [t_{arrival}, t_{departure}] \end{cases} \tag{3.21}$$

Equation (3.20) and (3.21) correspond to the situation that when an EV is in plug-in status, its charging rate can range from maximum V2G discharging rate to maximum charging rate. When the EV is disconnected from the charging station, all rates are zero which prevents any DR scheduling assigned to this EV.

Energy consumption of each EV is denoted by E_n. It represents the energy demand of the particular EV during its stay in the parking facility. It is obvious that the summation of the products of EV charging rate and time interval equals to the total energy demand, as in equation (3.12). According to level 2 charging standard (SAE-J1772, etc.), SoC is not able to be obtained from EV by the charging station. Most of the EV manufacturers does not provide any interface to allow third-party to retrieve the SoC information from their battery management system. So that we use our mixture user model to estimate EV user SoC demand.

According to the estimated results from CLSA, we know the density distribution of each behavior model and the probabilities of parameters within each model. The availability time interval $[t_{arrival}, t_{departure}]$ and energy consumption E_n of each EV can therefore be generated from these

behavior model. We use $P(\theta_i), i \in [1, k]$ to denote the density distribution of each behavior model and generate *k* charging rate boundaries from the *k* different behavior models. The combined day-ahead EV user mixture model is then:

$$R^{bound} = \sum_{i=1}^{k} P(\theta_i) R_i^{bound} \tag{3.23}$$

$$E^{bound} = \sum_{i=1}^{k} P(\theta_i) E_i \tag{3.24}$$

Figure 13 shows a comparison between the EV energy demand boundaries generated by mixture user model and completely uniform random behavior, where *N*=300 and the charging rate of each EV is set around 30kW, $P(\theta_i)$ is defined based on the density estimations of each behavior model in the results of the CLSA algorithm discussed previously, and *k* is 4 in our case. Although the total energy consumptions which are the area under the curve are similar, energy demands and availabilities across controllable time span are different.

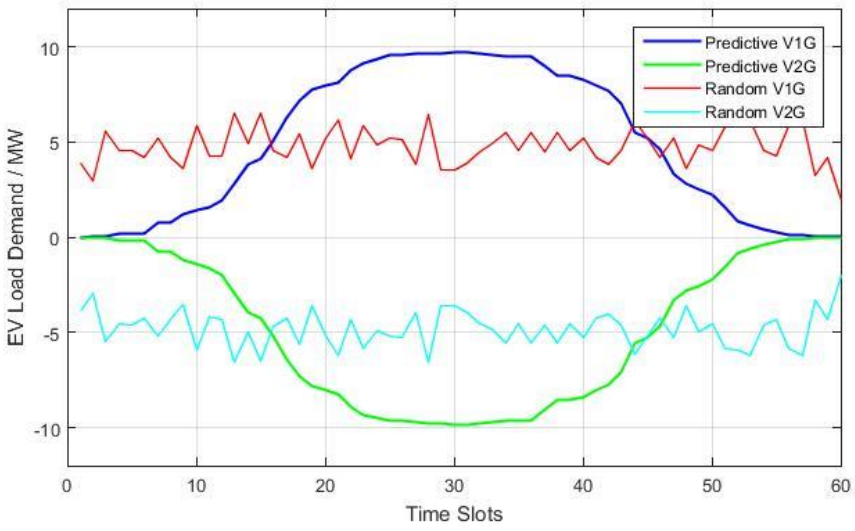

Figure 13. Predictive day-ahead EV energy demand boundary

3.6 V2G User Participation Time Analysis

An EV needs to be connected to the charging station and have sufficient energy in its battery in order to participate in V2G program to provide different kinds of grid services. Based on the EV user charging session data we have collected, we discuss possible ways for our current EV users to join V2G program and help to support the power grid. Figure 14 shows the number of overlapping charging sessions through a day across all charging stations operating in the UCLA campus parking lots. We show the record for 3 different days in colored lines.

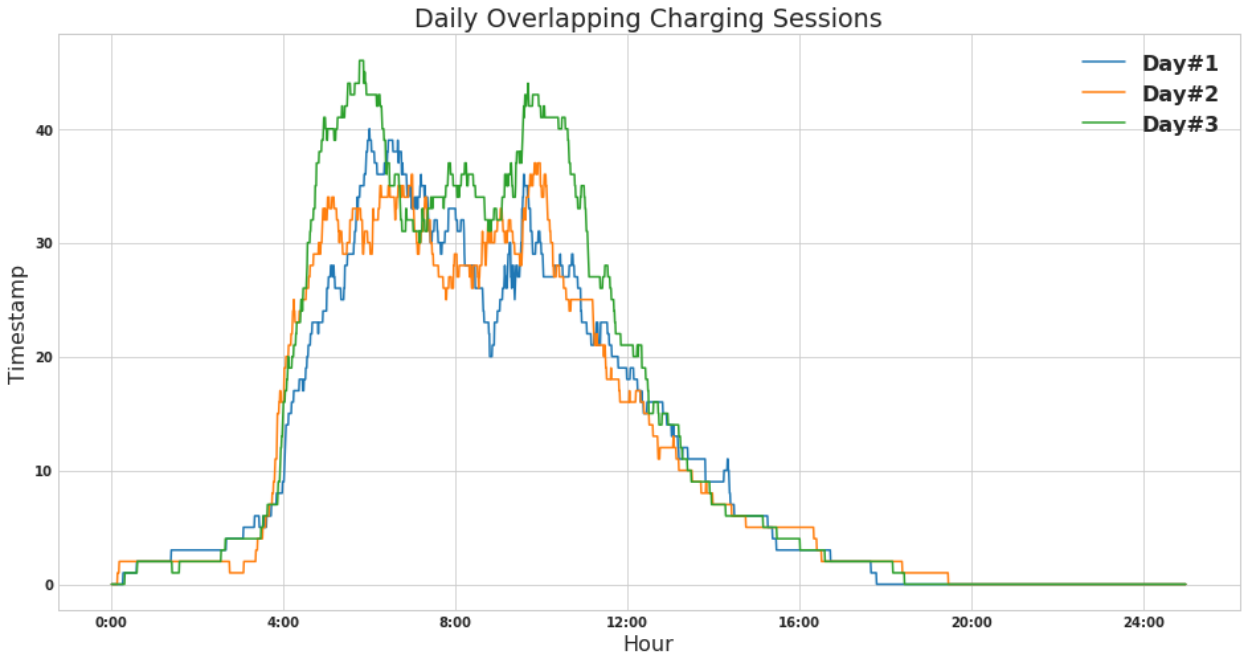

Figure 14. Overlapping charging sessions through a day

It can be seen in Figure 14 that a lot of EV users arrive early in the morning to avoid Los Angeles morning traffic. There is charging station usage peak at around 6 am. Another charging station usage peak appears at around 10:30 am, which may represent the people who choose to come to work after the morning traffic. We can find EV user gradually leave the charging station in the afternoon.

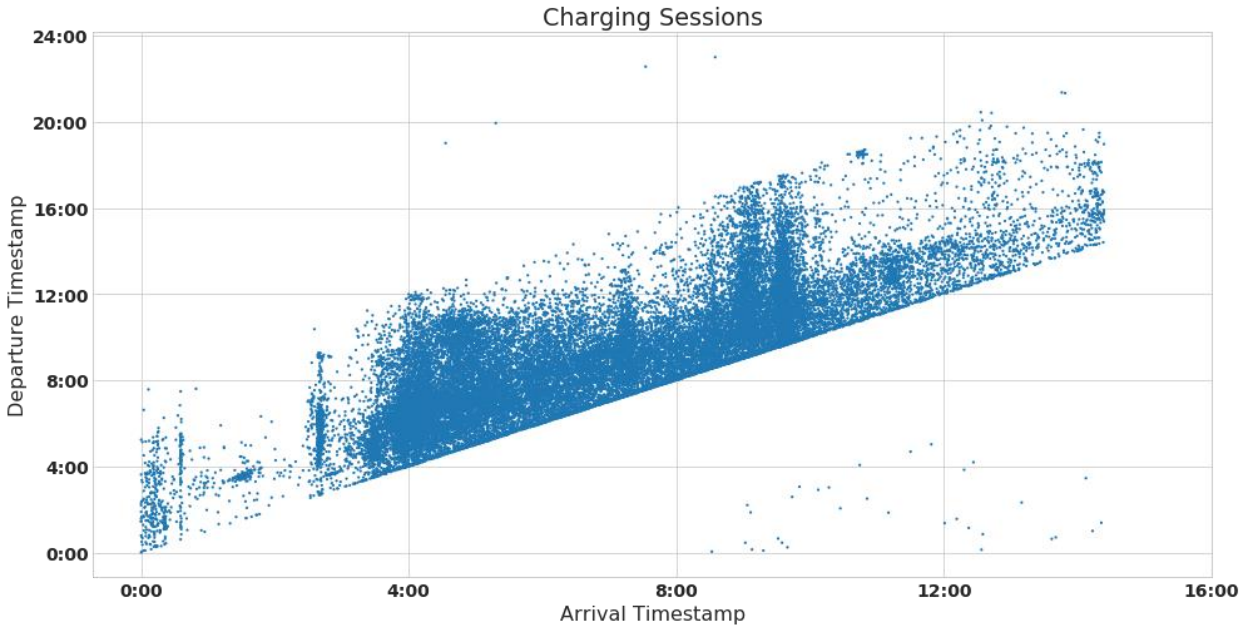

Figure 15. Charging sessions density map

Figure 15 shows the density map of charging sessions. In this figure we can find that EV users can be divided into two groups. Those who arrive early in the morning before 8 am mostly leave before noon time. EV users who arrive later than 8 am usually leave in the afternoon. We propose that it is possible to make the early morning group of EV user to participate in V2G program to support the morning power usage peak, since their EV batteries have been already charged for a certain amount of energy at the time of power grid morning demand peak, which occurs at around 8 am, as shown in Figure 16. The late morning group of EV user can provide V2G support to the power grid through the day time and the afternoon demand peak.

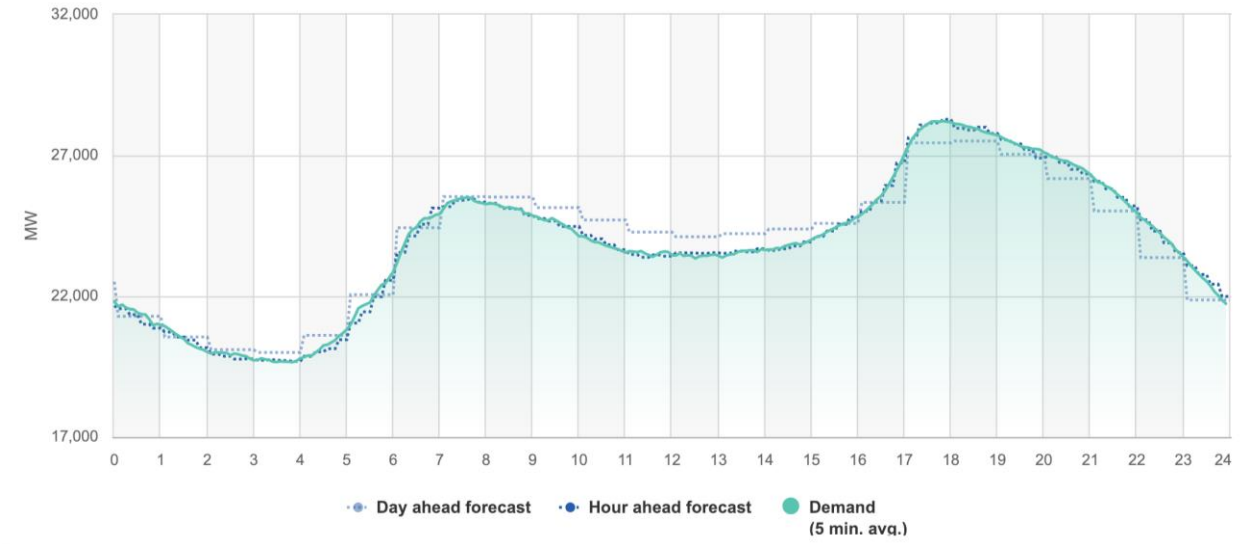

Figure 16. California power grid demand trend through a day [52]

3.7 Summary

In this chapter, we discussed three methods to analyze and predict electric user behavior. The general statistical method is simple but reliable on electric vehicle drivers whose traveling pattern is more regular and predictable. The clustering method is useful to distinguish different group and apply different energy management policy over them. The mixture user model is a generative model. It is proposed for generating a large amount of electric vehicle user samples using Monte Carlo which can be used in large scale simulation of optimal EV charging scheduling.

4 Chapter IV. Optimal Electric Vehicle Charging Scheduling

4.1 Introduction

With the proposed EV user behavior models at hand, we are able to make predictions and generate vivid artificial EV user charging session data for optimal charging scheduling algorithm design. This chapter will cover several smart EV charging scheduling algorithms proposed in this dissertation.

4.2 Predictive EV Scheduling Algorithm

With the emerging issues related to large scale EV integration, the following technical challenges can be identified: 1) energy price not considered in real-world implementations; 2) current multiplexing and power-sharing constraints in real-world implementations. Thus, we propose a predictive control paradigm that can perform on-line energy management for electric vehicles on the UCLA campus. The proposed EV charging algorithm is inspired by Model Predictive Control (MPC), which optimizes the energy management schedules adaptively by considering both the current and the predicted system states. In this scheduling algorithm, the estimated charging session parameters, including start time, duration and the energy demand can be estimated by users' historical records using methods covered in the previous chapter. Thus, the estimated stay duration and energy consumption are assumed to be known [53].The problem formulation is illustrated as follows:

4.2.1 EVSE Model

The EVSE being modeled may have multiple power sources, indicating that constraint for each charging outlet and the total power consumption for each power source should be applied:

$$0 \le r_n^k(t) \le r_k^{max} \cdot \eta, \ \ \forall \in \left[t_n^s, t_n^s + \hat{d}_n\right] \tag{4.1}$$

where $r_n^k(t)$ denotes the charging rate at time t for vehicle n connected to power source k. r_k^{max} denotes the limitation of power source k and η is the safety coefficient for each power source. t_n^s is the actual start time for vehicle n. For each power source k in the EVSE, we have:

$$0 \le \sum_{n \in N_k} r_n^k(t) \le r_k^{max} \cdot \eta, \qquad \forall t \in [t_n^s, t_n^s + \hat{d}_n] \tag{4.1}$$

where N_k denotes active charging sessions for power source k.

4.2.2 Battery Model

It is assumed in this scenario that the scheduling algorithm should allocate more energy than the demand value from each user. Thus, within the time range from start time t_n^s to leave time, denoted by $t_n^s + \hat{d}_n$, The actual energy consumption e_n should satisfy the following constraints:

$$e_n(t) = e_n(t - \Delta t) + r_n(t) \cdot \Delta t, \ \ \forall t \in [t_n^s, t_n^s + \hat{d}_n] \tag{4.2}$$

$$e_B > e_n\left(t_n^s + \hat{d}_n\right) \ge \hat{e}_n \tag{4.3}$$

4.2.3 Virtual Load Constraint

The uncertainties of user behaviors may render the pre-computed schedules in-valid when the power supply for each EVSE is limited. For instance, it is highly possible that the limited power source fails to deliver enough energy to satisfy the unexpected new charging demand and made the previous schedules infeasible. A method with virtual load constraint is proposed to limit the power supply for a future time window, ranging from $t + \Delta H$ to the end time T. Thus, more energy consumption will be shifted forward to $[t, t + \Delta H]$ to avoid infeasible solutions.

$$\sum_{\tau=t+\Delta H}^{\tau=T} \sum_{n \in N_k} r_n^k(\tau) < \lambda \cdot \sum_{\tau=t+\Delta H}^{\tau=T} r_k^{max}, \forall \tau \in [t+\Delta H, T] \quad (4.4)$$

This constraint is to limit the total power consumption for a specific EVSE by virtual load constraint coefficient λ.

4.2.4 Predictive Control

We formulate EV charging scheduling problem as a predictive control problem, which can be adapted to a variety of objectives, as long as the problem can be formulated as a convex optimization. Schedule optimization is performing every time step with the updated estimations of session parameters, including stay duration $\hat{d}_n$, and the energy demand $\hat{e}_n$ for each connected vehicle. Meanwhile, forecast solar generations are also considered in the model to compensate the EV charging load with the solar generations. The optimization objective is formulated follows:

$$\min_{r_n^k(\tau)} \sum_{\tau=t}^{\tau=T} P(\tau) \cdot max(\sum_{k \in K} \sum_{n \in N_k} r_n^k(\tau) - PV(\tau)), 0) \quad (4.5)$$

$s.t.\ (4.1) - (4.5)$

τ denotes the time when the optimization is initiated and T is the maximum time step for the scheduling horizon. $PV(\tau)$ is the forecast solar generation at time τ from the installed panels. $P(\tau)$ is the electricity price at time τ. At each time step, the optimal energy allocation schedules for all remaining steps are computed, however, only the first element from the computed schedule will be implemented, according to the paradigm of predictive control. Therefore, the algorithm will compare the output of solar generation and the aggregated EV demand and decide the best charging strategies, considering the energy prices at each time step. The whole procedure is illustrated in Algorithm 4.1 as follows:

Algorithm 4.1: Predictive EV Scheduling Algorithm

Generate price data

Retrieve forecast solar data

$\tau = t_0$

Do

For each power source k

Retrieve estimated session parameters;

Solve problem (4.6) ,subject to $(4.1) - (4.5)$;

If solution infeasible

Relax constraint (4.5) and set $\eta = 1$ in equation (4.1) and (4.2);

End

For each vehicle $n \in N_k$

Implement $r_n^k(\tau)$;

End

End

$\tau = \tau + \Delta t$

While $\tau \leq T$

4.2.5 Result and Discussion

The scheduling results by the algorithm 4.1 are shown in Figure 17, where the blue dotted curve is the original power consumption curve at this EVSE, and the red one denotes the optimized curved with minimal operational cost. The EV load peak in the early morning has been shifted to the later afternoon, due to 1) lower energy prices; 2) more solar PV generation. Interestingly, the EV power consumption actually follows the solar PV generation curve in the early morning when the generation value is comparatively lower. In each time step, the algorithm tends to evaluate the availability of solar energy to compensate the EV charging load. Without solar integration, the

original operational cost can be calculated as $7.02 while the new value by the predictive algorithm with solar integration is reduced to $3.01.

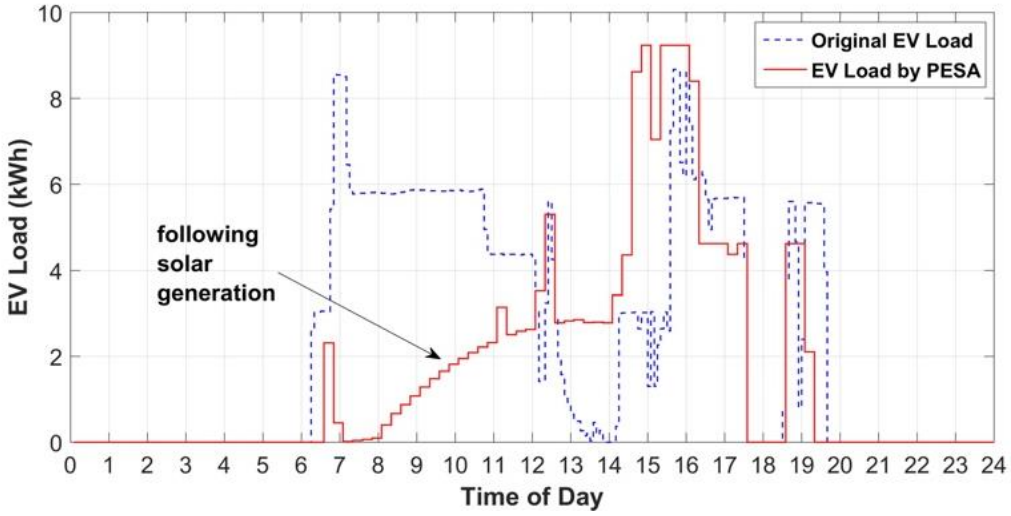

Figure 17. EV Load Scheduling Results

4.3 Distributed Optimal EV Charging Scheduling

Significant studies have been conducted to incorporate bi-directional power flow and grid services support from EVs, upgrading traditional dumb consumptions to controllable distributed energy resources (DERs) [8]. If one can combine EV charging and V2G service into a smart bi-directional charging strategy, EVs will become valuable assets to the power grid. However, distributed EV batteries must be aggregated on a large scale so that they can participate in the wholesale market to provide grid services. Such aggregation would require huge computational resources if it's performed by the traditional centralized control scheme. Smart bi-directional charging scheduling depends highly on EV driver behaviors. To facilitate the integration of EVs as DERs into the power grid, the following challenges should be addressed: 1) A bi-directional charging algorithm incorporates both smart charging and V2G service; 2) A decentralized control strategy which lowers computational cost with large-scale integration; Previous research has been done to patricianly

solve EV charging coordination problems. But none of them provides a comprehensive solution which addresses all the three aforementioned challenges based on real-world implementation. Gan et al. [18] use optimal control to allocate EV charging time and energy optimally, but the algorithm requires users to provide charging schedule, which may degrade customers' satisfaction by requiring inputs frequently. Wang et al. [28] provide two algorithms to aggregate EV charging with consideration of random user behavior model and renewable generation in the scheduling. Authors in [54] have developed smart charging strategy according to time-of-use (TOU) price from day-ahead predictions. These smart charging strategies can flatten the grid load profile by valley-filling but cannot do much during peak load. V2G can be performed to relieve the stress on the grid [26][36]. Methods for increasing smart charging and V2G scalability and interoperability are developed in [36], but large scale implementation strategy based on real-world data is rarely investigated.

We proposed a smart bi-directional charging scheduling algorithm that incorporates EV smart charging and V2G service for large scale implementation. An aggregated control center sends a control signal to all EV charging stations in its network. Each distributed charging station performs an optimization locally according to this control signal to update the EV bi-directional charging strategy and reports it to control center. Subsequently, the control center collects strategies from networked charging stations and then updates its original control signal. The iteration ends when the algorithm converges to an optimal charging strategy for all plug-in EVs in the network. Computational cost is shared by all charging stations which greatly lowers computing burden and time in the control center. In each iteration, the information update is asynchronous; there is no need for all charging stations to update their strategy. There is no strict rule for the control center to update control signal every iteration. These features are critical for a successful large-scale

implementation where prompt updating is impractical. User charging behavior and preference prediction are performed by mean estimation and linear regression using real-world EV usage data. Predicted EV user charging schedule and energy demand serve as input parameters for the proposed algorithm.

It is assumed that the utility or the microgrid operator can always provide a day-ahead prediction of the load profile in its service area or within the microgrid. Such prediction is defined as baseload in the scope of this algorithm. Control center of the smart charging infrastructure can retrieve baseload data from the service provider, i.e., utility or microgrid operator as input for its optimal bi-directional charging control algorithm. Control center makes a day-ahead prediction of user charging behaviors to obtain predicted charging start time, end time, energy demand for each EV users within its control network. Predicted data and control signal are then distributed to each networked EVSE for bi-directional charging profile optimization. Updated individual EV charging profiles are returned to the control center for control signal updating in a new iteration. All charging stations will interact with the centralized control center and cooperatively solve the optimization problem in a distributed fashion. The goal of the algorithm is to schedule the time and allocate the power flow for charging and V2G such that the load profile in the utility service area or within the microgrid are flattened and stabilized while all EV user demands are satisfied. The related research work can also be found in [33].

4.3.1 Constraints and Objective

The day-ahead predicted baseload is denoted as $B(t)$ with $t \in T$. $T = [1, 2, \dots T]$ is the time slot set where the algorithm will be performed, and *t* is the specific time slot. We define there are N EVs in total within the network. Each EV has a charging/discharging rate $p_n(t)$ with $n \in N = [1, 2, \dots N]$ at time slot *t*. Proposed algorithm aims to flatten the total load profile:

$$L(t) = \left(B(t) + \sum_{n=1}^{N} p_n(t) \right)^2 \tag{4.7}$$

To flatten the load curve, the summation of equation (4.7) over time must be minimized. It is easy to find out that a flat load curve $L(t)$ would be the optimal for this optimization problem.

The charging rate and V2G capacity of EVs made by different manufacturers are varied. We use $\overline{p_n}$ and $\overline{d_n}$ to denote the maximum charging rate and maximum V2G capacity of EV *n*, respectively. V2G discharging rate $\overline{d_n}$ is a negative value since the power flow is reversed. Thus, we have:

$$\overline{d_n} \le p_n(t) \le \overline{p_n} \tag{4.8}$$

In our proposed control scheme, $\overline{p_n}$ and $\overline{d_n}$ are regarded as upper bound and lower bound for the controllable charging rate. During the time between EV plug-in EVSE, t_{start}^{pred} and EV leave, t_{end}^{pred}, the charging rate can be set continuously within upper and lower bound, and it will be 0 otherwise:

$$\overline{p_n} = \begin{cases} p_n^{\max}, t \in \left[t_{start}^{pred}, t_{end}^{pred} \right] \\ 0, \quad \text{otherwise} \end{cases} \tag{4.9}$$

$$\overline{d_n} = \begin{cases} d_n^{\max}, t \in \left[t_{start}^{pred}, t_{end}^{pred} \right] \\ 0, \quad \text{otherwise} \end{cases} \tag{4.10}$$

Equation (4.9) and (4.10) are corresponding to the situation that when an EV is plugged in, its charging rate can range from maximum V2G discharging rate to maximum charging rate. When EV leaves the EVSE, all rates are zero which means there is no existing charging or discharging.

Energy consumptions of each EV are predicted using the aforementioned user behavior model. The predicted value E_n^{pred} represents the energy demand of the particular EV user during his or her

charging sessions. The summation of the product of EV charging rate and time interval equals to the energy demand:

$$\sum_{T} p_n(t)\Delta T = E_n^{pred} \tag{4.11}$$

where ΔT is constant since each time slot is a constant time value.

The control signal from the control center is the derivative of total load profile we intent on flattening multiplied by a tuning parameter:

$$c^i(t) = \frac{1}{\lambda N}\left(B(t) + \sum_{n=1}^{N} p_n(t) \right) \tag{4.12}$$

Where i represents the iteration number in the algorithm and λ denotes the control parameter. The algorithm converges when the difference between control signals in consecutive iterations smaller than a convergence criterion, i.e. $\left\| c^{i+1} - c^i \right\| \le \varepsilon$, where ε is a positive real number small enough to be the convergence criteria. It is not necessary to update control signal in every iteration for an optimal convergence.

Subsequently, each EVSE carries out an optimization of its plug-in EV locally, responding to the control signal. The objective is as follows:

$$\sum_{t=1}^{T} c^i(t) p_n^{i+1}(t) + \frac{1}{2}\left\| p_n^{i+1}(t) - p_n^i(t) \right\|^2 \tag{4.13}$$

Minimizing $\sum c(t)p(t)$ equals to move the first order derivative of (4.7) toward 0, which solves the optimization problem of minimizing the summation of equation (4.7) to flatten the load curve. The second term in equation (4.13) is a regularization to limit the charging rate variation to be

small. By minimizing this objective equation (4.13), EVSE will obtain an updated EV charging profile $p_n^{i+1}(t)$ and report it to the control center. Again, it is not necessary to report the updated charging profile to the control center in every iteration.

4.3.2 Optimal Distributed Bi-directional Charging Algorithm

The distributed algorithm to optimize EV charging energy allocation and scheduling are presented as following:

Algorithm 4.2: Optimal Distributed Bi-directional Charging

Obtain Day-ahead prediction of baseload data

Perform Day-ahead prediction of EV user behavior and energy demand

Initialize all EV charging profiles $p_n^0(t) = 0$, $n = 1,2,\ldots N$

Pick control parameter λ

Initialize control signal $c^0(t) = \frac{1}{\lambda N}\left(B(t) + \sum_N p_n^0(t)\right)$

While $\left\|c^{i+1} - c^i\right\| \geq \varepsilon$ **:**

  For each n EVSE in the network, $n = 1,2,\ldots N$

    Minimize (4.13)

    Subject to (4.8), (4.9), (4.10), (4.11)

  End

  If i mod u == 0

    Update control signal

  End

  If i mod v == 0

    Update charging profile;

  End

In algorithm 4.2, constant values u and v are used to emulate delay updating of the control signal and charging profile in real-world large-scale implementation. When the algorithm converges, the total load profile will be effectively flattened. Figure 18 shows the schematic of the proposed algorithm. Each EVSE performs optimization in its embedded system, which greatly lowers the computational burden of the control center.

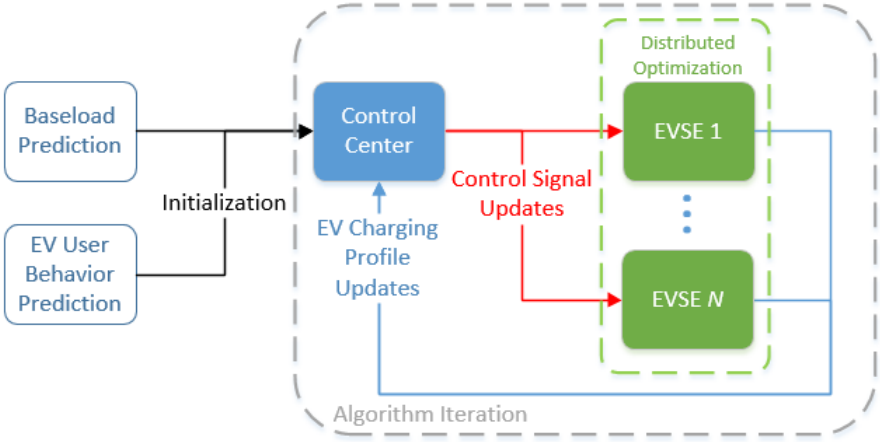

Figure 18. Schematic of the proposed charging control algorithm

4.3.3 Result and Discussion

UCLA Engineering IV building load profile on September 20, 2016 from 7 am to 7 pm is chosen as the baseload for proposed algorithm implementation. The 12 hours is divided into 60 time slots. The historical data in the database of UCLA SMERC smart EV charging system, including 30 EV drivers on UCLA campus, are extracted for user behavior modeling and prediction. There are power usage peak and valley in the load profile corresponding to the operation of some heavy energy consuming devices in the building. The fleet of 30 EVs will provide grid service to flatten the load under the control of the proposed algorithm. Such grid service can be possibly scaled up to support a microgrid or a utility service area with enough EV participation.

Before the implementation of the proposed algorithm, EV user behavior predictions are made based on the random selected historical charging record data from 30 EV users in the past three years. Charging start time, end time and energy demand are predicted for September 20, 2016 and then incorporated in the proposed algorithm. The algorithm converges to an optimal bi-directional charging strategy which effectively flattens the original baseload by peak shaving and valley filling, as shown in Figure 19.

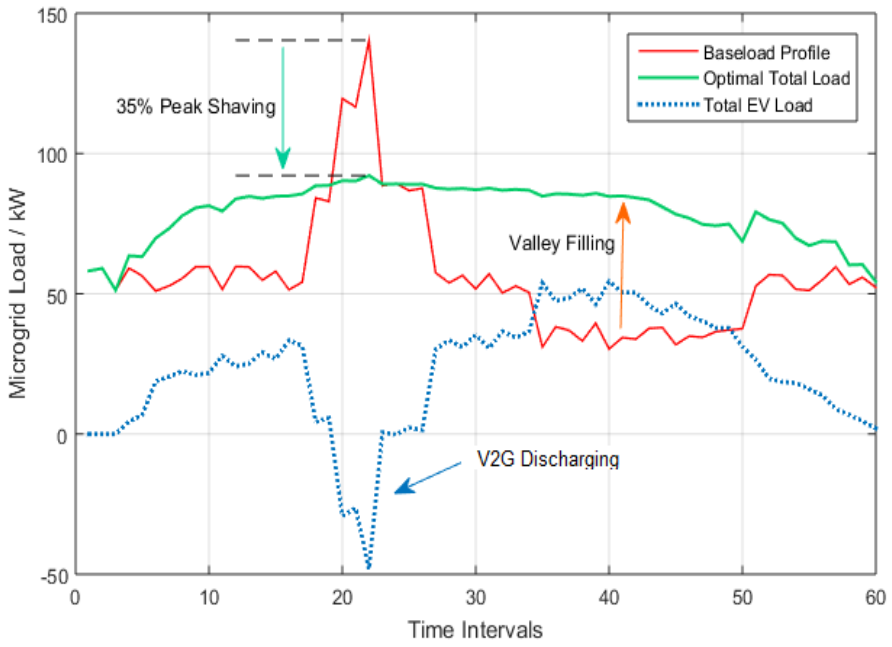

Figure 19. Baseload profile flattened by the proposed algorithm

In Figure 19 it can be seen that the baseload has power consumption peak from time slot No. 17 to time slot No. 27, and power usage valley from time slot No. 33 to No. 50. The optimal distributed bi-directional charging algorithm precisely tunes charging rate of each EV in the network, changing from high speed charging to discharging according to the trend of baseload profile. Almost all EVs are performing V2G discharging at baseload peak time, making the peak power consumption drops 35%, from 140 kW down to 90 kW. The Optimal total load curve, which is the combination of baseload and EV load profile, has been perfectly flattened. The optimal distributed bi-directional

charging algorithm shows its capability to integrate EVs into the power grid as DERs, providing various grid service to benefits the power grid.

The values of convergence criteria ε during algorithm iteration are plotted in Figure 20. It should be noticed zero is not an indication of convergence since control signal, and EV charging profiles are not updated in every iteration. The algorithm converges at around 32 iterations since ε becomes small enough. This asynchronous feature of the proposed algorithm shows its potential for large scale implementations where information transmission and updates are usually delayed.

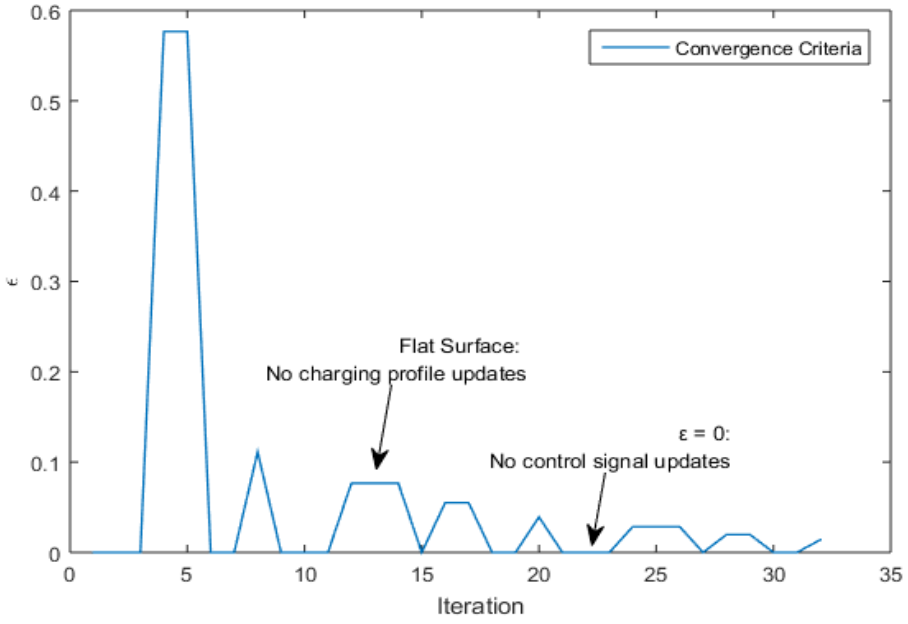

Figure 20. Convergence criteria in iterations

4.3.4 Conclusion

In this section, an optimal distributed bi-directional charging control algorithm is developed. The contributions of this algorithm can be summarized as 1) A distributed optimal bi-directional charging control algorithm implementation with real-world data; 2) Integrate EVs as DERs into the power grid to flatten load curves, correct voltage deviation, conduct voltage regulation, etc. It is implemented with real-world load profile and EV charging data with the result showing its

capability of integrating EVs into the power grid as DERs to perform grid service, flatten the load profile and stabilize the power grid. The algorithm has distributed and asynchronous features which greatly low the computational cost and ideal for large scale implementation.

4.4 Real-Time Charging Scheduling with Distribution Grid Implementation

While charging station becomes more and more accessible with the number of installation increases rapidly, bi-directional charging stations can discharge the electric energy in the EV battery back into the power grid, and provide ancillary service [55]. According to the SAE CCS and IEC15118 standards, the power limit of fast charging is up to 120kW, which can be equal to the total load of 30 to 40 households [56]. The gigantic energy consumption of EV chargers and V2G put challenges but also opportunities over the modern power grid. Although un-coordinated charging activities can cause voltage fluctuation, and power loss increase, especially when the number of charging sessions exceeds a certain level [36], coordinated smart charging can not only resolve the impact to the power grid but also turn EV charging demand to an opportunity to flatten the profile of the system [29].

Moreover, charging stations with SAE CCS or CHAdeMO [57] protocol have V2G capability, which transforms EVs from simple dumb loads to distributed energy resources (DER), providing grid services such as voltage regulation and peak load shaving [33]. With the fast increasing EV possession rate, EVs will become a great asset of the power grid as DERs in the near future, under the condition of being coordinated by well-designed control strategy [58]. However, controlling thousands or millions of EV charging load in power grid is challenging, which comes into the following aspects: 1) EV charging scheduling is heavily constrained by user availability; 2) Huge computational resources are required for optimal charging scheduling of a large number of EVs,

especially in real-time; 3) The impact of smart bi-directional charging at transmission level is still a question.

Recent years we have seen a lot of research works proposing optimal controllers for coordinated charging of EVs and prediction methods for EV user behavior. Gan et al. [7] used a distributed protocol to allocate EV charging time and energy optimally. Wang et al. developed an EV charging scheduling algorithm with minimum cost as its objective [29]. Authors in [26] analyzed the influence of bi-directional EV charging to a building and provided related control strategy. Kernel density estimation method is used in [31] to deal with the uncertainty of EV user behavior based on real-world data. Wang et al. [32] utilized sample average approximation to predict EV schedule and performed a simulation with 10 EVs within a distribution grid. In [59] the author targeted the charging demand of EV in commercial parking lots and determined charging strategy using two-stage approximate dynamic programming. Charging coordination for Valley filling and cost reduction was studied in [60] and found out global optimum is not possible. However, it is hard to find one among them which provides a comprehensive solution addressing all the challenges above based on real-world implementation requirements.

Accordingly, a decentralized control paradigm is introduced in this section and applied to a power grid to investigate the influence of large scale EV charging load on the electrical grid. In our proposed decentralized algorithm, the computational burden of optimal charging scheduling is distributed among the networked charging station equipped with an embedded controller, which significantly reduces the computational resources required at control center compared to traditional centralized control. Western System Coordinating Council (WSCC) 9-bus model is used as the simulation test case, where the grid load profiles are generated by scaling up real-world microgrid load profile collected by Cornell University [61], and they are assigned to the three PQ (load) buses

of the grid model. EV user charging record data obtained from UCLA SMERC smart charging infrastructure are used to model the EV charging load. The proposed decentralized charging control algorithm is performed over all EVs connected to the 9-bus system to flatten the total load profile in real time. Load flow analysis is carried out for worst cases before and after the implementation of the proposed algorithm to evaluate the effectiveness of the proposed algorithm in improving voltage profile and reducing line current and generation cost. Specifically, the worst cases are defined as when a large amount of EVs are plugged-in during peak hours while the grid baseload is also high. The related research work can also be found in [62].

4.4.1 System Simulation Configuration

To investigate the impact of large scale EV charging activities on the distribution grid, scaled-up EV load profiles are generated based on the collected EV charging historical data. EV loads are then applied to the WSCC 9-bus system model [63] for load flow analysis and algorithm performance evaluation.

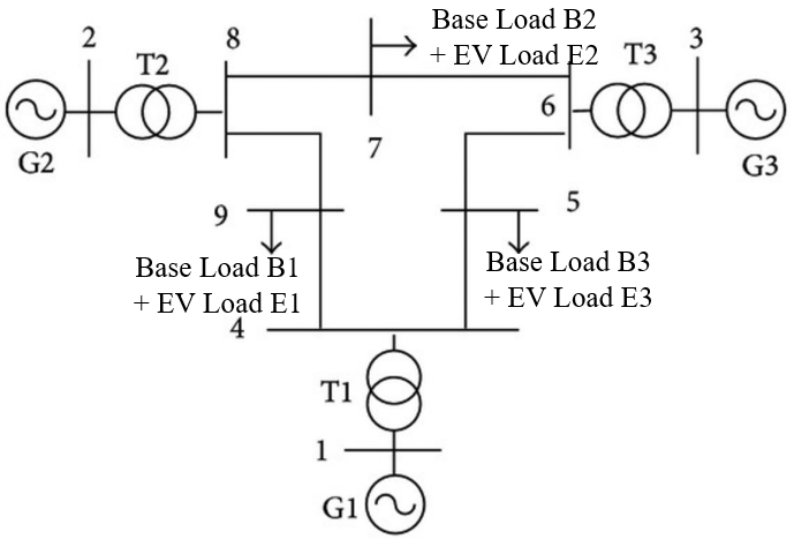

Figure 21. Single-line diagram of the distribution grid model

Three different base load and EV load profiles are applied to PQ bus 5, 7 and 9, as shown in Figure 21. The voltage level of these load buses is 230kV, and each of them represents a substation for a city region. Baseload for each load bus is the total power consumption for the city without EVs, and EV load is the total power demand from all EV charging activities in that city. Three generators are connected to the grid through buses 1, 2, and 3 where bus#1 is the swing bus. Hourly microgrid power consumption historical data is retrieved from Cornell University energy management portal and scaled up to the level of a small city with around 50,000 population, which is comparable to the cities in Los Angeles area such as Culver City and Beverly Hills. The obtained load profiles are applied to the three load buses in the test case, namely bus#5, bus#7 and bus#9 as the base load. Prediction of EV user daily traveling schedule and energy demand is carried out based on the historical data in UCLA SMERC smart charging infrastructure collected over past four years, and it is utilized as constraints in the proposed algorithm. The number of EVs assigned to each load bus is 15,000, consisting of 35% light-duty vehicles market shares as predicted for the year of 2040 in [64]. The simulation is carried out for different scenarios including 1) the worst case, where almost all EVs arrive and start charging at full capacity during peak demand hours; 2) the optimal case, where proposed algorithm shifts EV load and schedules V2G discharging sessions based on grid load condition and EV user behavior.

4.4.2 Load Flow Analysis

Load flow analysis is conducted before and after the implementation of the proposed algorithm to evaluate its contribution to the power quality. The relation between the current injected to each bus and the voltage of each bus of the grid model described in section II is shown by:

$$\begin{bmatrix} \bar{I}_1 \\ \vdots \\ \bar{I}_M \end{bmatrix} = \begin{bmatrix} \bar{Y}_{11} & \cdots & \bar{Y}_{1M} \\ \vdots & \ddots & \vdots \\ \bar{Y}_{M1} & \cdots & \bar{Y}_{MM} \end{bmatrix} \tag{4.14}$$

Or

$$\bar{I}_i = \sum_{j \in I} \bar{Y}_{ij} \bar{V}_j \tag{4.15}$$

Where I_i is the injected current at bus *i*, and V_j is the voltage at bus *j*. Y_{ij} is the admittance of the line connecting bus *i* to bus *j*, and $I = \{j | \bar{Y}_{ij} \neq 0\}$. The complex power injected to bus *i* is obtained by:

$$\bar{S}_i = P_i + jQ_i = \bar{V}_i \bar{I}^*{}_i = \bar{V}_i \sum_{j \in I} \bar{Y}_{ij} \bar{V}_j \tag{4.16}$$

Where P and Q are active power and reactive power, respectively. The bus voltage and line admittance can be written as:

$$\bar{V}_i = V_i e^{j\theta_i} \tag{4.17}$$

$$\bar{Y}_{ij} = Y_{ij} e^{j\alpha_{ij}} \tag{4.18}$$

By replacing (4.17) and (4.18) in (4.16). Basic load flow equations are obtained.

$$\begin{cases} P_i = V_i \sum_{j \in I} Y_{ij} \cos(\theta_i - \theta_j - \alpha_{ij}) \\ Q_i = V_i \sum_{j \in I} V_j Y_{ij} \sin(\theta_i - \theta_j - \alpha_{ij}) \end{cases} \tag{4.19}$$

Newton-Raphson method is used to solve the above nodal power equations and determine the voltage at each load bus. By comparing the voltage drop during the time interval where a large amount of EV charging activities taking places and the situation after charging control algorithm is applied, the impact of EV charging to the power grid and the effectiveness of scheduling algorithm can be evaluated.

4.4.3 Real-time Implementation of decentralized EV Charging Control Algorithm

We assume that the utility or grid operator can always predict the day-ahead load profile in the region where their services are provided. Control center of the smart EV charging infrastructure

retrieves the predicted base load as input data for the charging control algorithm. EVs can either absorb energy from the power grid to feed their battery or discharge the energy in their battery to feed the power grid. The decision of charging or discharging is determined by proposed charging control algorithm based on the condition of current grid load and the EV driver demand. Control center learns EV user behavior from historical charging data to predict parking schedule and possible state of charging (SoC) request, which is defined as the constraints in the optimal charging control algorithm. The decentralized control paradigm works as follows: 1) control center initializes and broadcasts control signal to all charging stations in its network; 2) each charging station updates its charging profile by performing an optimization only regarding to the EVs plugged in; 3) control center collects updated charging profiles from all charging stations, updates its control signal and broadcast it out again; 4) control algorithm is run in real-time with preset time interval and updated information. The goal of the proposed algorithm is to optimally schedule the bi-directional charging activities such that the load profile can be flattened, and load flow and voltage drop are kept in allowable range while all EV drivers' demands are fulfilled.

The prediction of baseload is denoted as $B^{\tau}(t)$ with $t \in T$ and $\tau \in H$. $T = [1, 2, \ldots T]$ is the time slot set where the algorithm will be performed, and *t* is the specific time slot. *H* is the time horizon where the charging control is moving forward. We assume that there are N EVs supplied by the smart charging system. Each EV has a charging and discharging rate $p_n^{\tau}(t)$ with $n \in N = [1, 2, \ldots N]$ at time slot *t* and time horizon τ. The aim of the proposed algorithm is to flatten the total load profile as described in (4.7), but with extra time horizon parameter:

$$L^{\tau}(t) = \left(B^{\tau}(t) + \sum_{n=1}^{N} p_n^{\tau}(t) \right)^2 \tag{4.20}$$

The charging rate and energy demand constraints are identical from equation (4.8) to (4.11). The control signal from the control center is the first order derivative of total load profile which we intend on flattening, multiplied by a tuning parameter [7]:

$$c^i(t) = \frac{1}{\lambda N}\left(B^\tau(t) + \sum_{n=1}^{N} p_n^\tau(t) \right) \tag{4.21}$$

Subsequently, by receiving the control signal, each charging station performs an optimization taking into consideration only the plugged-in EVs. The objective cost function is expressed as:

$$\sum_{t=1}^{T} c^i(t) p_n^{\tau^{i+1}}(t) + \frac{1}{2}\left\| p_n^{\tau^{i+1}}(t) - p_n^{\tau^i}(t) \right\|^2 \tag{4.22}$$

By minimizing the cost function, the charging station will update EV charging profile $p_n^{\tau^{i+1}}(t)$ and report it to the control center.

The distributed algorithm to optimize EV charging energy allocation and scheduling is presented as follows:

Algorithm 4.3: Real-Time Decentralized Bi-directional Charging

Initialize all EV charging profiles $p_n^0(t) = 0$, $n = 1,2,\ldots N$

Pick control parameter λ

Initialize control signal $c^0(t) = \frac{1}{\lambda N}\left(B(t) + \sum_N p_n^0(t)\right)$

While $\tau < H$

Updates prediction of baseload data

Updates prediction of EV user behavior and energy demand

While $\left\|c^{i+1} - c^i\right\| \geq \varepsilon$ **:**

For each n EVSE in the network, $n = 1,2,\ldots,N$

Minimize (4.22)

Subject to (4.8), (4.9), (4.10), (4.11)

End

$\tau = \tau + 1$

End

In the above algorithm, the control time horizon can be set to 24 hours, representing a day. The algorithm will update its control strategy every hour, i.e., $\tau \in [1,2,\ldots 24]$. When the algorithm converges, the total load profile defined in (5) will be effectively flattened. Figure 22 shows the schematic of the proposed algorithm running in real time. Each charging station performs optimization by its own embedded controller, which greatly lowers the computational burden of the control center.

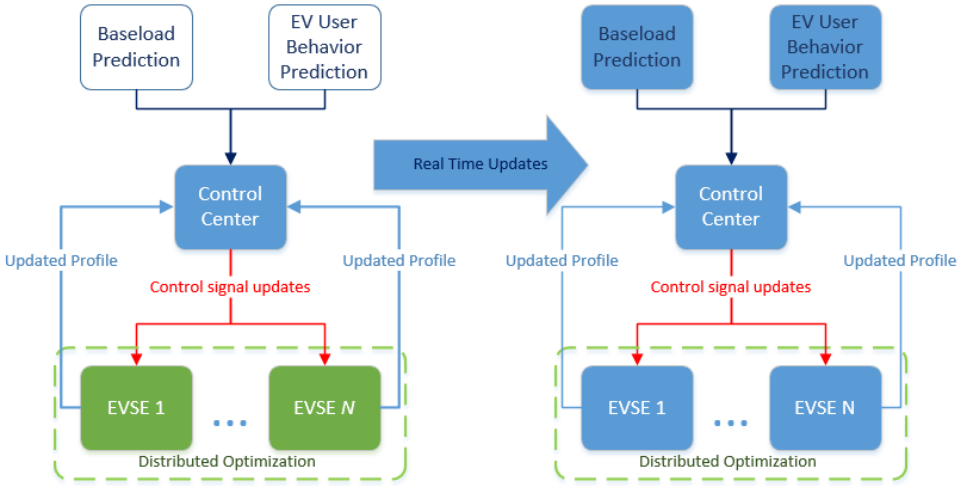

Figure 22. Schematic of the proposed charging control algorithm

4.4.4 Result and Analysis

In the condition that there is not any control or coordination over the EV charging stations, and all charging activities start immediately after EV is plugged in, total load can be too high for the power grid to stay in stable status.

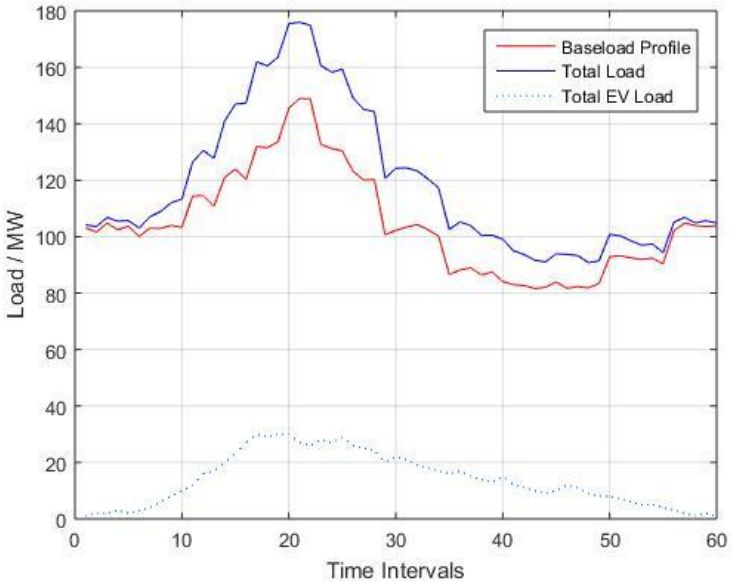

Figure 23. EV load peak overlap with grid peak demand

It can be seen in Figure 23 that when no charging control is implemented, EV charging peak overlaps with gird peak demand (time interval~20), which is not favorable to the power quality and power grid stability.

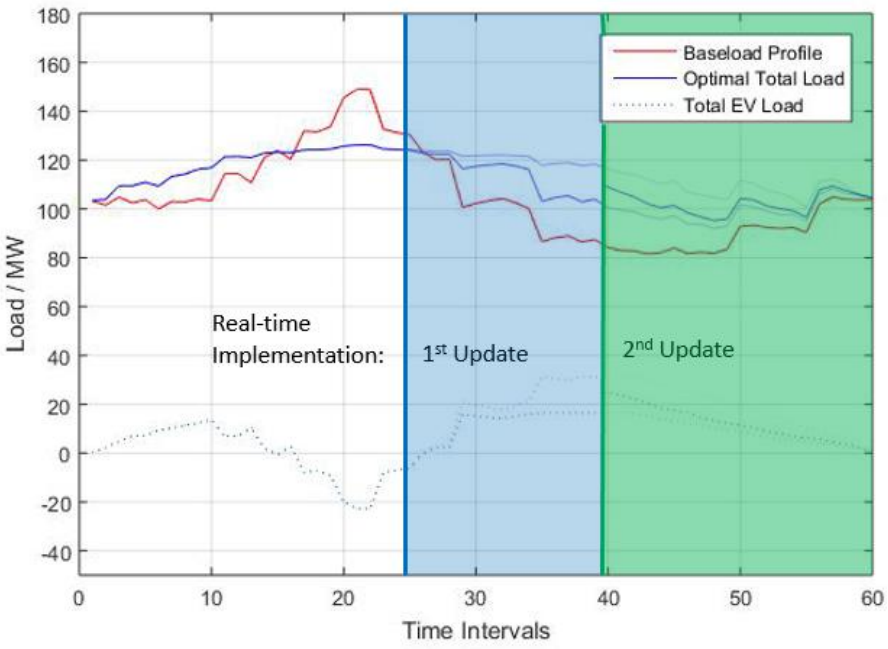

Figure 24. Optimal load profile with real-time update

Figure 24 shows the optimal total load profile, which is a combination of a grid base load and total EV charging load, and it is much flatter and smoother than the base load is. By comparing Figure 24 with un-coordinating charging scenario in Figure 23, it can be seen that the proposed charging algorithm arranges as much V2G discharging sessions as during grid peak hours, and then coordinates full capacity charging activity over its control network during low load demand time intervals from 35 to 55. Another look into the total load profile reveals that the peak load after algorithm implementation is 125MW, while it is 180MW in the worst case without coordination. Real-time implementation is demonstrated in the shaded areas of Figure 24, control center updates the EV user behavior prediction at time slot 25, according to current EV number and demand in the network, resulting in a new charging schedule and load profile. At time slot 40, second update is

made. New load profiles after updates are deeper blue color curves while previous profiles are shown in lighter color.

Load flow analysis results are shown in Table III, Table IV and Table V. It can be seen that the total line current is reduced by 40% after charging control is implemented. The power drawn from the swing bus is significantly decreased which results in generation cost reduction. Moreover, we observed 2% improvement of bus voltage profile over the grid while unacceptable voltage drops are seen at some of the buses, such as bus#5 and bus#9, before EV charging coordination. Therefore, it can be said that EV charging load coordination for load flattening yields overall system operation improvement.

Table III. Line Current Before / After Coordination

Line in the Grid		**Pre-control Line Current (A)**	**Post-control Line Current (A)**
From	**to**		
Bus 4	Bus 9	420.8	130.7
Bus 4	Bus 5	420.4	153.7
Bus 8	Bus 7	358.9	232.8
Bus 8	Bus 9	58.7	167.7
Bus 6	Bus 7	185.0	75.8
Bus 6	Bus 5	41.4	132.5

Table IV. Power Generation Before / After Coordination

Generator No.	**Pre-control Generation Complex Power (MW)**	**Post-control Generation Complex Power (MW)**
G1 (Swing)	329.66 + j112.01	105 + j48.75
G2	163 + j39.09	163 + j11.35
G3	85 + j25.03	85 – j2.25

Table V. Bus Voltage Profile Before / After Coordination

Bus #	**4**	**5**	**6**	**7**	**8**	**9**
Before	0.995	0.955	1.012	0.987	1.006	0.954
After	1.015	0.987	1.027	1.015	1.028	0.980

4.4.5 Conclusion

In this section, a real-time optimal decentralized EV charging algorithm is proposed and implemented. The contribution of this section can be summarized as 1) carrying out a large-scale simulation to evaluate the impact of large number bi-directional charging activities to the power grid; 2) running load flow analysis to evaluate the performance of the proposed algorithm in worst cases scenarios. A 30% peak load shaving and more than 2% of voltage drop reduction are observed when the EV charging load is controlled by the proposed algorithm. Also, the total line current of the power grid is reduced by 40% which significantly decreases the power loss.

4.5 Summary

Decentralized and real-time optimal charging scheduling algorithm with distributed grid implementation are designed and their performances are tested and validated with large scale simulation and real-world EV charging infrastructure and user dataset. Simulation results show that the proposed methods have great potential and favorable features for real-time optimal charging control. They can provide significant power grid stabilizing and computational burden relieving capability. Their performances are also tested on large-scale transmission and distribution grid implementation.

5 Chapter V. Vehicle Grid Integration and Demand Response

5.1 VGI for DR in public parking structure

5.1.1 Overview

The ideal VGI implementation scenario for the DR program is in the public parking structure, where a large amount of EV charging activities are taking place [65]. However, there are a lot of factors making it challenging to coordinate EV charging activities in public parking facilities at different locations to participate in the DR program as DERs while satisfying energy requests from EV drivers. Due to the availability and energy demand of each EV is highly stochastic and cannot be easily predicted, it is impossible to include EVs into wholesale energy market directly [59][66]. The performance of predictive control charging scheduling is affected by prediction accuracy and always cannot meet the optimal solution subject to the uncertainties. Real-time implementation of charging control can alleviate the negative effect of prediction error by implementing strategies like moving horizon but require extensive computation resources thus not scalable [67]. Previous research work has attempted to tackle this problem from multiple angles. For instance, data-driven approaches are utilized to determine the optimal EV operations, leveraging the monitoring data on existing EV-grid demonstration projects. In [32], stochastic programming approaches are applied on a sample test feeder to determine the optimal battery operations considering the uncertainties of driver behaviors.

Regarding controlling individual EV, the Kernel Density Estimator (KDE) is proposed in [31] to generate optimal personalized charging plans by dynamically estimating the stay duration and energy consumption values based on the historical charging sessions. As an implementable solution, an event-based control strategy is proposed in [28], where only pre-defined events can trigger the computation, i.e., re-optimization. V2G grid service is integrated into smart charging

for microgrid and building energy management in [68]. Model predictive control (MPC) for real-time control is investigated in [5] to handle the uncertainty of renewable generation and EV charging activities. Authors in [62] propose a real-time charging scheme to coordinate EV charging with grid load flow analysis and simulation. In [69] a stochastic programming approach is applied to analyze the impact of both price-based DR and incentive-based DR to EV users. Deep learning approach is introduced to do traffic and driver behavior modeling in [70]. The benefit of smart EV charging at non-residential locations is investigated in [71] but only TOU price is used and V2G is not considered. The ensemble learning method is applied in [72] to analyze the temporal behavior of load demand. K-Nearest Neighbors (kNN) is modified in [73] with novel similarity measure and Lazy-learning Algorithm. A data mining model which combined clustering, correlation and regression is proposed in [74] to characterize EV users based on data from 255 charging stations in the UK. However, to the best of authors' knowledge, none of them provides a comprehensive solution to address the implementation of optimal EV charging strategy which can resolve the challenges raised in user behavior analysis and optimal scheduling to use EV as DER. And most of the previous works are concluded with pre-defined assumption and simulation results, without knowledge of real-world implementation.

Two EV charging schemes are proposed to minimize the energy cost, by water -filling algorithm and two-stage optimizations in both wholesale and retail markets with predictive mixture user model. Historical EV charging records collected from all public charging stations within UCLA Smart Grid Energy Research Center (SMERC) smart charging infrastructure network is utilized for user behavioral analysis. A variation of latent semantic analysis is used to categorize all EV users into four behavioral models based on their statistical feature. A predictive user mixture model is generated from these behavioral models to define the day-ahead EV availability and energy

demand boundary. By obtaining the forecast baseload profile and day-ahead wholesale energy rate, an optimization is performed to minimize EV charging cost with the constraints from the user model. The first-stage optimization gives us the optimal EV load profile for the day-ahead wholesale energy market. On the next day, a real-time distributed optimization is performed over all charging station in the network with EV user and load information updating at each pre-defined time step. The second stage optimization provides real-time control over all online EVs in the system to follow the optimal load profile generated by the first-stage optimization, accommodating the DR requirement. In addition, the proposed water filling algorithm takes predicted user model and baseload as input and performs real-time control online over all charging stations within the network in a distributed paradigm. It is a lightweight fast converging algorithm without interior point methods thus can be used as an alternative solution for real-time charging scheduling. Simulations using real-world grid load and EV charging data under use cases with a different mixture of user groups are conducted and evaluated. The proposed smart charging scheme is implemented in the SMERC charging network to assess its performance. The related research work can also be found in [50].

5.1.2 Day-ahead EV Charging Scheme

Utility and independent system operator (ISO) use day-ahead wholesale energy price to incentivize a large number of consumers to participate in the DR program by planning their energy usage accordingly. During peak load, the electricity rate will be much higher than low demand time. But overall the wholesale price is much lower than TOU or other retail rates. The utility and ISO will also provide day-ahead power demand forecasting [75]. From a microgrid management operator's view, it is favorable to reduce consumption as much as possible during peak-time with highest energy price. In the first stage optimization, we use the day-ahead wholesale energy price as

guidance to generate the day-ahead EV charging scheme for the next day DR program. The objective of this optimization is to minimize the total cost of all charging activities through the controllable period:

$$\sum_{T}\left(B(t)+\sum_{N}\left(r_n(t)\right)\right)\cdot\pi(t) \tag{5.1}$$

Where $B(t)$ is the baseload at each time slot and $\pi(t)$ is the wholesale energy price at each time slot. The optimization will use the EV user model described in chapter III as constraints and generate optimal total EV load profile which will be used in the real-time control to be performed in the following day. For V2G incentives, we assume the energy price for purchasing energy for charging are the same as the prices for selling energy back to the grid via V2G services. The first stage optimization algorithm is generalized in algorithm 5.1:

	Algorithm 5.1: First Stage Wholesale Rate Optimization
1	Obtain day-ahead wholesale energy price from utility or ISO
2	Obtain day-ahead grid base load from utility or ISO
3	Minimize (5.1)
4	Subject to
5	(4.8), (4.9), (4.10), (4.11)

By making a summation of the result optimal charging rates of all online EVs at each time slot and overlapping with baseload forecasting, a total optimal load profile $L(t)$ is obtained:

$$L(t)=\sum_{N}r_n(t)+B(t) \tag{5.2}$$

5.1.3 Real-time Decentralized Electric Vehicle Charging Control

The aim of real-time EV charging control is to ensure the real-time load profile following the optimal profile in (5.2) exactly, by making adjustments to conditions different from user model. We use the following function to represent the gap between real-time and planned profile:

$$G(t) = \left(\hat{B}(t) + \sum_{N} \hat{r}_n(t) - L(t) \right)^2 \tag{5.3}$$

Where the hat represents real-time value. A variation of the derivative of this gap equation will be used as the objective function to be minimized. The real-time EV charging control is a decentralized algorithm which intended to protect the privacy of each EV driver and execute the control command in an asynchronous manner. In the decentralized control paradigm, control signals are distributed to each networked charging station for bi-directional charging profile optimization. Charging stations only carry out the optimization regarding the EV connected to them. Updated individual EV charging profiles are returned to the control center for updating the control signal in a new iteration. All charging stations will interact with the centralized control center and cooperatively solve the optimization problem in a distributed fashion. The conceptual control signal issued by the control center is the first derivative of (5.3) with tuning parameter γ, and γ is the Lipschitz constant. The smaller γ is, the easier the algorithm converges:

$$c^i(t) = \frac{1}{\gamma \widehat{N}} \left(\hat{B}(t) + \sum_{\widehat{N}} \hat{r}_n(t) - L(t) \right) \tag{5.4}$$

where i denotes the iteration steps number and $\widehat{N}$ is the number of EVs currently online. We can imagine the control signal $c^i(t)$ as price, so that we minimize the first term to reduce the charging cost. The second term in (15) is for regularization, so that charging rate will change in a smooth manner. By minimizing the objective equation, each charging station will obtain an updated EV

charging profile $\hat{r}_n^{i+1}(t)$ and report it back to the control center. The iteration stops when the difference between control signals in consecutive iterations smaller than a convergence criterion, i.e. $\left\|c^{i+1} - c^i\right\| \leq \varepsilon$, where ε is an arbitrary small positive real number. The proposed decentralized algorithm has an asynchronous feature that it is not necessary to update control signal in every iteration for an optimal convergence. Subsequently, each charging station carries out an optimization of its plug-in EV locally, using the control signal as input. The objective is as following:

$$\sum_T c^i(t)\hat{r}_n^{i+1}(t) + \frac{1}{\rho}\left\|\hat{r}_n^{i+1}(t) - \hat{r}_n^i(t)\right\|^2 \tag{5.5}$$

By minimizing the objective equation, each charging station will obtain an updated EV charging profile $\hat{r}_n^{i+1}(t)$ and report it back to the control center. Again, it is not necessary to report the updated charging profile to the control center in every iteration.

The decentralized EV charging control algorithm is summarized in Algorithm 5.2 as follows:

	Algorithm 5.2: Decentralized Bi-directional Charging Control
1	Obtain day-ahead optimal load profile from the first stage
2	Collect current EV status over the whole network
3	Initialize all EV charging profiles $\hat{r}_n^0(t) = r_n(t)$, n = 1,2,…N
4	Pick tuning parameter γ
5	Pick $l2$ regularization parameter ρ
6	Initialize control signal $c^0(t) = \frac{1}{\gamma \hat{N}}\left(\hat{B}(t) + \sum_{\hat{N}} \hat{r}_n^0(t) - L(t)\right)$
7	
8	**While:** $\left\|c^{i+1} - c^i\right\| \geq \varepsilon$
9	**For** EV #n in the network, n = 1,2,…N
10	Minimize (5.5)
11	Subject to
12	(4.8), (4.9), (4.10) with real-time value
13	And
14	$\sum_T r_n(t) \cdot \Delta t \geq E_n$
15	**End**
16	Update EV charging profile
17	Update control signal
	End

Here we make a relaxation of the constraint in (4.11), allowing charging energy more than demand to reach the optima where equality constraint may not be feasible. In each time slot within the whole controllable period, control center and charging stations will collect and update information of current online EV status and grid load, then perform the optimization to adjust the EV charging scheme in the following future time slots. The whole EV charging control schematic is shown in Figure 25below.

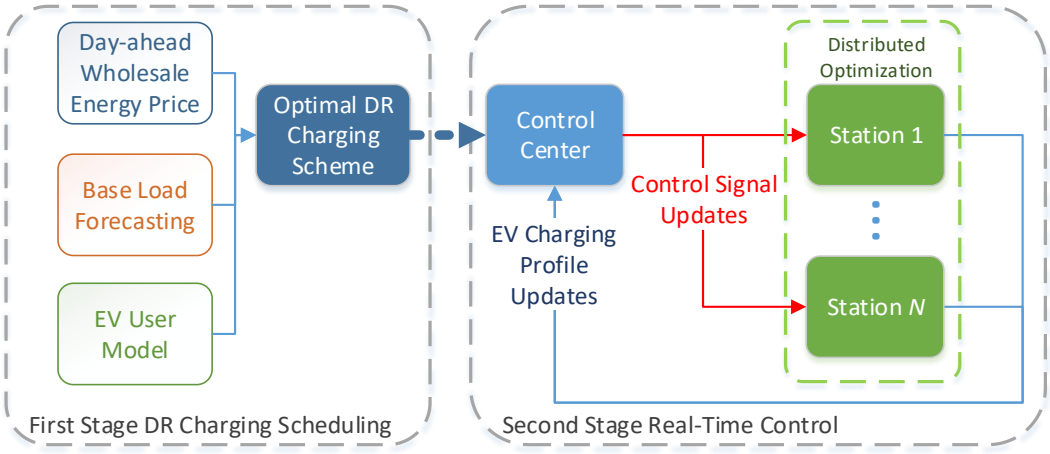

Figure 25. Schematic of the proposed charging control algorithm

5.1.4 Real-time Decentralized Electric Vehicle Charging Control II

The second charging scheduling solution utilizes the idea of the water filling algorithm from information theory for optimal power allocation [76]. In this research, the algorithm is modified for EV charging scheduling, performing real-time valley filling and peak shaving to accommodate DR program.

At every time slot we assume there is an optimal total load level where the scheduling algorithm tries to reach, we define it as a control signal $p^i(t)$:

$$p^i(t) = \frac{1}{N}\left(\sum_N \hat{r}_n^i(t) + \hat{B}(t)\right) \tag{5.6}$$

Which represents the average of optimal total load or ideal water level at time slot t. Control signal must satisfy the following constraint:

$$\begin{cases} \min\limits_t \left(\hat{r}_n^{min}(t) + \widehat{B_n}(t)\right) \le p^i(t) \\ \max\limits_t \left(\hat{r}_n^{max}(t) + \widehat{B_n}(t)\right) \ge p^i(t) \end{cases} \tag{5.7}$$

And the sum of charging rates must satisfy the energy demand constraint in (4.11). Based on (5.6) (5.7) the upper and lower bound of control signal feasible space of EV n can be derived as:

$$l_n = \min_t \left(p^i(t) - \hat{r}_n^i(t) + \hat{r}_n^{min}(t) \right) \tag{5.8}$$

$$u_n = \max_t \left(p^i(t) - \hat{r}_n^i(t) + \hat{r}_n^{max}(t) \right) \tag{5.9}$$

We can use the bisection method to search in this space set up by (5.8) (5.9) to find control signal $p^{i+1}(t)$ which can make the charging rate profile satisfies or very close to the energy demand defined in (5.7). The term $p^i(t) - \hat{r}_n^i(t)$ equals to a fraction of the baseload. After obtained the target control signal, the charging schedule can be updated using:

$$\hat{r}_n^{i+1}(t) = \hat{r}_n^i(t) - p^i(t) + p^{i+1}(t) \tag{5.10}$$

Equation (5.10) can also be interpreted as the change of charging rate. The value is determined by the difference between the load level $p(t)$ in previous and current iteration. When the control signal becomes stable, i.e. $\left\| p^{i+1} - p^i \right\| \leq \varepsilon$, we can terminate the algorithm since the target optimal total load curve is reached. The complete algorithm flow is generalized as follows:

Algorithm 5.3: Distributed Water-filling Charging Control

Obtain day-ahead grid base load from utility or ISO
Obtain predicted user charging profile from mixture user model
Collect current station status over the whole network
Initialize all EV charging rate $\hat{r}_n^0(t) = \underline{r_n}(t)$, $n = 1,2,\ldots N$
While: $\left\|p^{i+1} - p^i\right\| \geq \varepsilon$
  For EV #n in the network, $n = 1,2,\ldots N$
    Get upper and lower bound u_n, l_n from (5.8), (5.9)
    While: $\|u_n - l_n\| \geq \varepsilon$
      $m_n = \frac{1}{2}(u_n + l_n)$
      $\hat{r}_{tmp}^i(t) = \hat{r}_n^i(t) - p^i(t) + m_n$
      If $\sum_t \hat{r}_{tmp}^i(t) > E_n$
        $m_n = u_n$
      Else
        $m_n = l_n$
    End
    Update EV profile using (5.10) with $p^{i+1}(t) = m_n$
    Update control signal: $p^{i+1}(t) = \frac{1}{N}\left(\sum_N \hat{r}_n^{i+1}(t) + \hat{B}(t)\right)$
End

The proposed water-filling charging control algorithm does not depend on the convex optimization solver but uses the bisection method instead, which significantly reduce the computation time, thus more ideal for real-time implementation. The water-filling algorithm uses prediction from clustering station model for future timestamp scheduling, but independent from electricity pricing model. It can be used as an alternative to the two-stage optimization charging control.

5.1.5 Result and Discussion

Simulation of the proposed smart EV charging control algorithm is performed using the UCLA SMERC smart charging network infrastructure as a testbed. Historical EV charging record data collected for the past four years are used to build the EV mixture user model. Day-ahead wholesale energy price is provided by the California Independent System Operator (CAISO) [77]. TOU price is obtained from Southern California Edison (SCE) TOU-8 commercial plan for consumers with more than 500kW consumption [78]. The base load is generated using the CAISO demand and forecasting data as guidance [52]. In the simulation, we assume there are N=300 EVs participated through the day. There are four user behavior models with probability distribution $P(\theta_i) \in [0.2, 0.45, 0.4, 0.05]$which are estimated by CLSA. To improve the fidelity of the simulation of such EV charging system, the simulation platform considers the historical EV charging load and historical load curves, as well as the instantaneous EV charging behaviors. During the simulation, cross-validation methods are utilized. Specifically, a portion of the experiment days are selected as the base datasets, which are used to predict the day-ahead system baseload and the EV drivers' preferences. Another portion of experiment days will be selected as the test days, when the proposed decision-making algorithms will be used to generate the optimal EV control plans, assuming limited knowledge of the future system states. Therefore, the uncertainties of the EV charging behaviors and model fidelity can be preserved in this simulation platform. The simulation is discretized by each time step when the real-time charging station status changes, the control algorithm will update the charging profile in a moving horizon fashion.

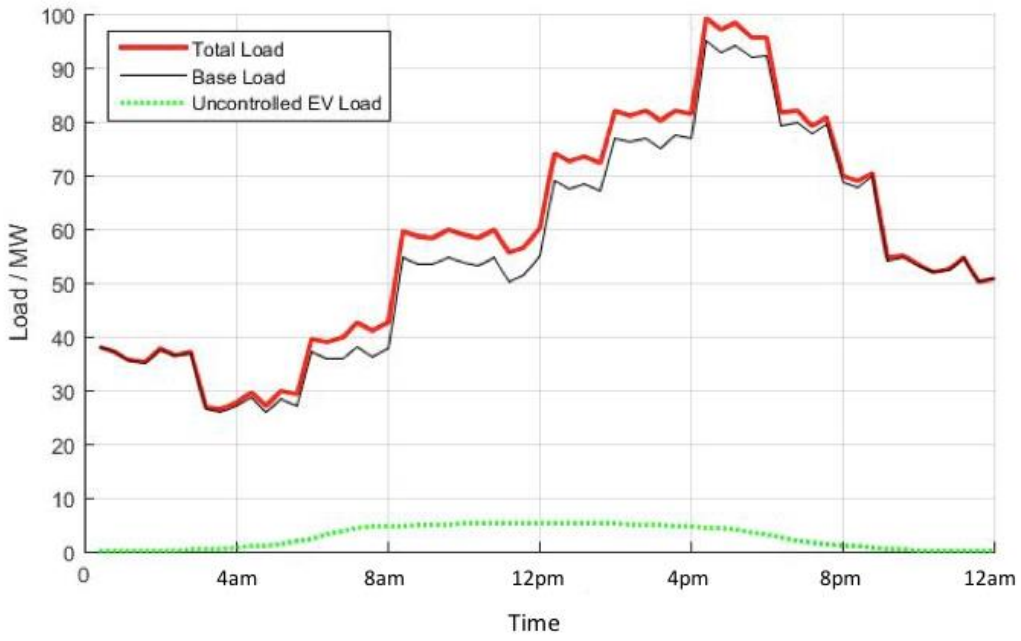

Figure 26. Load profile without control

Figure 26 shows the base load and the EV charging load without any control. It can be seen that one-third of the EV charging loads overlap with the peak base load. This situation is not favorable both to the utility and consumer.

5.1.5.1 Load Shifting Performance

The first-stage optimization is performed using wholesale energy price, and the optimal load profile is generated and plotted in Figure 27 in red dot line.

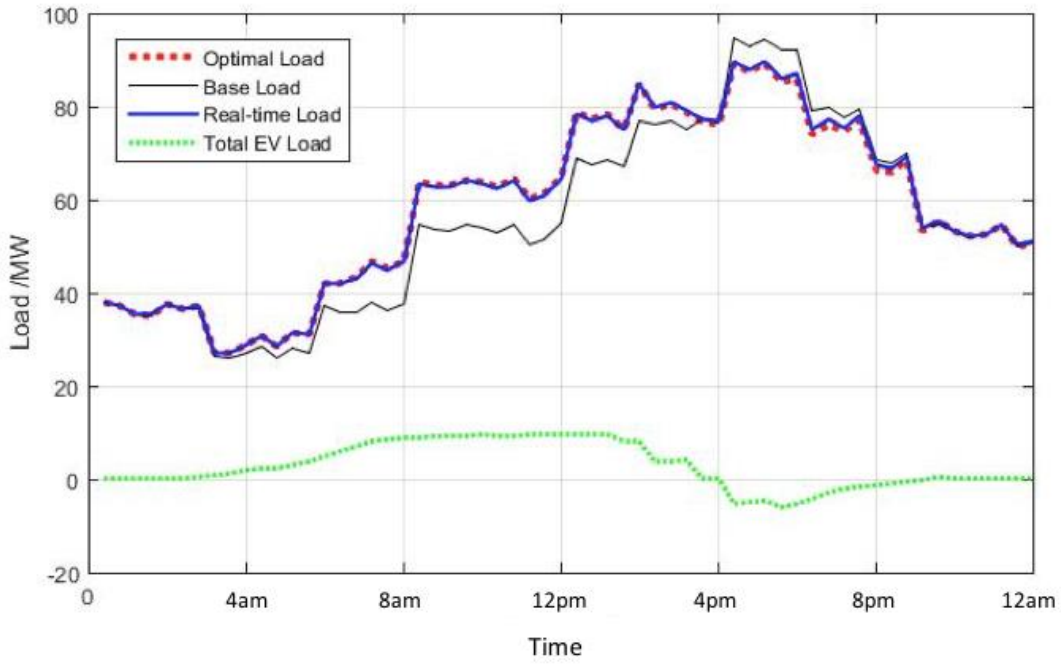

Figure 27. Load profile following algorithm performance

In Figure 27 we can find that the algorithm schedules high power charging during off-peak hours when the electricity price is lowest. The charging load reaches its peak around noon when most of the EVs are online. Most of the charging activities are paused or even switched to V2G mode to shift the load and support the DR program when the energy price is increasing. Around 6 pm, which is peak-hour, it can be seen that with the help of our scheduling algorithm, the optimized EV charging load does not overlap with the base load peak demand. On the contrary, the algorithm tries to control all qualified EVs to perform V2G to reduce the peak load in the power grid. Charging activities resume to normal after peak hour. The peak of baseload is 95MW, with the help of the two-stage optimization algorithm scheduled V2G, the total load drops to 85MW.

For the second-stage real-time EV charging control implementation, we expect to see that the real-time EV charging load follows the optimal charging scheme generated by the first-stage optimization without affected by differences between the EV user model prediction and real-time situation. The second-stage EV charging control, decentralized optimization is conducted with re-

initialized EV user model, representing the difference between prediction and the real case. In Figure 27, it can be seen that the blue curve, which is the real-time load profile, follows almost exactly with the optimal profile in red with minimal deviations. The difference is the result of the prediction error in reality. Performance of the water-filling algorithm and comparison between the two proposed charging controls are shown in Figure 28.

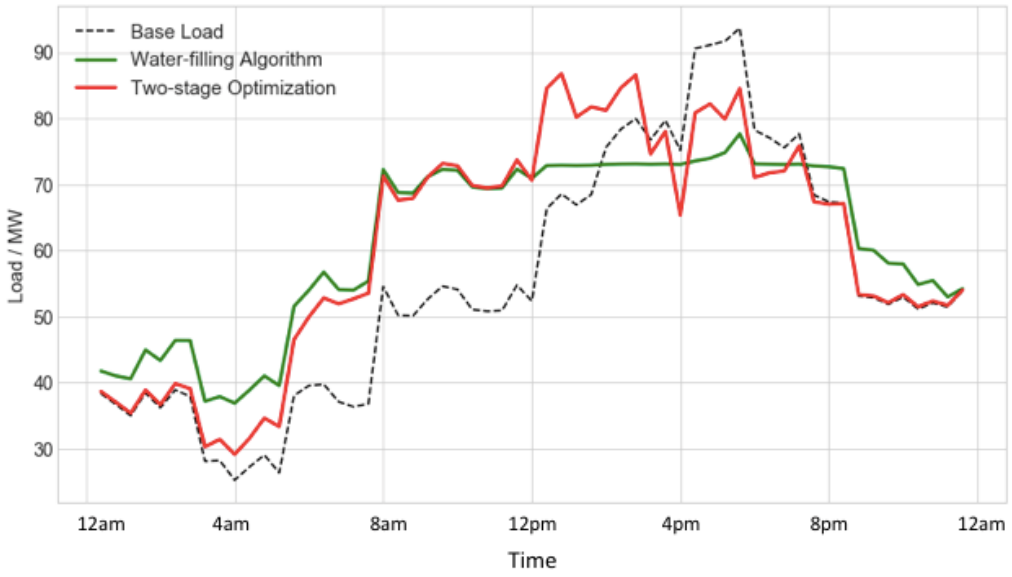

Figure 28. Comparison between two proposed charging control schemes

We can find that both charging control algorithms are trying to schedule more charging during off-peak hours when the electricity price is the lowest. With the help of algorithm scheduled V2G, the total load drops to 85MW as discussed previously, and even lower to 75MW with the help of the water-filling algorithm. It can also be seen from Figure 28 that the water-filling algorithm outperforms the two-stage optimization in valley-filling and peak-shaving. The total load curve generated by the water-filling algorithm is relatively more flattened since the algorithm is trying to allocate load at every time slot towards an average load level under the constraints of availability and demand. However, the two-stage optimization is price-based and trying to shift load according to the electricity price curve. A comparison between the EV total energy consumption with and

without the proposed algorithms implementation is shown in Figure 29. We can find that both proposed algorithms have scheduled more charging during off-peak and mid-peak hours, and V2G during peak time. But water-filling algorithm performs load shifting more aggressively, while two-stage optimization is more subjected to the price curve.

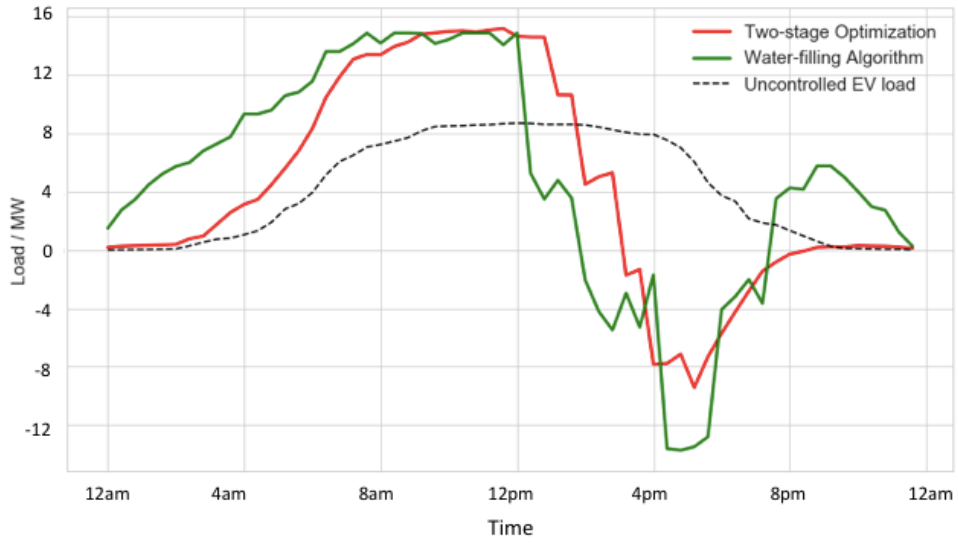

Figure 29. Comparison between two proposed charging control schemes

5.1.5.2 Energy Cost Saving

The purpose of the proposed two algorithms is to both reduce the energy cost and shift peak load. The first-stage optimization tends to allocate more charging activities during the wholesale energy price is low and then pause or reverse charging during the energy price going high. The water-filling algorithm is independent of the pricing policy. But since it can flatten the load curve, the algorithm is also a good choice for the DR program. Without charging control, all charging stations will serve in 'plugging in and charging' mode. There is no variable charging power or V2G session. Due to the energy constraint in (4.11) used in the first-stage optimization, and the relaxed of (4.11) used in second-stage real-time control, the wholesale energy purchased through two-stage optimization charging control can be equal or less than the real-time demands. Thus, enough energy has to be purchased during real-time control via the retail energy market with TOU price.

For V2G incentives, the mechanism of V2G rewards may be more sophisticated in reality, but in the scope of this research, we just define it to be the negative TOU price for simplicity. Based on the wholesale price and (5.2) the energy saving can be calculated:

$$\delta = \sum_{T}\sum_{N}\left(r_n^{\mathrm{w}}(t) - r_n^{\mathrm{w/o}}\right)\cdot\pi(t) - \Delta e_n\,(t)\cdot\lambda(t) \tag{5.11}$$

where $\Delta e_n(t)$ is the difference between real-time demand and prediction, and $\lambda(t)$ is the TOU price. $r_n^{\mathrm{w}}(t)$ represents the charging rate controlled by the proposed algorithm while $r_n^{\mathrm{w/o}}$ is the charging rate without proposed control. Based on the price data from CAISO, the number of vehicles and other setups used in this simulation, energy cost saving can be calculated. Energy cost without smart charging control can be obtained by multiplying power consumption rate through the day with energy price. Cost reduction rate can be obtained by calculating the portion of energy cost saving with proposed control to the energy cost without charging control using equation (5.12):

$$\text{Cost Reduction Rate} = \frac{\delta}{r_n^{\mathrm{w/o}}\cdot\tau(t)} \times 100\% \tag{5.12}$$

Charging cost, V2G reward and total cost are plotted in Figure 30 for one-day operation with and without charging control implementation.

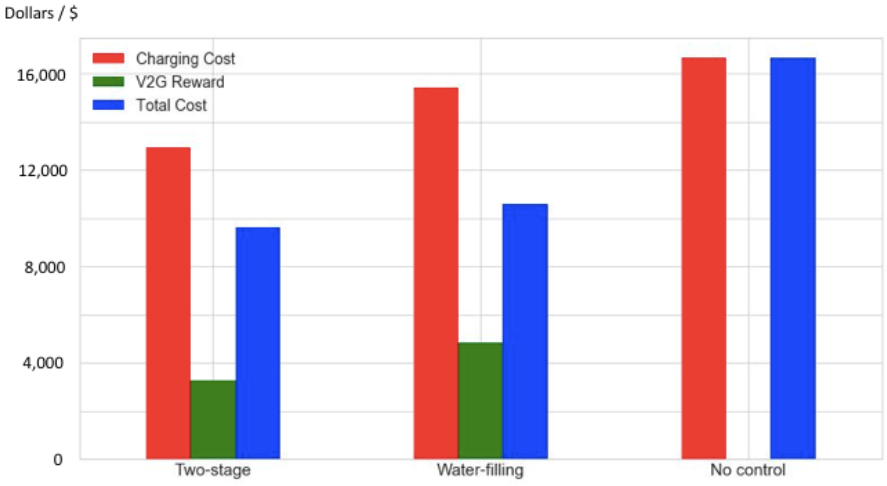

Figure 30. Charging cost comparison for one-day operation

It can be seen from Figure 30 that the two-stage optimization charging control can help to obtain the most cost saving, since this algorithm is price-based optimization. Although the water-filling algorithm has better performance on load shifting, it still yields more total cost than the two-stage optimization. Both proposed algorithms help the grid operator reduce EV charging cost and do load shifting to accommodate the DR program.

5.1.5.3 Performance Evaluation

In real-world control implementation, it is impossible to guarantee our EV user model perfectly predict the real-time situation. The control algorithm should be able to adapt to variance in real-time. We use two criteria to measure the deviations. Mean absolute percentage error (MAPE) is used to evaluate the prediction accuracy of the EV user model against actual user behavior in (5.13). And the resulting load profile following quality is quantified by the root mean square error (RMSE) in (5.14).

$$\mathrm{MAPE} = \frac{1}{\mathrm{T}} \sum_{\mathrm{T}} \sum_{\mathrm{N}} \left| \frac{\hat{\mathrm{r}}_{\mathrm{n}}(\mathrm{t}) - \mathrm{r}_{\mathrm{n}}(\mathrm{t})}{\hat{\mathrm{r}}_{\mathrm{n}}(\mathrm{t})} \right| \tag{5.13}$$

$$\mathrm{RMSE} = \sqrt{\sum_{\mathrm{T}} \mathrm{G}(\mathrm{t})} \tag{5.14}$$

where again $\hat{\mathrm{r}}_{\mathrm{n}}(\mathrm{t})$ is the actual user behavior on a particular day and $\mathrm{r}_{\mathrm{n}}(\mathrm{t})$ is the predicted value. $\mathrm{G}(\mathrm{t})$ is the objective function used in second-stage control to follow the day-ahead profile. We have generated five use cases with a different portion of random charging behavior mixed into EV user mixture model prediction to emulate the real-time variance. Simulations are conducted for these use cases and we investigate the energy cost reduction and saving percentage. Results are listed in Figure 31 and Table VI.

Table VI. Performance Evaluation against Prediction Error

Prediction Error (MAPE)	Load Profile Following Error (RMSE)	Cost Reduction / Day ($)	Saving Percentage
0.205	0.3001 MW	3185	18.08%
0.262	0.3123 MW	3053	17.99%
0.344	0.8187 MW	2574	14.57%
0.521	1.6662 MW	1785	10.35%
0.683	2.5413 MW	1034	6.46%
0.991	3.5420 MW	-3355	-20.17%

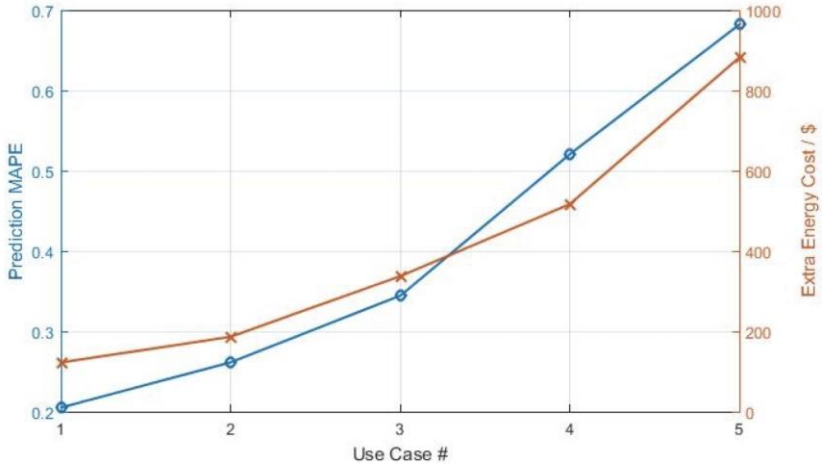

Figure 31. Prediction MAPE with extra energy purchasing

From Table VI it can be seen that if an accurate prediction was made by our EV user mixture model, the proposed algorithm could achieve almost 18.08% of energy cost reduction against uncoordinated charging activities. Figure 31 shows the extra energy cost needed to be paid due to different levels of prediction MAPE. With the prediction error increasing, the profile following error grows almost linearly. But when the prediction is not too far away from the real case and stays in a reasonable range, the curve following algorithm can still provide some control to available resources and accommodate a portion of DR program.

In real-time control implementation, computation time is an important factor to take into consideration. Too much delay in decision making will result in losing control effectiveness. Table

VII shows the convergence speed of two proposed algorithms when performing on a different number of charging stations.

Table VII. Total Convergence Speed Analysis

Number of EVs	Two-stage Optimization	Water-filling Algorithm
50	147.083 s	0.062 s
100	282.109 s	0.079 s
200	554.439 s	0.154 s
1,000	2,817.119 s	0.660 s

From Table VII we can conclude that the runtime of the water-filling algorithm is much faster than the two-stage optimization. With fast convergence speed, the water-filling algorithm can be used to perform time-critical real-time control and will be less sensitive to prediction error. Two-stage optimization is relatively slow in convergence. But since it is a decentralized algorithm to be performed in every charging station, when the total time is averaged over all charging stations, each station will only share a 3 seconds computation, which is still acceptable for real-time charging control.

5.1.6 Conclusion

In this section, two decentralized algorithms are proposed to coordinate electric vehicle charging activities and utilize electric vehicle as a distributed energy resource in public parking facilities within the microgrid / power grid for demand response program. The first-stage optimization provides an optimal electric vehicle charging scheme based on day-ahead wholesale energy price and prediction. Second stage optimization performs distributed real-time control to follow the optimal electric vehicle charging scheme. Simulation results show the proposed algorithm can reduce around 18.08% energy cost with decent prediction and have a certain level of robustness against prediction error. The alternative water-filling algorithm provides a fast convergence speed

for real-time charging control with a slightly lower cost saving. The decentralized feature lowers the computational cost at the control center and greatly reduces convergence time, which provides great potential for scalability.

5.2 VGI for Renewable Generation Smoothing and DR

5.2.1 Mitigate the PV duck-curve with focus on V2G and grid-to-vehicle infrastructure

As PV output usually peaks around noon which does not typically coincide with the power grid peak load, over-generation from this renewable source occurs and could cause problems. In this section, it is shown that by using the grid to the vehicle, or G2V or also known as V1G, we managed to mitigate this over-generation. Such over-generation is typically known as the Duck Curve. The results from our G2V approach are demonstrated using data from the Santa Monica Civic Center PV system and charging stations. Here in Figure 15 (left) presents the PV output profile of a typical day and a typical load. For the PV data, we choose the data collected on a random date (02/01/2017) as an example for discussion. For the typical load, in the absence of Santa Monica Civic Center building load profile due to access limitations, we utilize the regular EV charging loads in that building to serve as the proxy of the building load. As shown in the figure, between 11-2 the energy generated by solar PV is greater than the building load. We focus on this region and add additional EV fast charger load to demonstrate how EV fast charging loads could mitigate this over-generation, which is shown in Figure 32 (right). This EV fast charging load is with a constant load of 28 kW; it significantly eliminates the gap between PV generation and original building load.

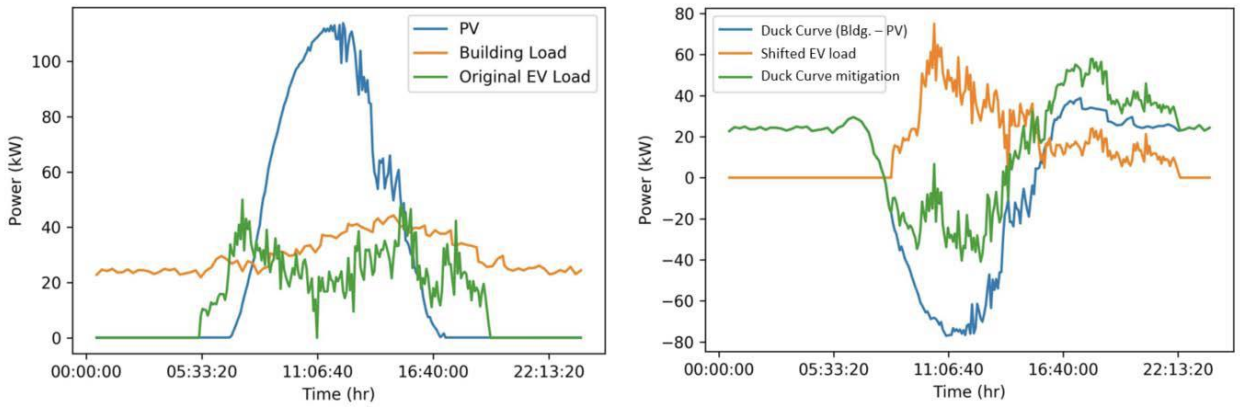

Figure 32: PV generation against building load and duck curve mitigation

For the entirety of 2016, 325 days of data are collected, and 237,001 kWh energy harvested, with a daily average of 729 kWh. The reasons there are 40 days without data input include monitoring system firmware/software upgrades, on-site metering system running other energy applications, and PV system switched turn-off by the site-host. Figure 33 presents the maximum instance of power by month. Observations can be made that it follows the variation of how much sunshine the PV system is exposed to. Throughout this period, we performed 12 sessions of monitored V1G/V2G operations. A typical load profile of V1G/V2G can be found in Figure 34.

The V1G can rapidly increase consumption to 28 kW in a short amount of time (two minutes) and is capable of covering the period when the solar output reaches its maximum output. In a typical summer day when the PV system outputs a maximum of 120 kW, this fast charging session accounts for 23.3 percent of the total generation, while in a typical winter day when the maximum is halved, or 60kW, the fast charging session could consume a total of 46.7 percent of the total generation.

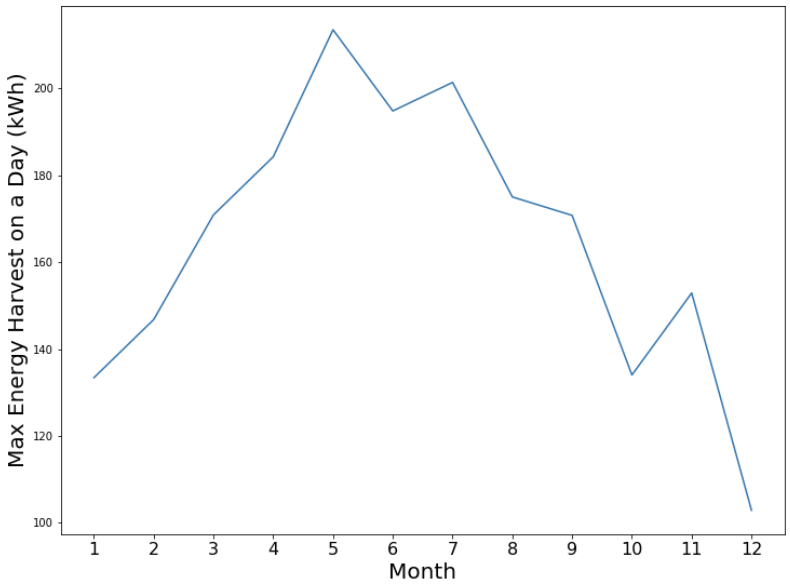

Figure 33. PV Maximum Instance Power by Month

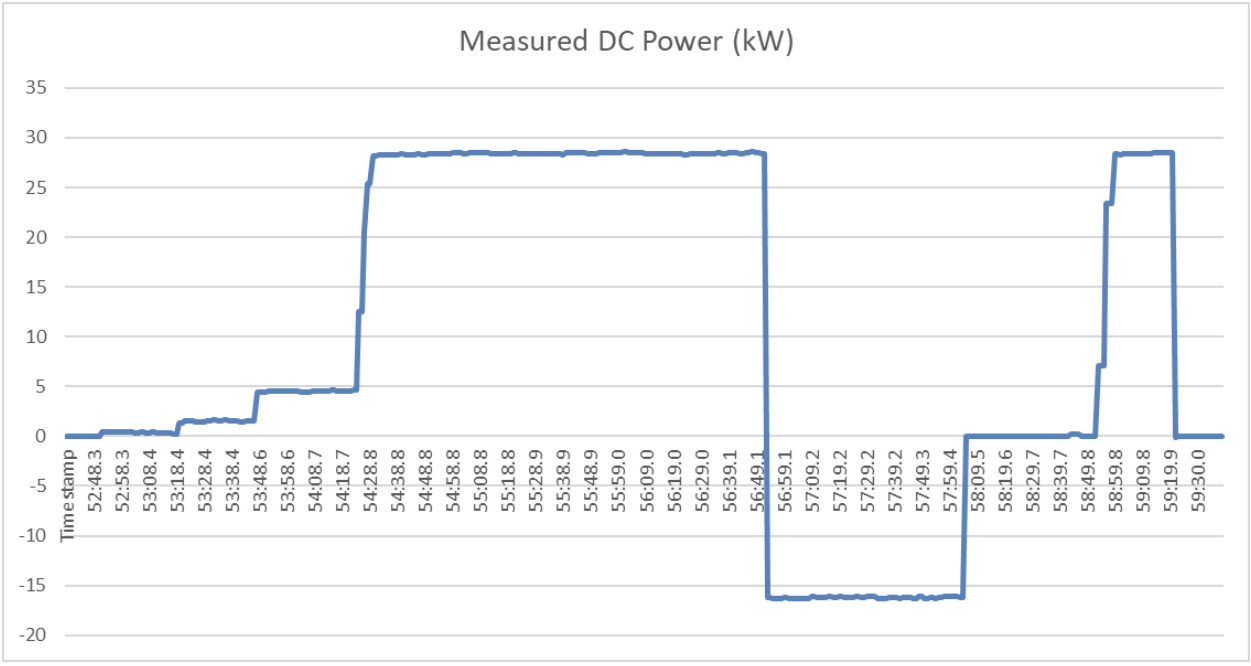

Figure 34. V2G Operation Load Profile

From these statistics, simulation is performed. Assuming that the fast charging has the capability ranges from (0, 28) kW. Two fast charging systems are considered in this simulation. The maximum instant power by day for 2017 is extracted, with baseload subtracted from it, the distribution of load consumption difference and load balancing can be observed in Figure 35. As

could be observed from the histogram, the number of days when the difference between generation and load being near zero increase dramatically as the number of fast charging system increases.

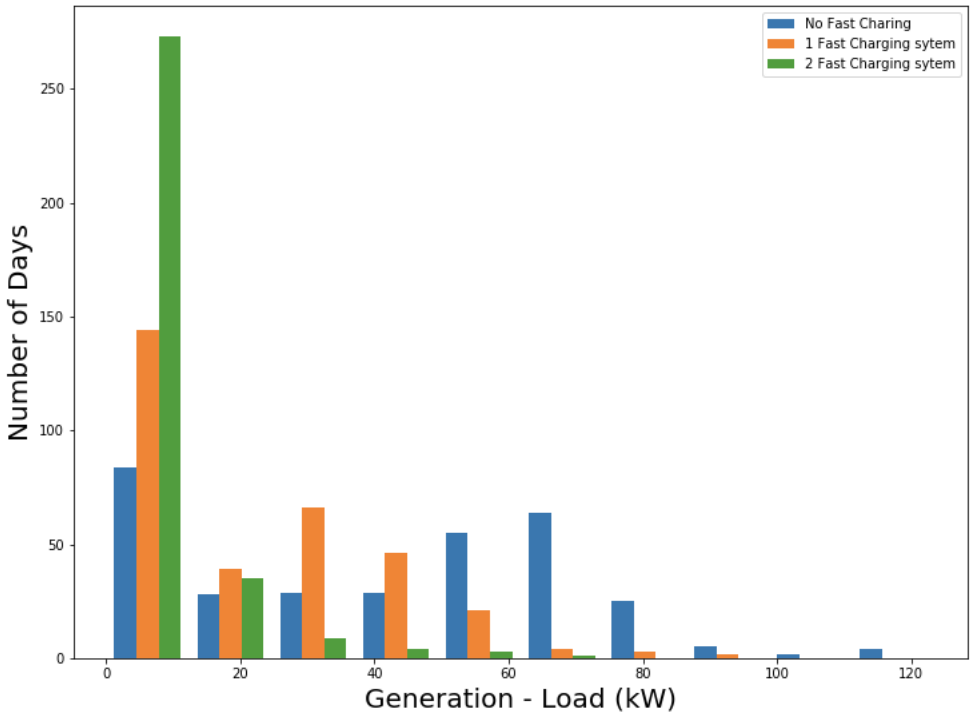

Figure 35. Over-Generation Damping with Fast Charging

A conclusion could be drawn that, since the base load is only around 90 kW as shown in Figure 32, the V2G system with proper number of instances being installed (in this case, 2 systems are sufficient), the system should be able to fill the gap between load and generation not just during most of the peak hours, but also most of the time throughout a day.

5.2.2 VGI for Demand Response

There are two types of DR considered in this analysis: Pure DR and DR with V2G. For pure DR, the power from the charger to the vehicle is reduced to an absolute minimum. For DR with V2G, the discharging power is used to perform reverse power flow and provides effective V2G capability that is more than the pure DR. The result for pure DR is shown in Table VIII.

Table VIII. Pure Demand Response Power Reduction

Begin Power (w)	Min Power (w)	Ave. Power (w)	Start Time	Stop Time
14031	3629.63	3303.370787	6/3/17 14:12	6/3/17 14:21
11805.04	2052.17	1636.363636	6/2/17 18:50	6/2/17 18:57
17278.4	4195.05	3854.389722	6/2/17 15:15	6/2/17 15:30
6565.74	3425.46	7092.537313	6/2/17 13:58	6/2/17 14:03
5557.98	2602.64	3904.411765	6/2/17 13:38	6/2/17 13:48

Source: UCLA SMERC © 2014-2017

Begin power is the power when DR is initiated (in units of Watts). Minimum power is the minimum total power consumption for the Civic Center during the period of DR. Average power is the average consumption power of all stations summed together, calculated from main energy. The result for DR with V2G is:

Table IX. DR with V2G support

Consumed Energy (kWh)	Backfeed Energy (kWh)	Start Time	Stop Time	Pure (kWh)
0.76	-2.13	2/25/17 12:10	2/25/17 12:18	-1.37
0	-0.944	2/25/17 12:22	2/25/17 12:24	-0.944
0.6	-4.239	2/25/17 12:40	2/25/17 12:49	-3.639
0.81	-4.49	3/20/17 11:00	3/20/17 11:09	-3.68
1.72	-4.658	4/28/17 9:17	4/28/17 9:26	-2.938
2.14	-4.122	4/28/17 9:40	4/28/17 9:48	-1.982
2.46	-4.815	4/28/17 10:00	4/28/17 10:09	-2.355
0.72	-2.581	5/31/17 11:10	5/31/17 11:16	-1.861
0.56	-1.498	5/31/17 11:22	5/31/17 11:25	-0.938
1.67	-4.545	6/28/17 19:07	6/28/17 19:16	-2.875
0.89	-2.571	6/28/17 19:22	6/28/17 19:27	-1.681
1.64	-4.65	7/26/17 18:21	7/26/17 18:30	-3.01
0.69	-1.979	7/26/17 18:35	7/26/17 18:39	-1.289
0.5	-1.583	7/26/17 18:46	7/26/17 18:49	-1.083
0.09	-0.515	8/24/17 14:01	8/24/17 14:03	-0.425

Source: UCLA SMERC © 2014-2017

5.3 Summary

In this chapter, strategies for VGI in public parking structure are proposed. VGI for solar generation duck curve mitigation and building load support is discussed. It can be seen that by utilizing the V2G capability of EV with proposed grid integration control algorithms, EVs can become a valuable resource for the power grid and support for renewable generation. Results from

real-world implementation in our Santa Monica test site proved the effectiveness of proposed methods.

6 Chapter VI. Smart Charging System Design

6.1 DC Fast Charging

6.1.1 Overview

J1772 level 2 charging station developed in our lab can change the charging power and current to the EV based on charging control command issued from the smart charging control center. It also has the multiplexing feature which can charge four plugged-in EVs at the same time with different power outputs for each EV. With the increasing of battery capacity, the charging speed of level 2 AC charging station cannot satisfy customer's need in the future, and level 3 fast DC charging will become more and more popular. Currently, all the J1772 DC charging stations in the market can only charge one car at a time with a fixed current. We plan to develop a J1772 level 3 fast DC charging station with varying current and multiplexing features.

6.1.2 Implementation Approach

Under SAE J1772 standard, level 2 charging station output current is defined by the duty cycle of PWM signal on the pilot control line. Most of the charging control signal between EV and EVSE are exchanged via the pilot control line. But in SAE Combo Charging Standard (CCS) specification, the PWM signal on pilot control line no longer plays such a key role in the EV-EVSE charging control communication. Powerline-Communication (PLC) system is installed in both the EVSE and EV which is going to handle the communication for level 3 fast DC charging. Most of the charging control signal in J1772 level 3 fast DC charging is transferred by PLC in XML dataframe [79]. And the pilot control line is used for PLC communication. The schematics of PLC communication for charging control is shown in Figure 36.

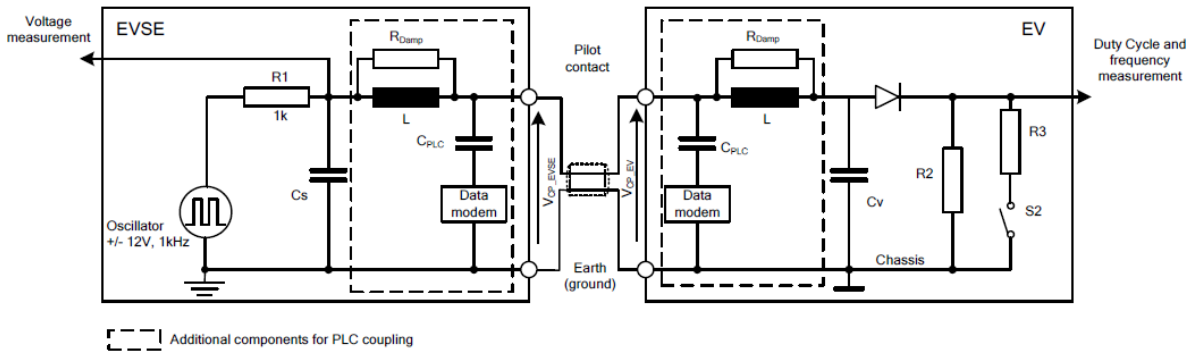

Figure 36. PLC between level 3 DC charging station and EV [80]

In J1772 level 2 charging station the output current is controlled by the duty cycle of PWM signal on the pilot control line, the relationship is shown in Figure 37.

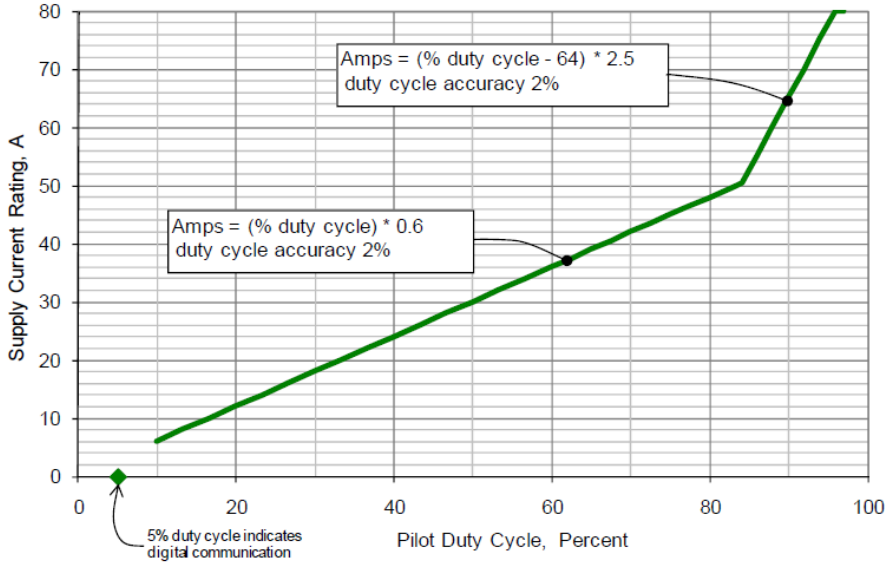

Figure 37. Supply current rating vs. pilot control duty cycle [23]

In J1772 level 3 DC charging station, the duty cycle on the pilot control line is fixed at 5% during charging process which indicates digital communication, as shown in Figure 37. The digital communication is performed on PLC using HomePlug Green PHY 1.1 protocol [81].

Before the J1772 level 3 DC charging station and EV start energy transfer, there is an initialization process called handshake. In the handshake phase, EVSE and EV exchange some important

charging parameters by PLC, including the voltage and current limits the EVSE can provide and the EV can accept. After the handshaking, connector in the charging station will be closed and energy transferring begins. The charging voltage and current are defined in the handshaking. Figure 38 shows the charge current request signal and the charge current. The Vehicle regulates the energy delivery by managing Voltage Request and Current Request signals to the DC Supply with a cyclic message (7a). The DC supply reports its present output current and output voltage, its present current limit and voltage limit, and its present status back to the PEV in the message (7b) [23]

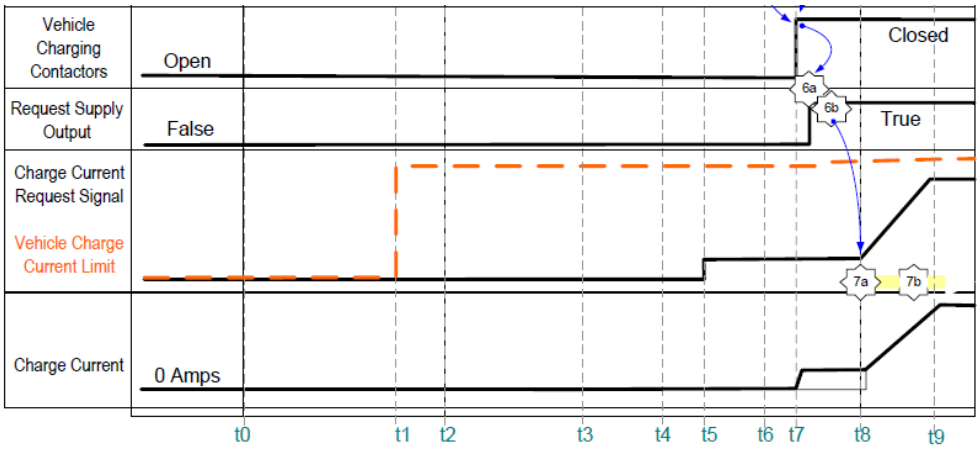

Figure 38. Charge current request signal and charge current

The possibility of designing a J1772 level 3 DC combo charging station lies on the current request signal. In the level 2 smart charging station case, we can change the charging current by changing the duty cycle of PWM signal on the control pilot. In the level 3 charging station case, there is an information exchange about the current and voltage limit and demand between the EVSE and EV. On the EVSE side, we can design a feature in the hardware and firmware which can change the EVSE output current limit information as needed. If a lower charging current is requested by our smart charging algorithm, the firmware will tune down the value in the EVSE output current limit; the EV side will then adjust its energy receiver to reduce charging current. In this way, we can

control the charging current in the level 3 DC fast charging process. In the future, ISO15118, where SAE CCS standard is developed from, will be merged with SAE CCS standard. ISO15118 will become the most widely used EV charging standard in the U.S.

6.1.3 Communication for DC Fast Charging

A DC combo charging station was bought to act as the test bed for level 3 smart charging station design, as shown in Figure 39.

Figure 39. DC combo charger for level 3 fast DC charging

A pair of PLC adapters are used to help develop PLC communication in the level 3 smart charging station design. The PLC adapter pair is shown in Figure 40.

Figure 40. PLC adapter pair for PLC communication design

According to the previous analysis, the level 3 smart charging station must be able to generate a various output current limits message and send via PLC to the EV to control the charging current. The first step to develop this feature is to get and analyze the PLC message exchanged between EVSE and EV. The method to get the PLC charging control message is to connect a PLC adapter to the EVSE control pilot line, use a computer with an EV emulator software installed. The EVSE will consider the computer as a plugged-in EV and sending charging control message out. The message then will be caught and save by PLC control software installed in the connected computer. The PLC control software used here is called Qualcomm Atheros Open Powerline Toolkit, which is used for controlling the Atheros PLC chip in the adapter to send, receive, listen to PLC message and more.

We initially chose Raspberry Pi as the core controller for our future level 3 smart charging station. First, we used it to test the ability to catch and save a PLC message. Once it is clear how to obtain the content of PLC communication on the powerline, we can then proceed to connect it to the EVSE to get charging control message.

Currently, we can use the Qualcomm Atheros Open Powerline Toolkit to run some command on the PLC adapter such as monitor the PLC network, test transmission speed. And we can use the port listening command to catch PLC command transferring between the PLC adapter pair, as shown in Figure 41. With the same method, we can obtain charging control command from EVSE.

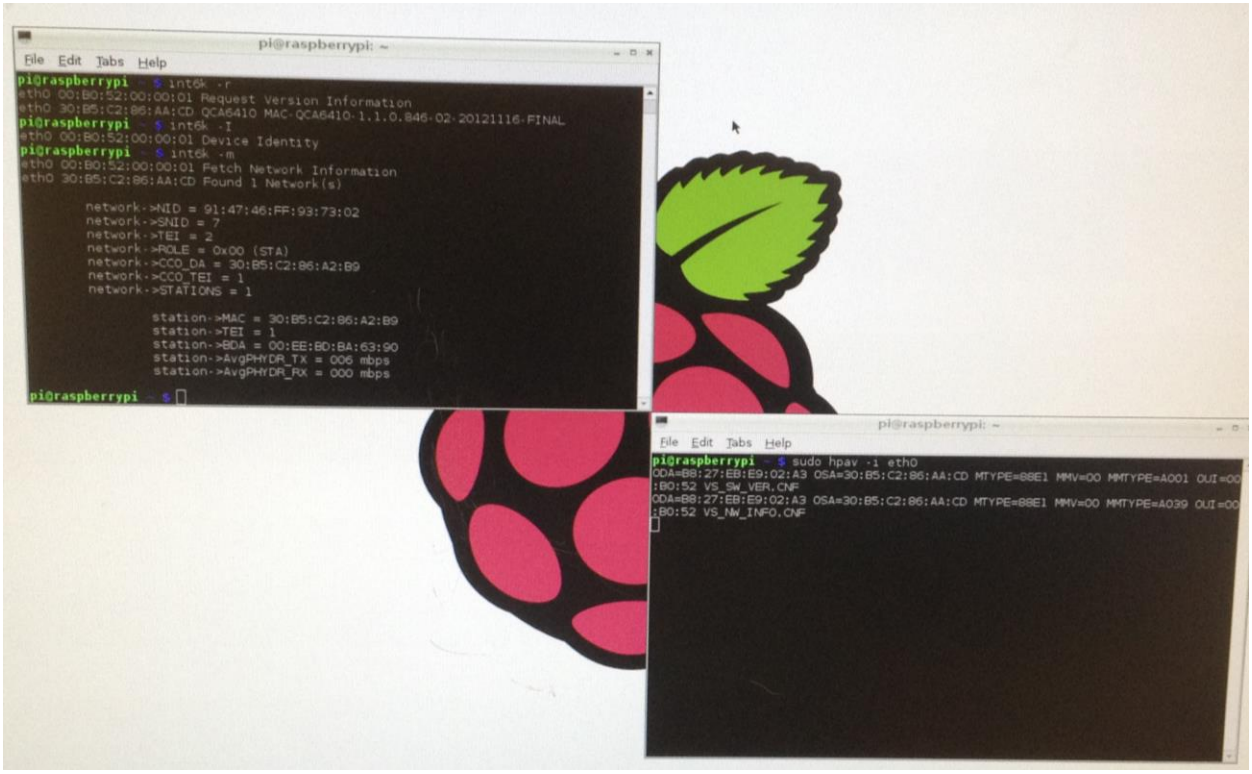

Figure 41. PLC message between two PLC adapter caught by the software

6.2 V2G controller

6.2.1 The V2G Charging Station

The Princeton Power C1-30 V2X Fast Charger is a DC fast EV charger with V2G capability. This CHAdeMO compliant charging station has a 30kW maximum charge rate. It can provide up to 50 miles of range in less than 20 minutes. It can also discharge an EV at the rate of 30kW to the power grid with V2G compatible EVs. The charger is a ‘kiosk-style’ charging station which is available

to the public. The power source for this charger is 3 phase 480V AC. The maximum DC output is 120A. The power factor of this charger is more than 0.95 above 20% rated power.

The Princeton Power fast charger can support all EVs with CHAdeMO type connector. It can be operated by its front panel or by remote control. Figure 42 shows the charger charging a Nissan Leaf in Santa Monica Civic Center Parking lot.

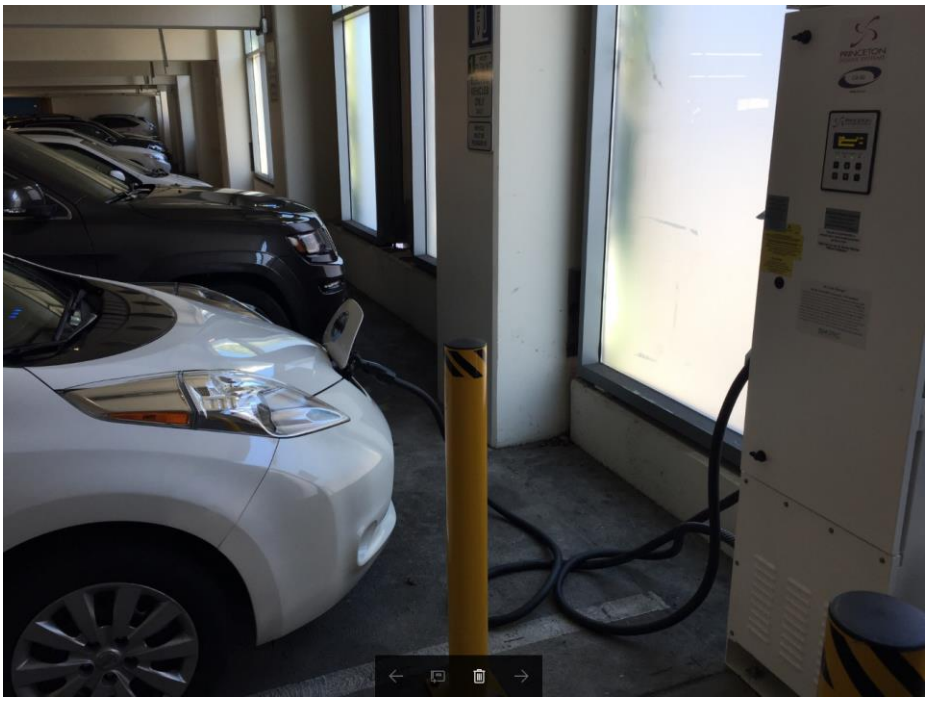

Figure 42. Princeton Power charging station in charging session

6.2.2 Communication Network

The charging station can be interfaced via Modbus TCP protocol [82]. To realize remote control and data collection, we have installed a router as a gateway for the network communication and a smart meter to measure power consumption data. The equipment is installed in a SMERC box next to the charger as shown in Figure 43.

Figure 43. Network Communication equipment box

A 277V to 110V step-down transformer was installed to obtain power from one line of the 3-phase power source to provide power for the gateway. Figure 44 shows the inside view of the SMERC box. One the left-hand side is the gateway router for the network communication. On the bottom of the box are the transformer and power outlet. Right-hand side is the smart meter. The blue Ethernet cable connects to the gateway with the charger, and the gateway is connected to SMERC control center via the Internet.

Figure 44. Inside view of the network equipment box

The communication network layout is shown in Figure 45. Voltage and current data are measured by smart meter between the charger and power source. The smart meter communicates with the gateway using Zigbee protocol [83]. The charger is connected with the gateway using an Ethernet connection. The communication protocol between the charger and remote-control center is Modbus TCP via this Ethernet and Internet connection. Control center is located in SMERC lab in UCLA campus, which is around 10 miles from the charger installation site.

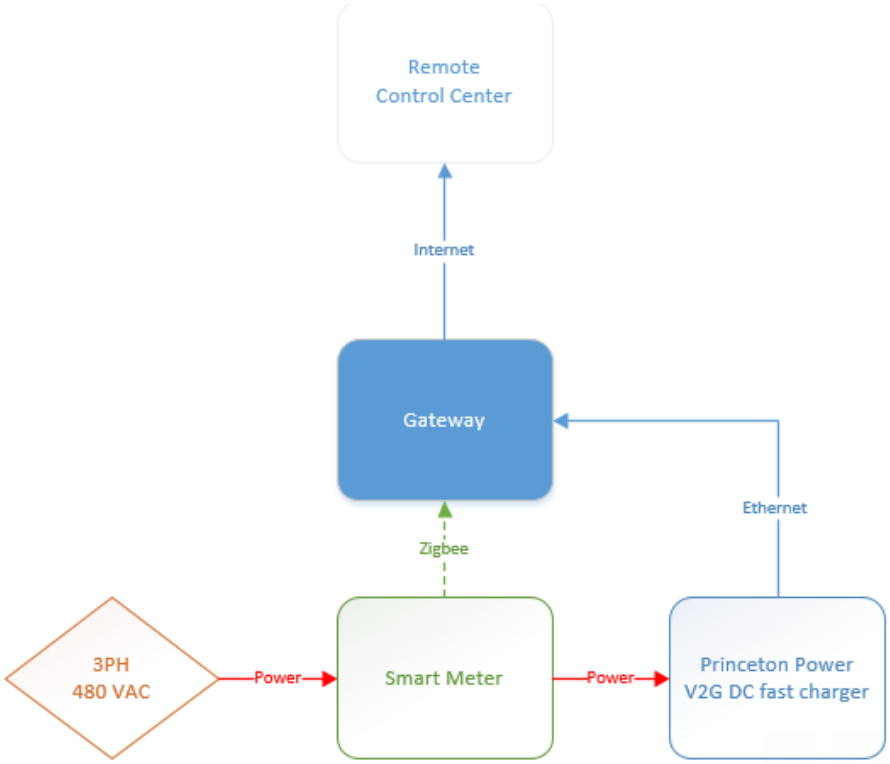

Figure 45. Charging Station Communication Layout

The power consumption is monitored by the smart meter installed between the power source and the charger 24/7 with a one-minute sampling interval. The data can also be collected directly on site via Modbus TCP interface. Figure 46 shows the data collection procedure on-site with a laptop.

Figure 46. On-site data collection

During on-site data collection with Modbus interface, data can be sampled with 1-second interval. Figure 47 and Figure 48 show the same session with both charging and discharging, collected by a smart meter and on-site respectively.

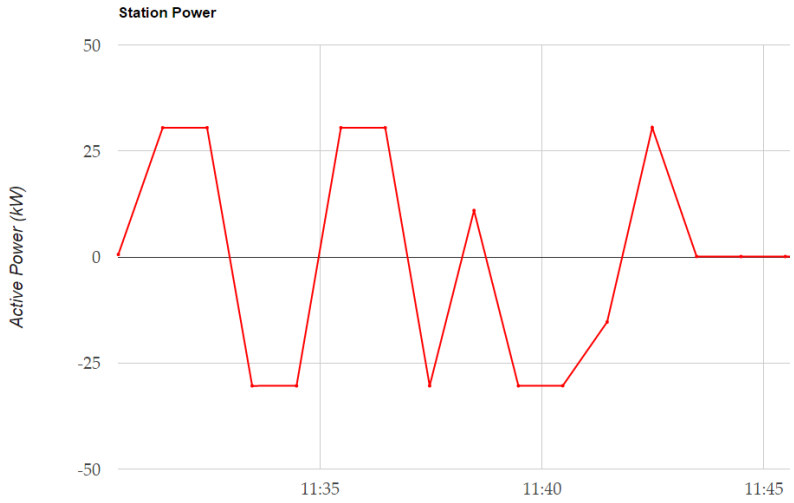

Figure 47. Charging and discharging data collected by smart meter

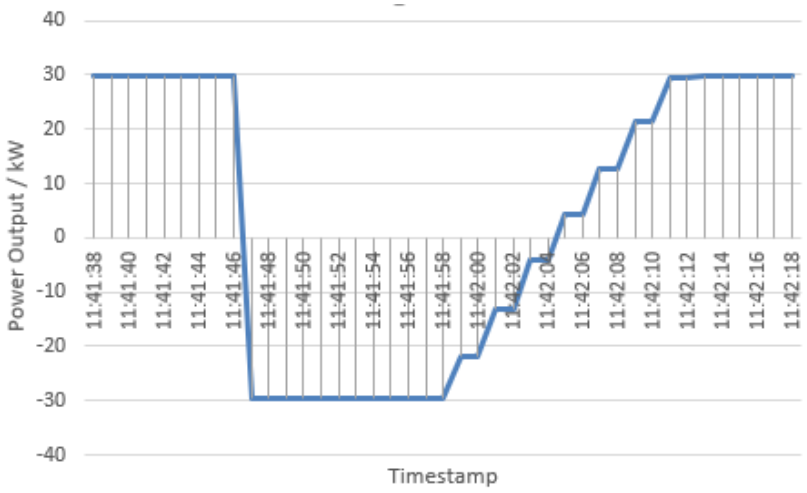

Figure 48. Onsite data collection via Modbus interface

Table X shows the testing sessions performed using V2G charging station

Table X. Charging and Discharging Sessions on Princeton Power DCFC

Date/Time	Testing Type	Total Charging Energy (kWh)	Total Discharging Energy (kWh)	Starting SoC	Ending SoC
2/25/2017 12:25	charging/discharging / incremental	8.8	6.85	30%	40%
3/20/2017 11:00	charging/discharging / incremental	5.87	4.49	64%	52%
4/28/2017 9:28	charging/discharging	21.45	13.6	39%	55%
5/31/2017 11:00	charging/discharging	8.81	4.08	59%	69%
6/28/2017 19:05	charging/discharging	12.31	7.12	76%	77%
7/26/2017 18:14	charging/discharging	8.3	8.2	97%	77%
8/8/2017 15:18	charging	7.91	0	60%	90%
8/24/2017 13:18	charging/discharging	13.5	0.51	30%	90%
9/29/2017 17:05	charging/discharging	6.79	3.76	71%	84%
10/13/2017 18:37	charging/discharging	7.16	1.25	43%	80%
11/30/2017 10:42	charging/discharging	4.87	0.99	57%	78%

12/22/2017 16:24	charging/discharging	5.84	3.95	88%	93%

6.2.3 V2G Controller Firmware Design

The V2G controller is built on a Raspberry Pi. The firmware of the V2G controller consists of two parts: an HTTP server and a database. The database is used as a buffer to collect real-time charging station metering data. It will upload charging session record in batch once the capacity threshold is reached. The database is linked to the HTTP server. The HTTP server is a program written in Python which keeps running in the Raspberry Pi. The flow chart of the HTTP server is shown in Figure 49.

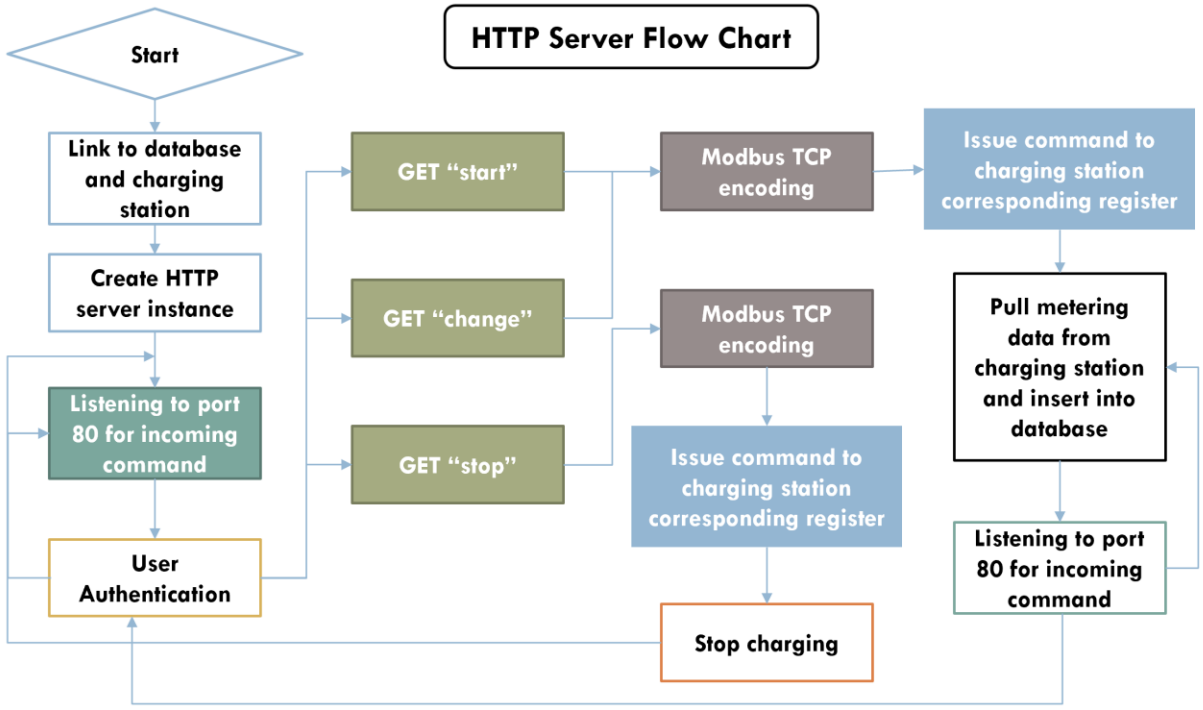

Figure 49. HTTP server program flow chart

The HTTP server works in an infinite loop to keep listening to the HTTP message from SMERC control center. Once received, it will decode the message and extract charging control command

and parameters. The server will then encode the command using IEEE hex code format into Modbus TCP data frame. The encoded charging control command goes into charging station via local Ethernet cable using Modbus TCP protocol. Corresponding registers in the charging station will be set and charging mode and parameter will be changed.

6.3 Safety Feature of Charging Station

6.3.1 Charging Station Ground Fault Circuit Interrupter

To provide a safe, smart technology for charging EVs, a safety system has been designed for all levels of control. The administrator can turn the relays of the charging stations on or off and check their status by transmitting commands. The charging stations can be reset manually or automatically on schedule as long as the connection between the server and the charging stations exists. Any emergency action taken at the top level will have a delay time that depends on the condition of wireless communication including 3G, WIFI, ZigBee, and Cloud. Thus, a fast-acting local unit is implemented to stop charging in case of an emergency.

To prevent electrical hazards, there should be no voltage on the handle of the charging cable until it is plugged into an EV. The detection of the EV plug-in status is implemented in the state machine of the firmware of the control unit based on the J1772 standard. The voltage of the pilot signal pin on the handle should be +12V when there is no EV connected to the charging station. After plugging in the EV, the voltage will be +9V or +6V depending on whether or not the EV is ready to accept energy. The EV plug-in status detection is implemented in the state machine in the firmware of the control unit. Furthermore, the charging station is required to shut off the power immediately to prevent the hazard of electric shock when there is an abnormal diversion of current from one of the hot wires. The Ground Fault Circuit Interrupter (GFCI) detects the difference of

current between two hot wires and shuts off the safety relay when the difference has crossed the threshold amperage. Unlike a traditional GFCI which requires manually pressing the reset button, a pure hardware GFCI with a remote reset function is used to increase the reliability. The power to the EV can be controlled by the server, the control unit of the charging station.

6.3.2 Voltage Detector

The voltage detector is another safety feature added to our level 2 smart charging station. It is used to monitor the output of the relay to find possible electric leakage or relay welding. The voltage detector is connected to each relay output in the smart charging station and keep reading the voltage of the output. If there is undesired voltage on the relay output, the voltage detector will send a signal to the controller to trigger related safety process written in the firmware (e.g., stop charging station or report problems). Figure 50 shows the design schematic of the voltage detector.

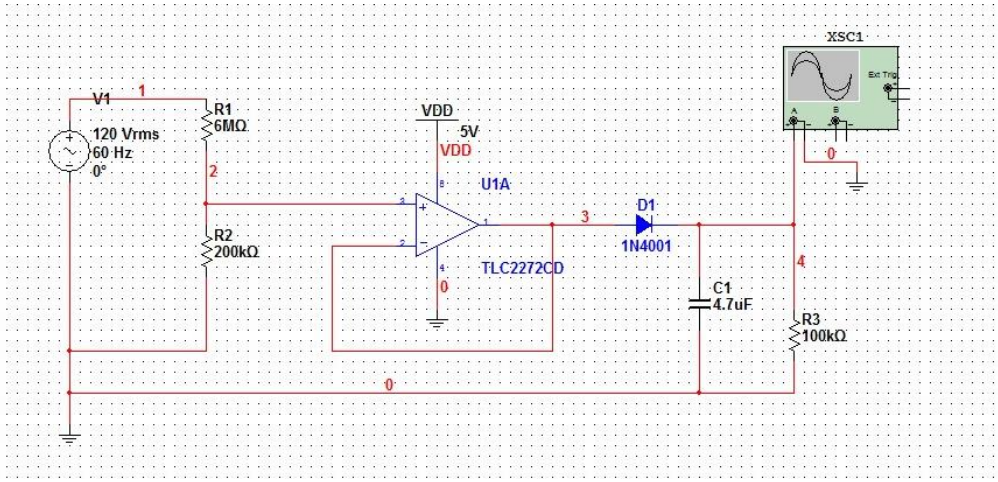

Figure 50. Schematic of voltage detector

The voltage detector directly connects to the output of relay, then a 31:1 voltage divider follows the input to lower the input voltage from 110V to 3.5V. The 3.5V input goes into an op-amp which is working as a voltage follower. The op-amp is used to isolate the high voltage part which is connected to the relay output and low voltage part which is connected to the charging control

electronics. The output of voltage follower connects to a half-wave rectifier. The half-wave rectifier is made by a diode, a capacitor, and a resistor. The diode removes negative voltage input, the capacitor and resistor pair can tune the alternate current sinusoid wave closed to DC signal. This DC signal is the indicator of the voltage status of the relay output and will go into the microprocessor in the charging control electronics for decision making. When there is no charging going on, the output voltage of the voltage detector should stay low. When the charging has enabled the output of the voltage detector is shown in Figure 51.

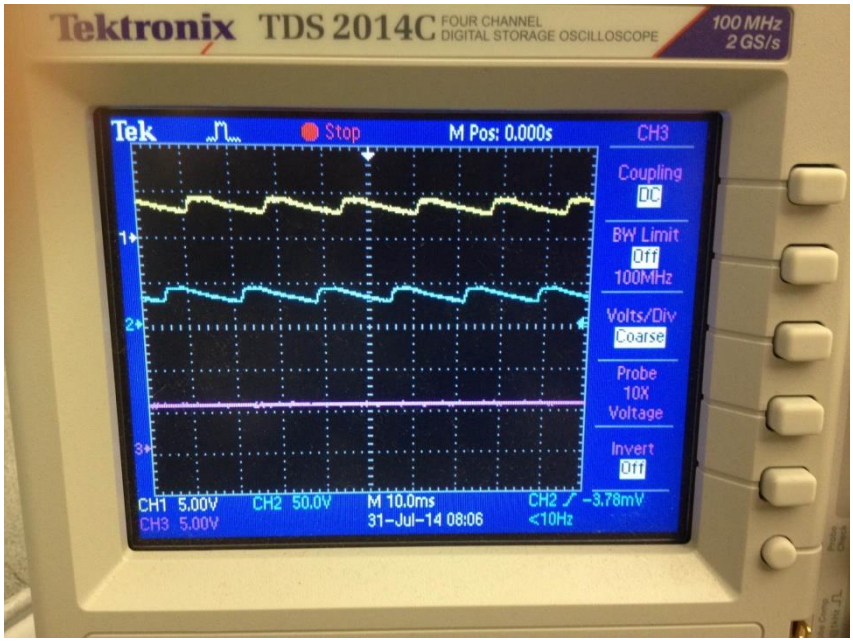

Figure 51. Oscilloscope image of voltage detector output

6.4 IEC 61850 Integration

6.4.1 Introduction

Most of the smart charging implementations are data-driven, which means the energy consumption decisions made by algorithms should be based on the real-time power data retrieved from multiple sources, including 1) meters for EV chargers, 2) meters for baseload monitoring, 3) mobile applications on the user side, etc. So far, most information is encapsulated and exchanged among

the communication networks with different standards or proprietary protocols. However, the scalability of such smart charging infrastructure and interoperability with smart grid and other grid device are limited due to lack of standardization in communication. Also, different protocols and data formats make it difficult for system diagnosis and maintenance. Therefore, to facilitate the integration process of intelligent charging system into the smart grid environment, the following challenges should be addressed: 1) A universal standard and data models for data exchange among distribution network and EV users; 2) An accessible service that efficiently converts data in multiple proprietary formats into the universal standard.

There are many existing standards and protocols used in a smart grid such as IEEE 802.3, SEP 2.0, IEC 61850 [84]. Among them, IEC 61850 is an international communication standard for electrical substation and power utility automation. Integration with IEC 61850 can provide more interoperability and reliability, making it easier to configure the smart device in the network. Previous research work has been done about the implementation of IEC 61850 in different systems. The authors in [85] present a way to standardize the power system protection settings using IEC 61850 to improve its interoperability. The reliability of a substation automation system communication network using IEC 61850 is evaluated in [86]. The challenge and possible method to integrate EV into power grid for aggregated control are discussed in [87], but not using IEC 61850 standard. The authors in [88] provide a review of today's state of the art in ISO/IEC standardization of the V2G Interface. The integration of IEC 61850 into a Vehicle to Grid (V2G) system is conducted in [89]. However, yet no research has been done on the integration of IEC 61850 into an EV smart charging system to standardize charging control commands, session parameters and other data formats exchanged among different components of the system.

In this section, we proposed a method to integrate IEC 61850 into EV smart charging infrastructure

developed by SMERC. The data transmitted between EVSE and the aggregated control center includes charging control commands, power metering data and user interactions, etc. IEC 61850 is integrated to standardize these data strings, making them immediately available to other devices. New features such as power-sharing, current multiplexing and mobile app charging control are also integrated. The overall processes are:

1) Summarize the information and charging session parameters exchanged among the smart charging system;
2) Design the IEC 61850 Service framework to describe the components in the smart charging infrastructure
3) Design IEC 61850 data set to map the charging parameters and data into the system framework
4) Construct a Substation Configuration Language (SCL) file based on the data models from (2) and (3);
5) Develop web service to manipulate variables in SCL file, integrate the IEC 61850 system framework into existing control center program, serving as the communication interface

Related research can also be found in [53].

6.4.2 IEC61850 Service Framework Design

In the IEC 61850 service framework, the root of the system is the physical device, which has an IP address that can be accessed by other smart devices in the network. A physical device is defined as an Intelligent Electronic Device (IED) in IEC 61850 in the smart grid network. We define the EVSE as IED in the system. An IED contains some logical devices (LD), which are the function blocks inside the IED. Each LD is a collection of logical nodes (LN) that implement particular functions. LNs carry the data set to describe the IED status. LNs in the IED contain all charging data and session parameters, such as energy consumption, charging current, user ID, charging time,

etc. This data is made immediately available to other IEC 61850 devices. Figure 52 shows the smart charging infrastructure described by the IEC 61850 service framework.

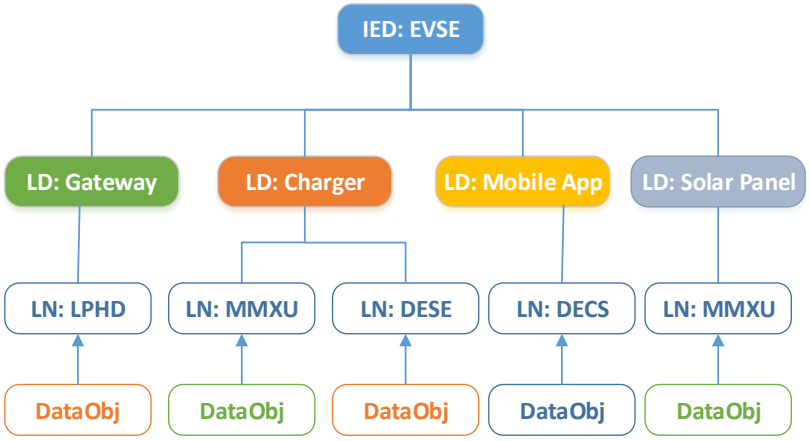

Figure 52. Smart charging infrastructure in IEC 61850 framework

There are one gateway and 4 EV chargers in each EVSE. Each charger is associated with one mobile app, *i.e.*, one user can only use his mobile app to access data of the charger plugged in his EV. The data in each IED should be made available to all other IEDs in the network. Logical device gateway acts as an interface between the EVSE and outside network and not responsible for any data measuring and processing tasks. Logical device charger performs all interactions with EV from authentication to charging control and monitoring. There are two logical nodes assigned to the charger, *i.e.*, MMXU for data measuring and DESE for authentication and monitoring. Logical device mobile app is the user end charging control interface. User preference in the mobile should also be made accessible by IEDs. Thus, a DECS logical node is assigned to the mobile app to satisfy this need. Logical device solar panel provides the real-time value of generated power by the solar panel to control center for charging scheduling algorithm decision making. A logical node MMXU is assigned to this measurement unit.

6.4.3 Logical Node and Dataset Design

Several chapters of IEC 61850 are used in the logical node data set design. IEC 61850-7-2 is used for the design of data set, and it defines the structure of data objects (DO) in the logical node. IEC 61850-7-3 is used to define the common data class (CDC) in the communication structure. IEC 61850-7-4 is used to select logical node classes and data classes. IEC 68150-90-8 is for a logical node related to E-mobility, EV and EVSE. Data set of 4 different types of logical node in IED are shown in Table XI.

Table XI. LN: MMXU IN CHARGER

MMXU Class			
DO	DA	CDC	Explanation
Timestamp	stVal	INC	Charging session start time
PhV	mag	MV	Charging voltage
A	mag	MV	Charging current
Hz	mag	MV	Grid frequency
PF	mag	MV	Power factor
W	mag	MV	Charging active power
VA	mag	MV	Charging apparent power
TotWh	mag	MV	Total active power consumption

MMXU is a measurement type of LN. MMXU logical node in the charger LD has 8 data objects. They represent the charging parameters in real-time including the charging voltage, current, power and total energy consumed, etc. Charging parameters are retrieved by the control center via a gateway with a predefined time interval for smart charging algorithm analysis. A data object (DO) is the elements in the SCL file contain the definition of a data and data value in IEC 61850 format. Data attribute (DA) is the element inside a DO which defines the data type of a data object. DA can be a status value (stVal), magnitude (mag), etc. Common data class (CDC) is the properties of the data object. CDC is mapped into concrete object definitions that are to be used for a particular protocol (e.g., MMS) for communication. In Table XI there are two CDC types, where INC stands

for controllable integer status and MV stands for measured value.

Table XII shows another logical node named DESE inside the charger logical device. DESE records user information and charger status. The data sets in DESE are obtained at the beginning of the charging session except for DutCycle, which contains the PWM duty cycle on the control pilot line between EVSE and EV. The duty cycle determines the charging current rate and may be changed during the charging session by the control of the smart charging algorithm.

Table XII. LN: DESE IN CHARGER

DESE Class			
DO	DA	CDC	Explanation
MeterStatus	stVal	INC	A flag shows meter on/off
RelayStatus	stVal	INC	A flag shows charger relay status
DutCycle	mag	MV	Current PWM duty cycle on CP
ID	stVal	INC	ID number of charger
Organization	stVal	INC	The organization EVSE belong to
AccessUsername	stVal	INC	Name of charger user
Availability	stVal	INC	Charger is ready for charging
Offline	stVal	INC	Whether the charger is offline

Table XIII. LN: DECS IN MOBILE APP

DECS Class			
DO	DA	CDC	Explanation
Price	stVal	INC	Real time energy price
Threshold	mag	MV	User price preference level
requireEnergy	stVal	INC	Indicate the user charging demand
EnergyRequired	mag	MV	The amount of energy needed
StartTime	stVal	MV	Charging start time
Duration	mag	MV	Whole charging session time span

Table XIII is the logical node data set in the mobile app logical device. These data are exchanged between the control center and user mobile app, representing user charging preference and demand. Table XIV is a logical node in the solar panel, showing the photovoltaic power generated by solar panels connected with the smart charging infrastructure.

Table XIV. LN: MMXU IN Solar Panel

MMXU Class			
DO	DA	CDC	Explanation
PV	mag	MV	Power generated by solar panels

6.4.4 SCL File and C# Web Service

With all of these charging data and parameters mapped into IEC 61850 abstract data model, an SCL file is then written to carry the data. SCL file is used in IEC 61850 standardized communication between smart grid devices

Before IEC 61850 integration, charging data and parameters are communicated in JSON and proprietary string format between EVSE, control center and mobile apps. To integrate with IEC 61850 in the communication, a web service is developed to extract data from JSON files and strings, then map them into IEC 61850 SCL file data objects. The web service can also read data values in the SCL file and map them back to JSON and string files. The web service serves as the interface to standardize communication in the smart charging infrastructure. The sequence diagram of smart charging system with IEC 61850 web service is shown in Figure 53.

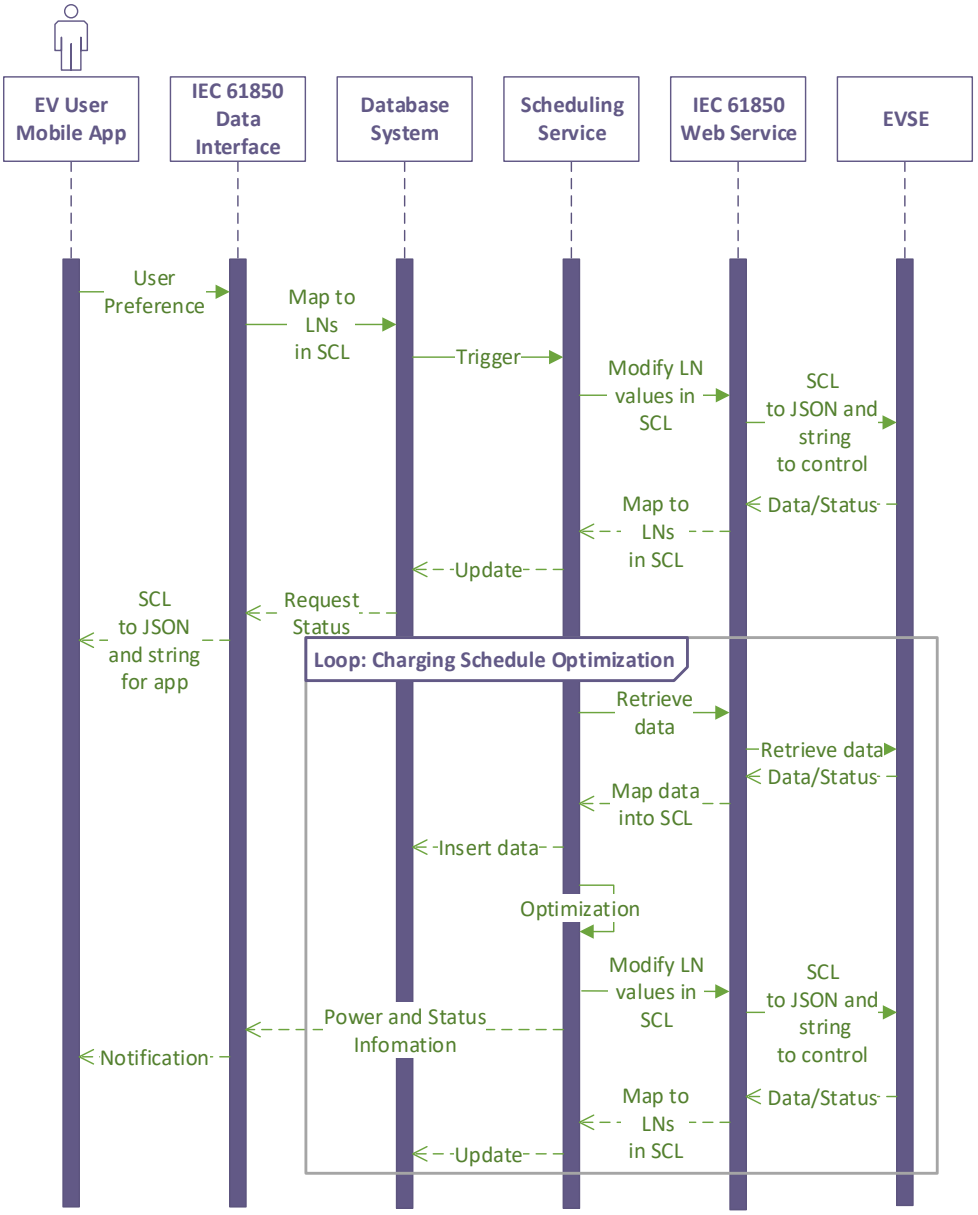

Figure 53. UML Sequence Diagram for IEC 61850 web service integration in smart charging infrastructure

The web service interface guarantees that all the charging-related data inside the control center are in IEC 61850 format. With the integration of IEC 61850 by web service interface, all incoming charging data to the control center are standardized into IEC 61850 SCL format, thus open to all other IEDs and smart grid applications in the network using IEC 61850 to read and manipulate, greatly improving the interoperability. All outgoing data are converted back to private protocols to be processed by particular local devices.

6.4.5 Result and Discussion

To test the feasibility and evaluate the performance, real-world EV charging data is used to set up the simulation experiments. Charging records for a randomly selected day, including users' start charging time, stay duration, and energy demand values, are extracted from the database system. The properties of the dataset on the test day are shown in Table XV:

Table XV. Charging Records on 17th, Marth, 2015

No.	User Index	Start Time	Duration (h)	Energy Demand (kWh)
1	CE1*	06:10:12	9.33	8.561
2	F42*	6:42:33	2.02	4.468
3	BFE*	7:07:44	6.87	12.207
4	155*	7:17:24	9.92	9.185
5	9CA*	14:08:58	7.3	6.154
6	8D5*	15:30:23	4.2	11.11
7	2E7*	18:31:56	1.05	5.722

Figure 54 shows the visualization of integrated charging information with IEC 61850 data frame in the SCL file. The information and data models are extracted during the simulation of real-world charging events. Left-hand side of Figure 54 is the hierarchy architecture of IEC 61850 model, while on right-hand side are some data object value extracted from hardware and meter reading. Charging data and user preference are processed by the web service and stored in certain SCL data object. As shown in the figure, solar panel generation, charging power, real-time energy price, estimated remaining charging duration etc. are mapped into the standardized IEC 61850 SCL data objects and ready to use by the charging scheduling algorithm.

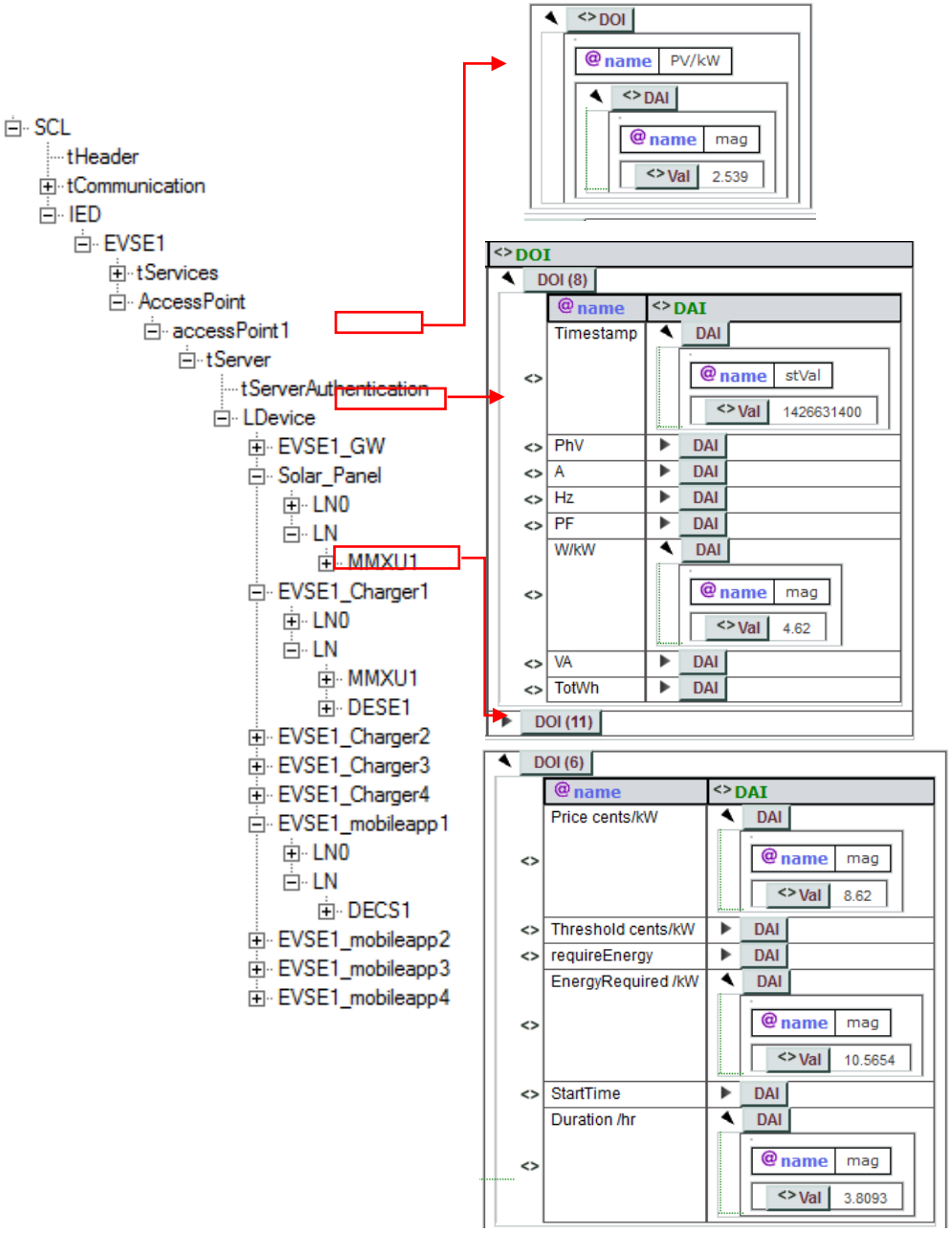

Figure 54. IEC 61850 SCL file visualization

6.4.6 Conclusion

In this section IEC 61850 abstract data model, supporting web service and interface are designed and tested for the smart charging infrastructure. With this IEC 61850 integration, the smart charging data and new features such as mobile app and current sharing are standardized into SCL configuration file, making them immediately available to any smart grid device and applications.

Thus, the works in this here not only extend the content of IEC 61850 in the smart charging field but also greatly improve the scalability and interoperability of smart charging infrastructure.

6.5 Summary

In this chapter, the hardware and firmware design for V2G control and communication system, the safety and reliability components for charging station and the integration of IEC61850 standard into smart charging network for standardized and reliable communication are discussed in detailed. Our designs have all been developed, manufactured and installed in our smart charging infrastructure network for public access.

7 Chapter VII. Conclusion and Future Works

In this research work, a systematical design for the completed Optimal Vehicle Grid Integration strategy for smart EV charging system which consists of regular level 2 AC charging station, fast DC charging station and V2G charging station is proposed and implemented. It is designed based on real-world system infrastructure implementation and EV user usage history. The charging control strategy is tested in simulation for large scale implementation and proved to be able to support the power grid with smart charging and V2G based on the real-world evaluation within our smart charging network infrastructure.

Major findings of this research consist of methods to estimate EV availability and demand, Optimal Vehicle Grid Integration strategy for large scale distributed real-time EV charging control. All designs have been implemented and evaluated for their performance and effectiveness against real-world scenario and use cases.

In the future, there will be more and more extreme EV charging stations connect to the power grid with more than 300kW power output. Advanced V2G technology will finally be commercialized and brought into the energy market. Different V2G options such as AC V2G and DC V2G deserve more investigations for their potential and use cases. The research of EV smart charging and V2G should be continued with the modernization of smart grid.

8 Bibliography

[1] "'Governor Brown Takes Action to Increase Zero-Emission Vehicles, Fund New Climate Investments – Governor Edmund G. Brown Jr.' [Online]. Available: https://www.gov.ca.gov/2018/01/26/governor-brown-takes-action-to-increase-zero-emission-vehicles-fund-new-climate-investments/. [Accessed: 29-Apr-2018]."

[2] Y. Mu, J. Wu, N. Jenkins, H. Jia, and C. Wang, "A Spatial–Temporal model for grid impact analysis of plug-in electric vehicles," *Appl. Energy*, vol. 114, pp. 456–465, Feb. 2014.

[3] A. Foley, B. Tyther, P. Calnan, and B. Ó Gallachóir, "Impacts of Electric Vehicle charging under electricity market operations," *Appl. Energy*, vol. 101, pp. 93–102, Jan. 2013.

[4] "'Tariffs.' [Online]. Available: https://www.pge.com/tariffs/index.page. [Accessed: 29-Apr-2018]."

[5] L. Gan, A. Wierman, U. Topcu, N. Chen, and S. H. Low, "Real-time Deferrable Load Control: Handling the Uncertainties of Renewable Generation," *SIGMETRICS Perform Eval Rev*, vol. 41, no. 3, pp. 77–79, Jan. 2014.

[6] N. Chen, L. Gan, S. H. Low, and A. Wierman, "Distributional analysis for model predictive deferrable load control," in *53rd IEEE Conference on Decision and Control*, 2014, pp. 6433–6438.

[7] L. Gan, U. Topcu, and S. Low, "Optimal decentralized protocol for electric vehicle charging," in *2011 50th IEEE Conference on Decision and Control and European Control Conference*, 2011, pp. 5798–5804.

[8] "California Energy Storage Showcase, 'LA Air Force Base Vehicle to Grid Demonstration,' [Online]. Available: http://www.energy.ca.gov/research/energystorage/tour/af_v2g/."

[9] D. Lew and N. Miller, "Reaching new solar heights: integrating high penetrations of PV into the power system," *IET Renew. Power Gener.*, vol. 11, no. 1, pp. 20–26, 2017.

[10] H. O. R. Howlader, M. Furukakoi, H. Matayoshi, and T. Senjyu, "Duck curve problem solving strategies with thermal unit commitment by introducing pumped storage hydroelectricity amp; renewable energy," in *2017 IEEE 12th International Conference on Power Electronics and Drive Systems (PEDS)*, 2017, pp. 502–506.

[11] R. Torabi, A. Gomes, and F. Morgado-Dias, "The Duck Curve Characteristic and Storage Requirements for Greening the Island of Porto Santo," in *2018 Energy and Sustainability for Small Developing Economies (ES2DE)*, 2018, pp. 1–7.

[12] J. Geske and D. Schumann, "Willing to participate in vehicle-to-grid (V2G)? Why not!," *Energy Policy*, vol. 120, pp. 392–401, Sep. 2018.

[13] M. A. Masrur *et al.*, "Military-Based Vehicle-to-Grid and Vehicle-to-Vehicle Microgrid—System Architecture and Implementation," *IEEE Trans. Transp. Electrification*, vol. 4, no. 1, pp. 157–171, Mar. 2018.

[14] L. Noel, G. Zarazua de Rubens, J. Kester, and B. K. Sovacool, "Beyond emissions and economics: Rethinking the co-benefits of electric vehicles (EVs) and vehicle-to-grid (V2G)," *Transp. Policy*, vol. 71, pp. 130–137, Nov. 2018.

[15] P. Staudt, M. Schmidt, J. Gärttner, and C. Weinhardt, "A decentralized approach towards resolving transmission grid congestion in Germany using vehicle-to-grid technology," *Appl. Energy*, vol. 230, pp. 1435–1446, Nov. 2018.

[16] Q. Wang, C. Zhang, Y. Ding, G. Xydis, J. Wang, and J. Østergaard, "Review of real-time electricity markets for integrating Distributed Energy Resources and Demand Response," *Appl. Energy*, vol. 138, pp. 695–706, Jan. 2015.

[17] T. K. Kristoffersen, K. Capion, and P. Meibom, “Optimal charging of electric drive vehicles in a market environment,” *Appl. Energy*, vol. 88, no. 5, pp. 1940–1948, May 2011.
[18] L. Gan, U. Topcu, and S. H. Low, “Optimal decentralized protocol for electric vehicle charging,” *IEEE Trans. Power Syst.*, vol. 28, no. 2, pp. 940–951, May 2013.
[19] H. Zhang, Z. Hu, Z. Xu, and Y. Song, “Evaluation of Achievable Vehicle-to-Grid Capacity Using Aggregate PEV Model,” *IEEE Trans. Power Syst.*, vol. 32, no. 1, pp. 784–794, Jan. 2017.
[20] W. Kempton and J. Tomić, “Vehicle-to-grid power fundamentals: Calculating capacity and net revenue,” *J. Power Sources*, vol. 144, no. 1, pp. 268–279, Jun. 2005.
[21] Devin Reeh, Francisco Cruz Tapia, Yu-Wei Chung, Benham Khaki, Peter Chu, Rajit Gadh, “Vulnerability Analysis and Risk Assessment of EV Charging System under Cyber-Physical Threats,” in *IEEE Transportation Electrification Conference and Expo*, 2019.
[22] Mohsenian-Rad, Hamed, “UC-Lab Center for Electricity Distribution Cybersecurity,” in *UC-National Lab Collaborative Research and Training Awards*, 2018.
[23] Hybrid - EV Committee, “SAE Electric Vehicle and Plug in Hybrid Electric Vehicle Conductive Charge Coupler,” SAE International.
[24] 14:00-17:00, “ISO 15118-1:2013,” *ISO*. [Online]. Available: http://www.iso.org/cms/render/live/en/sites/isoorg/contents/data/standard/05/53/55365.html. [Accessed: 16-Dec-2018].
[25] C.-Y. Chung, P. Chu, and R. Gadh, “Design of Smart Charging Infrastructure Hardware and Firmware Design of the Various Current Multiplexing Charging System,” City of Los Angeles Department, DOE-UCLA-00192-5, Oct. 2013.
[26] Y. Wang, H. Nazaripouya, C.-C. Chu, R. Gadh, and H. R. Pota, “Vehicle-to-grid automatic load sharing with driver preference in micro-grids,” presented at the Innovative Smart Grid Technologies Conference Europe (ISGT-Europe), 2014 IEEE PES, 2014, pp. 1–6.
[27] C.-Y. Chung, J. Chynoweth, C.-C. Chu, and R. Gadh, “Master-Slave Control Scheme in Electric Vehicle Smart Charging Infrastructure,” *The Scientific World Journal*, 2014. [Online]. Available: https://www.hindawi.com/journals/tswj/2014/462312/. [Accessed: 16-Dec-2018].
[28] B. Wang, Y. Wang, C. Qiu, C. Chu, and R. Gadh, “Event-based electric vehicle scheduling considering random user behaviors,” in *2015 IEEE International Conference on Smart Grid Communications (SmartGridComm)*, 2015, pp. 313–318.
[29] B. Wang, B. Hu, C. Qiu, P. Chu, and R. Gadh, “EV charging algorithm implementation with user price preference,” in *2015 IEEE Power Energy Society Innovative Smart Grid Technologies Conference (ISGT)*, 2015, pp. 1–5.
[30] “Open Automated Demand Response,” *Wikipedia*. 22-May-2018.
[31] B. Wang, Y. Wang, H. Nazaripouya, C. Qiu, C. c Chu, and R. Gadh, “Predictive Scheduling Framework for Electric Vehicles Considering Uncertainties of User Behaviors,” *IEEE Internet Things J.*, vol. PP, no. 99, pp. 1–1, 2016.
[32] Y. Wang, W. Shi, B. Wang, C.-C. Chu, and R. Gadh, “Optimal operation of stationary and mobile batteries in distribution grids,” *Appl. Energy*, vol. 190, pp. 1289–1301, Mar. 2017.
[33] Y. Xiong, C. Chu, R. Gadh, and B. Wang, “Distributed optimal vehicle grid integration strategy with user behavior prediction,” in *2017 IEEE Power Energy Society General Meeting*, 2017, pp. 1–5.

[34] B. Wang *et al.*, “Predictive scheduling for Electric Vehicles considering uncertainty of load and user behaviors,” in *2016 IEEE/PES Transmission and Distribution Conference and Exposition (T D)*, 2016, pp. 1–5.
[35] A. Gensler, J. Henze, B. Sick, and N. Raabe, “Deep Learning for solar power forecasting #x2014; An approach using AutoEncoder and LSTM Neural Networks,” in *2016 IEEE International Conference on Systems, Man, and Cybernetics (SMC)*, 2016, pp. 002858–002865.
[36] Y. Xiong, B. Wang, Z. Cao, C. Chu, H. Pota, and R. Gadh, “Extension of IEC61850 with smart EV charging,” in *2016 IEEE Innovative Smart Grid Technologies - Asia (ISGT-Asia)*, Melbourne, Australia, 2016, pp. 294–299.
[37] T. Zhang, W. Chen, Z. Han, and Z. Cao, “Charging Scheduling of Electric Vehicles With Local Renewable Energy Under Uncertain Electric Vehicle Arrival and Grid Power Price,” *IEEE Trans. Veh. Technol.*, vol. 63, no. 6, pp. 2600–2612, Jul. 2014.
[38] M. Majidpour, C. Qiu, P. Chu, R. Gadh, and H. R. Pota, “Fast Prediction for Sparse Time Series: Demand Forecast of EV Charging Stations for Cell Phone Applications,” *IEEE Trans. Ind. Inform.*, vol. 11, no. 1, pp. 242–250, Feb. 2015.
[39] B. Pitt, “Applications of data mining techniques to electric load profiling,” Ph.D., University of Manchester, 2000.
[40] R. Selbaş, A. Şencan, and E. U. Küçüksille, “Data Mining Method For Energy System Aplications,” *Knowl.-Oriented Appl. Data Min.*, Jan. 2011.
[41] “Data mining and graph theory focused solutions to Smart Grid challenges - ProQuest.” [Online]. Available: https://search.proquest.com/openview/29d48ca26257bafe80819c60de985b76/1?pq-origsite=gscholar&cbl=18750&diss=y. [Accessed: 16-Dec-2018].
[42] V. Figueiredo, F. Rodrigues, Z. Vale, and J. B. Gouveia, “An electric energy consumer characterization framework based on data mining techniques,” *IEEE Trans. Power Syst.*, vol. 20, no. 2, pp. 596–602, May 2005.
[43] T. Zhang, G. Zhang, J. Lu, X. Feng, and W. Yang, “A New Index and Classification Approach for Load Pattern Analysis of Large Electricity Customers,” *IEEE Trans. Power Syst.*, vol. 27, no. 1, pp. 153–160, Feb. 2012.
[44] S. Ramos and Z. Vale, “Data mining techniques application in power distribution utilities,” in *2008 IEEE/PES Transmission and Distribution Conference and Exposition*, 2008, pp. 1–8.
[45] Y. Xiong, B. Wang, C. Chu, and R. Gadh, “Electric Vehicle Driver Clustering using Statistical Model and Machine Learning,” in *2018 IEEE Power Energy Society General Meeting (PESGM)*, 2018, pp. 1–5.
[46] “*k*-means clustering,” *Wikipedia*. 14-Dec-2018.
[47] “Multilayer perceptron,” *Wikipedia*. 02-Oct-2018.
[48] “Mean absolute percentage error,” *Wikipedia*. 13-Dec-2018.
[49] “Latent semantic analysis,” *Wikipedia*. 18-Nov-2018.
[50] Y. Xiong, B. Wang, C. Chu, and R. Gadh, “Vehicle grid integration for demand response with mixture user model and decentralized optimization,” *Appl. Energy*, vol. 231, pp. 481–493, Dec. 2018.
[51] “Expectation–maximization algorithm,” *Wikipedia*. 13-Dec-2018.
[52] “California Independent System Operator, ‘Today’s Outlook’. [Online] Available: http://www.caiso.com/outlook.html.”

[53] Y. Xiong, B. Wang, Z. Cao, C. c Chu, H. Pota, and R. Gadh, “Extension of IEC61850 with smart EV charging,” in *2016 IEEE Innovative Smart Grid Technologies - Asia (ISGT-Asia)*, 2016, pp. 294–299.
[54] Y. Cao *et al.*, “An Optimized EV Charging Model Considering TOU Price and SOC Curve,” *IEEE Trans. Smart Grid*, vol. 3, no. 1, pp. 388–393, Mar. 2012.
[55] “Princeton Power, ‘V2X Fast Charger – CA-30/CA-10’, 2015. Available:https://www.princetonpower.com/images/CA10_30_SellSheet_November2015.pdf.”
[56] “U.S. Energy Information Administration, ‘How much electricity does an American home use’, October 2016. Available: https://www.eia.gov/tools/faqs/faq.php?id=97&t=3.”
[57] “Chademo Association, ‘CHAdeMO Protocol’, 2010. Available: http://chademo.com.”
[58] R. Gough, C. Dickerson, P. Rowley, and C. Walsh, “Vehicle-to-grid feasibility: A techno-economic analysis of EV-based energy storage,” *Appl. Energy*, vol. 192, pp. 12–23, Apr. 2017.
[59] L. Zhang and Y. Li, “Optimal Management for Parking-Lot Electric Vehicle Charging by Two-Stage Approximate Dynamic Programming,” *IEEE Trans. Smart Grid*, vol. 8, no. 4, pp. 1722–1730, Jul. 2017.
[60] Maigha and M. L. Crow, “Cost-Constrained Dynamic Optimal Electric Vehicle Charging,” *IEEE Trans. Sustain. Energy*, vol. 8, no. 2, pp. 716–724, Apr. 2017.
[61] “Cornell University Facilities Services, ‘Real Time Building Utility Use Data’. Available: http://portal.emcs.cornell.edu.”
[62] Y. Xiong, B. Khakit, C. Chu, and R. Gadh, “Real-Time Bi-Directional Electric Vehicle Charging Control with Distribution Grid Implementation,” in *2018 IEEE/PES Transmission and Distribution Conference and Exposition (T D)*, 2018, pp. 1–5.
[63] “WSCC 9-Bus System - Illinois Center for a Smarter Electric Grid (ICSEG).” .
[64] “Bloomberg New Energy Finance, ‘Electric vehicles to be 35% of global new car sales by 2040’, February 2016. Available: https://about.bnef.com/blog/electric-vehicles-to-be-35-of-global-new-car-sales-by-2040/.”
[65] T. Chen, H. Pourbabak, Z. Liang, W. Su, and P. Yu, “Participation of electric vehicle parking lots into retail electricity market with evoucher mechanism,” in *2017 IEEE Transportation Electrification Conference and Expo, Asia-Pacific (ITEC Asia-Pacific)*, 2017, pp. 1–5.
[66] D. Guo and C. Zhou, “Realistic modeling of vehicle-to-grid in an enterprise parking lot: A stackelberg game approach,” in *2018 IEEE Texas Power and Energy Conference (TPEC)*, 2018, pp. 1–6.
[67] L. Danxi, Z. Bo, Q. Yan, and X. Yu-jie, “Optimal control model of electric vehicle demand response based on real — time electricity price,” in *2017 IEEE 2nd Information Technology, Networking, Electronic and Automation Control Conference (ITNEC)*, 2017, pp. 1815–1818.
[68] Y. Wang, B. Wang, C.-C. Chu, H. Pota, and R. Gadh, “Energy management for a commercial building microgrid with stationary and mobile battery storage,” *Energy Build.*, vol. 116, pp. 141–150, Mar. 2016.
[69] M. Shafie-khah *et al.*, “Optimal Behavior of Electric Vehicle Parking Lots as Demand Response Aggregation Agents,” *IEEE Trans. Smart Grid*, vol. 7, no. 6, pp. 2654–2665, Nov. 2016.

[70] Z. Zhao, W. Chen, X. Wu, P. C. Y. Chen, and J. Liu, “LSTM network: a deep learning approach for short-term traffic forecast,” *IET Intell. Transp. Syst.*, vol. 11, no. 2, pp. 68–75, 2017.
[71] E. C. Kara, J. S. Macdonald, D. Black, M. Bérges, G. Hug, and S. Kiliccote, “Estimating the benefits of electric vehicle smart charging at non-residential locations: A data-driven approach,” *Appl. Energy*, vol. 155, pp. 515–525, Oct. 2015.
[72] X. Qiu, L. Zhang, Y. Ren, P. N. Suganthan, and G. Amaratunga, “Ensemble deep learning for regression and time series forecasting,” in *2014 IEEE Symposium on Computational Intelligence in Ensemble Learning (CIEL)*, 2014, pp. 1–6.
[73] M. Majidpour, C. Qiu, P. Chu, H. R. Pota, and R. Gadh, “Forecasting the EV charging load based on customer profile or station measurement?,” *Appl. Energy*, vol. 163, pp. 134–141, Feb. 2016.
[74] E. Xydas, C. Marmaras, L. M. Cipcigan, N. Jenkins, S. Carroll, and M. Barker, “A data-driven approach for characterising the charging demand of electric vehicles: A UK case study,” *Appl. Energy*, vol. 162, pp. 763–771, Jan. 2016.
[75] “PJM - 7-Day Load Forecast.” [Online]. Available: https://www.pjm.com/markets-and-operations/energy/real-time/7-day-load-forecast.aspx. [Accessed: 17-Dec-2018].
[76] N. Chen, C. W. Tan, and T. Q. S. Quek, “Electric Vehicle Charging in Smart Grid: Optimality and Valley-Filling Algorithms,” *IEEE J. Sel. Top. Signal Process.*, vol. 8, no. 6, pp. 1073–1083, Dec. 2014.
[77] “California Independent System Operator, ‘Locational Marginal Prices (LMP)’. [Online] Available: http://oasis.caiso.com/mrioasis/logon.do.”
[78] “Southern California Edison, ‘Schedule TOU-8’, Sep 2017. [Online] Available: https://www.sce.com/NR/sc3/tm2/pdf/ce54-12.pdf.”
[79] “XML,” *Wikipedia*. 08-Dec-2018.
[80] Hybrid - EV Committee, “Broadband PLC Communication for Plug-in Electric Vehicles,” SAE International.
[81] “HomePlug | HomePlug Green PHY™: perfect fit for Smart Energy / Internet of Things (IoT) applications.” [Online]. Available: http://www.homeplug.org/tech-resources/green-phy-iot/. [Accessed: 17-Dec-2018].
[82] “Modbus,” *Wikipedia*. 13-Dec-2018.
[83] “Zigbee,” *Wikipedia*. 16-Dec-2018.
[84] “IEC TR 61850-1:2003 | IEC Webstore | LVDC.” [Online]. Available: https://webstore.iec.ch/publication/20071. [Accessed: 17-Dec-2018].
[85] Q. Hong, S. M. Blair, V. M. Catterson, A. Dyśko, C. D. Booth, and T. Rahman, “Standardization of power system protection settings using IEC 61850 for improved interoperability,” in *2013 IEEE Power Energy Society General Meeting*, 2013, pp. 1–5.
[86] N. Liu, M. Panteli, and P. A. Crossley, “Reliability evaluation of a substation automation system communication network based on IEC 61850,” in *12th IET International Conference on Developments in Power System Protection (DPSP 2014)*, 2014, pp. 1–6.
[87] J. Heuer, P. Komarnicki, and Z. A. Styczynski, “Integration of electrical vehicles into the smart grid in the Harz.EE-mobility research project,” in *2011 IEEE Power and Energy Society General Meeting*, 2011, pp. 1–6.
[88] J. Schmutzler, C. A. Andersen, and C. Wietfeld, “Evaluation of OCPP and IEC 61850 for smart charging electric vehicles,” in *2013 World Electric Vehicle Symposium and Exhibition (EVS27)*, 2013, pp. 1–12.

[89] R. Huang *et al.*, “Integration of IEC 61850 into a Vehicle-to-Grid system with networked electric vehicles,” in *Innovative Smart Grid Technologies Conference (ISGT), 2015 IEEE Power Energy Society*, 2015, pp. 1–5.